ISSN 1881-7831 Online ISSN 1881-784X

DD&T

Drug Discoveries & Therapeutics

Volume 16, Number 4
August 2022

IRCA BSSA

IACMHR

www.ddtjournal.com

DD&T
Drug Discoveries & Therapeutics

ISSN: 1881-7831
Online ISSN: 1881-784X
CODEN: DDTRBX
Issues/Year: 6
Language: English
Publisher: IACMHR Co., Ltd.

Drug Discoveries & Therapeutics is one of a series of peer-reviewed journals of the International Research and Cooperation Association for Bio & Socio-Sciences Advancement (IRCA-BSSA) Group. It is published bimonthly by the International Advancement Center for Medicine & Health Research Co., Ltd. (IACMHR Co., Ltd.) and supported by the IRCA-BSSA.

Drug Discoveries & Therapeutics publishes contributions in all fields of pharmaceutical and therapeutic research such as medicinal chemistry, pharmacology, pharmaceutical analysis, pharmaceutics, pharmaceutical administration, and experimental and clinical studies of effects, mechanisms, or uses of various treatments. Studies in drug-related fields such as biology, biochemistry, physiology, microbiology, and immunology are also within the scope of this journal.

Drug Discoveries & Therapeutics publishes Original Articles, Brief Reports, Reviews, Policy Forum articles, Case Reports, Communications, Editorials, News, and Letters on all aspects of the field of pharmaceutical research. All contributions should seek to promote international collaboration in pharmaceutical science.

Editorial Board

Editorial and Head Office:

Pearl City Koishikawa 603,
2-4-5 Kasuga, Bunkyo-ku,
Tokyo 112-0003, Japan
E-mail: office@ddtjournal.com

Drug Discoveries & Therapeutics

Editorial and Head Office

Pearl City Koishikawa 603, 2-4-5 Kasuga, Bunkyo-ku,
Tokyo 112-0003, Japan

E-mail: office@ddtjournal.com
URL: www.ddtjournal.com

Original Article

Brief Report

Commentary

Letter to the Editor

Original Article

DOI: 10.5582/ddt.2022.01053

Binding of phenochalasin A, an inhibitor of lipid droplet formation in mouse macrophages, on G-actin

Keisuke Kobayashi[1,2], Daisuke Matsuda[1], Hiroshi Tomoda[1,3,*], Taichi Ohshiro[1,2,*]

[1] Department of Microbial Chemistry, Graduate School of Pharmaceutical Sciences, Kitasato University, Tokyo, Japan;
[2] Medicinal Research Laboratories, School of Pharmacy, Kitasato University, Tokyo, Japan;
[3] Laboratory of Drug Discovery, Graduate School of Pharmaceutical Sciences, Kitasato University, Tokyo, Japan.

SUMMARY Phenochalasin A, a unique phenol-containing cytochalasin produced by the marine-derived fungus *Phomopsis* sp. FT-0211, was originally discovered in a cell morphological assay of observing the inhibition of lipid droplet formation in mouse peritoneal macrophages. To investigate the mode of action and binding proteins, phenochalasin A was radio-labeled by ^{125}I. Iodinated phenochalasin A exhibited the same biological activity as phenochalasin A. [^{125}I]Phenochalasin A was found to be associated with an approximately 40 kDa protein, which was identified as G-actin. Furthermore, detail analyses of F-actin formation in Chinese hamster ovary cells (CHO-K1 cells) indicated that phenochalasin A (2 μM) caused elimination of F-actin formation on the apical site of the cells, suggesting that actin-oriented specific function(s) in cytoskeletal processes are affected by phenochalasin A.

Keywords Phenochalasin, cytochalasin, actin, lipid droplet, macrophages

1. Introduction

Marine-derived microorganisms are a promising natural resource for new drug discovery because they produce a wide range of structurally diverse compounds. Phenochalasins A and B, produced by the marine-derived fungus *Phomopsis* sp. FT-0211 which was isolated from seawater collected near Ponape Island (*1,2*), were originally discovered in a cell morphological assay of observing the inhibition of lipid droplet formation in mouse peritoneal macrophages (*3*). These compounds belong to the well-known cytochalasan family (*4,5*). Intriguingly, phenochalasin A (Figure 1) possesses a unique phenol moiety in the structure, and this type of cytochalasans has not been reported to date. Thus, the marine-derived *Phomopsis* sp. FT-0211 is valuable for phenochalasin A production. Furthermore, cytochalasans are generally considered as mycotoxins showing cytotoxic activity to mammalian cells by binding to the actin filaments (*6*). Importantly, phenochalasin A inhibited lipid droplet formation in mouse macrophages without cytotoxic effect (*3*). These findings prompted us to investigate the mechanism of action of phenochalasin A on lipid droplet formation in mouse macrophages. In this study, we examined the action of phenochalasin A compared to cytotoxic cytochalasin on actin filament formation.

2. Materials and Methods

2.1. Materials

Phenochalasin A was produced by fermentation of the marine-derived fungus *Phomopsis* sp. FT-0211 in the production medium (seawater concentration was changed from 50% to 25%) at 27°C for 4 days according to a previously reported method (*1*). From the 10 L culture, pure phenochalasin A (15 mg) was obtained as white powder. Cytochalasin E, phosphatidylcholine, phosphatidylserine, dicetylphosphate, cholesterol, G-actin (derived from rabbit muscle), Ham's F-12 medium, and bovine serum albumin (BSA) (fatty acid free, fraction V) were purchased from Sigma-Aldrich (now Millipore Sigma, St. Louis, MO, USA). Iodination Beads were purchased from Pierce (now Thermo Fisher Scientific, Waltham, MA, USA). [^{125}I]Sodium iodinate and [^{14}C]oleic acid were purchased from PerkinElmer (Waltham, MA, USA). GIT medium was purchased from Nippon Seiyaku Co. (Tokyo, Japan). Penicillin (10,000 units/mL) and streptomycin (10,000 mg/mL) were purchased from Invitrogen (now Thermo Fisher Scientific, Waltham, MA, USA).

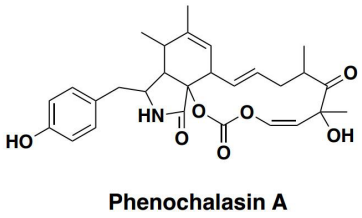

Phenochalasin A

Figure 1. The structure of phenochalasin A.

2.2. Preparation of [^{125}I]phenochalasin A

Preparation of [^{125}I]phenochalasin A was performed according to the instruction manual for Iodination Beads(*7-9*) with a slight modification. In brief, 100 µg of phenochalasin A (0.20 µmol) was dissolved in 500 µL of 20% methanol/phosphate-buffered saline (PBS)(-), and then 5.0 µL of [^{125}I]sodium iodinate (20.0 MBq) was added. After 30-min incubation at room temperature, the supernatant was collected and the beads were washed with 100 µL PBS(-). The aqueous solutions were two times extracted with 500 µL of ethyl acetate. The organic layer was collected and ethyl acetate was evaporated under nitrogen atmosphere. [^{125}I]Phenochalasin A solution was prepared at a concentration of 1 mg/mL using acetonitrile and stored at -20°C until use.

2.3. Cell culture

CHO-K1 cells (a generous gift from Dr. Kentaro Hanada, National Institute of Infectious Diseases, Tokyo, Japan) were maintained at 37°C in 5% CO_2 in medium A containing Ham's F-12 medium supplemented with 10% heat-inactivated FBS, penicillin (100 units/mL) and streptomycin (100 mg/mL) using a method described previously (*10*).

2.4. Assay for [^{14}C]neutral lipid synthesis in mouse macrophages

The assay for the synthesis of neutral lipid from [^{14}C] oleic acid was conducted according to a previously described method (*11*). In brief, primary mouse peritoneal macrophages (5×10^5 cells/250 µL of GIT medium) in each well of a 48-well plastic plate (Corning Co., Corning, NY, USA) were incubated at 37°C in 5% CO_2 for 2 h. The medium was then replaced with 250 µL of DMEM containing 8% (v/v) lipoprotein-deficient serum (LPDS), penicillin (100 units/mL) and streptomycin (100 mg/mL) (hereafter referred to as medium B). After another 2-h preincubation, a test compound (2.5 µL in acetonitrile solution) and liposomes (10.0 µL, 1.0 µmol phosphatidylcholine, 1.0 µmol phosphatidylserine, 0.20 µmol dicetylphosphate and 1.5 µmol cholesterol, suspended in 1.0 mL of 0.3 M glucose) together with [^{14}C]oleic acid (5 µL (1.85 kBq) in 10% ethanol/PBS(-) solution) were added to each well. Following 14-h incubation, the medium was removed and the cells in each well were washed three times with PBS(-). The cells were lysed with 250 µL of 10 mM Tris·HCl/PBS(-) containing 0.1% (w/v) sodium dodecyl sulfate (SDS), and the cellular lipids were extracted by the method of Bligh and Dyer (*12*). After concentrating the organic solvent, the total lipids were separated on a TLC plate (silica gel F254, 0.5 mm thick, Merck, Darmstadt, Germany) and analyzed with a BAS-2000 (Fuji Film, Tokyo, Japan).

2.5. Binding of [^{125}I]phenochalasin A to macrophage cell lysate and G-actin

2.5.1. Preparation of lysate of mouse peritoneal macrophages

The microsomes of mouse peritoneal macrophages were prepared according to a previously described method (*13,14*). Briefly, mouse peritoneal macrophages (2×10^8 cells) were homogenized in 3.0 mL of cold Tris·HCl (pH 7.8) containing protease inhibitor cocktail (Roche) in a Teflon homogenizer. The supernatant was collected by centrifugation at 10,000 rpm for 15 min at 4°C. The lysate was prepared at a concentration of 5 mg of protein/mL and stored at -80°C until use.

2.5.2. Binding assay using [^{125}I]phenochalasin A

The macrophage lysate or G-actin (derived from rabbit, 40 µg or 10 µg in 80 µL of Tris·HCl (pH 7.8), respectively) was incubated with cytochalasin E (10 µL, 0-400 µmol) at 4°C for 15 min, then [^{125}I]phenochalasin A (370 kBq, 4 µmol, 2 µL) was added, and the samples were incubated at 4°C for 15 min. The binding assay was stopped by transferring an equal amount of 2× sample buffer containing 2.0% of 2-mercaptoethanol, which was boiled for 5 min at 95°C and centrifuged. A portion of supernatant was separated by SDS-PAGE at a constant current of 20 mA for 2 h. [^{125}I]Phenochalasin A binding proteins were detected by radioactivity using image analyzer BAS-2000.

2.6. Analysis of actin filaments in CHO-K1 cells by confocal microscopy

CHO-K1 cells (3×10^3 cells in 200 µL of medium A) in each well of an 8-well of glass chamber slide (Nalge Nunc International K.K., Rochester, NY, U.S.A.) were incubated at 37°C in 5% CO_2. Following the overnight recovery, a sample (2.0 µL in acetonitrile solution) was added to each well. After 1 and 6 h of incubation, cells were washed three times with 200 µL of PBS(-), and then fixed by soaking in 100 µL of 3.7% formalin for 20 min at room temperature. After washing three

times with PBS(-), actin filaments were stained with Alexa Fluor 594-phalloidin (0.66 µM, 100 µL in 3% BSA/PBS(-)) for 1 h at room temperature under shading condition. After washing three times with PBS(-), the cells were mounted with Prolong Antifade reagent (Thermo Fischer Scientific) according to the manufacturer's instructions. The formation of actin filaments was examined by confocal laser scanning microscopy (LSM-510 META, Carl Zeiss, Oberkochen, Germany).

2.7. MALDI-TOF-MS analysis of phenochalasin A treated-G-actin

A complex of a test sample (phenochalasin A and cytochalasin E) and G-actin was prepared by incubation of 2.1 µM of actin with 20 µM of a test sample in milliQ for 3 h on ice. The molecular weight of the actin incubated with or without a test sample was determined by a MALDI-TOF/MS spectrometer (AXIMA-CFR, SHIMADSU, Kyoto, Japan). Sinapinic acid (for proteome research, Wako) was used as the matrix for the measurement.

3. Results

3.1. Inhibition of macrophage-derived lipid droplet formation by iodinated phenochalasin A

As demonstrated in the previous study, phenochalasin A blocked the lipid droplet formation by selectively inhibiting cholesteryl ester (CE) synthesis (IC_{50}, 0.61 µM) without any cytotoxic effect (even at the highest dose of 20 µM) in mouse peritoneal macrophages. Furthermore, the target site of phenochalasin A is limited to within the prelysosomal stages of cholesterol metabolism in the lipid droplet synthetic process (*3*). To investigate the target molecule of phenochalasin A in this process, radiolabeled phenochalasin A was prepared by taking advantage of having a phenol residue in the structure to produce [^{125}I]phenochalasin A. During the setup conditions for the iodination reaction, monoiodinated ([I]) and diiodinated ([I_2])phenochalasin A were prepared. We confirmed that [I]- and [I_2] phenochalasin A exhibited inhibitory activity of lipid droplet formation and CE synthesis (Figure 2) in mouse macrophages analogous to phenochalasin A. Indeed, their IC_{50} values of CE synthesis were the range of 0.1 to 1.0 µM (Figure 2). Finally, under 30 min reaction time for the iodination, [^{125}I]phenochalasin A (including [^{125}I] and [$^{125}I_2$]phenochalasin A) was prepared and used in the subsequent experiments.

3.2. Analysis of [^{125}I]phenochalasin A-binding proteins in macrophage lysate

After the macrophage lysate (40 µg protein) was incubated with [^{125}I]phenochalasin A (370 kBq, 4 µmol), proteins in the lysate were separated by SDS-PAGE and radiolabeled proteins were detected by autoradiography. As shown in Figure 3 (right 3 lanes), an approximately 40 kDa protein was mainly radiolabeled. Preincubation of the lysate with excess of cytochalasin E (40 and 400 µmol) caused elimination of the radioactivity from the protein, suggesting that [^{125}I]phenochalasin A is strongly bound to actin filaments in the lysate. To validate this, pure G-actin (10 µg) was similarly treated with [^{125}I]phenochalasin A and analyzed (Figure 3 left 3

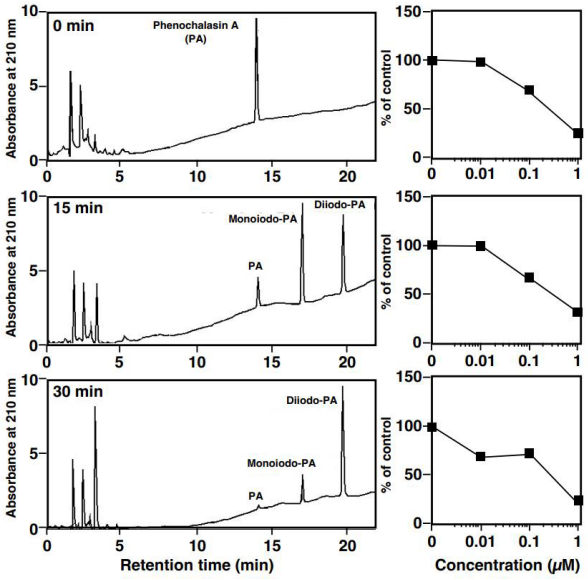

Figure 2. Iodination of phenochalasin A and its inhibitory effect on CE synthesis. Left lane shows HPLC chromatogram of iodination at indicated times. HPLC conditions were as follows; column, YMC-Pack D-ODS-5 (4.6 × 250 mm); mobile phase, 30-70% acetonitrile/H_2O-0.1% H_3PO_4 20-min linear gradient; flow rate, 1.0 mL/min; detection, UV at 210 nm. Right lane shows the inhibitory activity of CE synthesis of mixture of iodinated phenochalasin A at indicated reaction times.

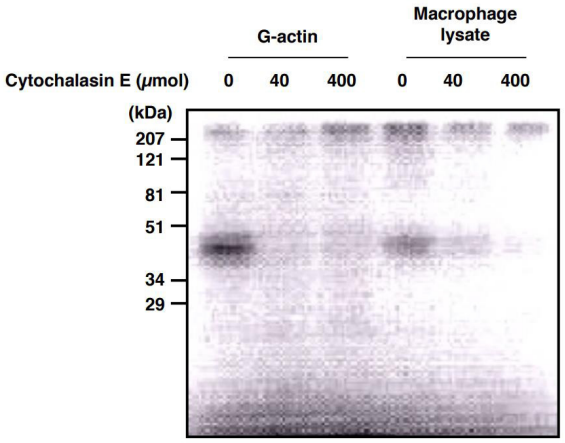

Figure 3. Binding of [^{125}I]phenochalasin A on G-actin and macrophage lysate. G-actin or macrophage lysate was incubated with [^{125}I]Phenochalasin A (4 µmol, 370 kBq) after the preincubation with cytochalasin E (0, 40, 400 µmol). Bound proteins were analyzed using SDS-PAGE and radio autography.

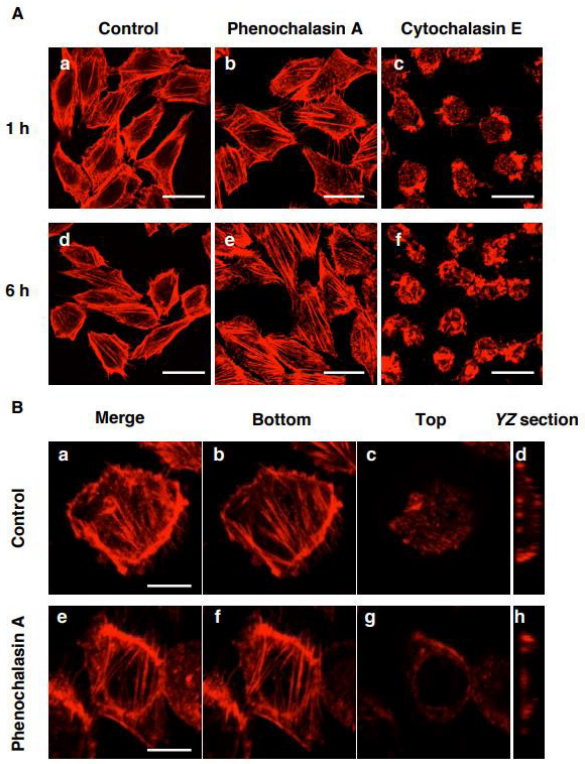

Figure 4. Effect of phenochalasin A on F-actin in CHO-K1 cells. **(A)** CHO-K1 cells were treated with phenochalasin A (2 μM) or cytochalasin E (2 μM). Following 1-h and 6-h incubation, cells were stained with Alexa Fluor 594-phalloidin. **a**, **d**: control cells; **b**, **e**: phenochalasin A-treated cells; **c**, **f**: cytochalasin E-treated cells. Bars, 20 μm. **(B)** CHO-K1 cells were treated with (**e-h**) or without phenochalasin A (2 μM) (**a-d**). Following 6-h incubation, cells were stained with Alexa Fluor 594-phalloidin. **a**, **e**; whole scanning images, **b**, **f**; bottom scanning images, **c**, **g**; top scanning images, **d**, **h**; sectioning images. Bars, 10 μm.

lanes). G-actin was found to be radiolabeled with [^{125}I] phenochalasin A, but not radiolabeled by preincubation with cytochalasin E. Thus, it was concluded that phenochalasin A is exclusively bound to actin filaments of mouse macrophages.

3.3. Effect of phenochalasin A on actin filament formation in CHO-K1 cells.

Since it is difficult to observe actin filaments in intact mouse peritoneal macrophages, CHO-K1 cells were used to investigate the effect of phenochalasin A on actin filament formation. Confocal microscopical observation (Figure 4A) indicated that ostensibly similar F-actin filaments were formed in control cells and phenochalasin A-treated cells, whereas F-actin filaments were fragmented/broken (at 1 h) and aggregated (at 6 h) in cytochalasin E-treated cells. To search for the difference between control and phenochalasin A-treated cells, F-actin formation was compared at the bottom (basal) and top (apical) sites between the cells (Figures 4B-g and -h). Intriguingly, F-actins disappeared at the top site of phenochalasin A-treated cells, suggesting that the specific function of actin is affected by phenochalasin A.

4. Discussion

In the previous study (*3,15*), we reported that 7 cytochalasans tested (two phenochalasins, three cytochalasins and two aspochalasins) inhibited macrophage-derived lipid droplet formation. Six cytochalasans except phenochalasin A caused morphological abnormality in macrophages at the doses corresponding to the IC_{50} values (0.20-3.0 μM) for CE synthesis. Only phenochalasin A did not induced such morphological abnormality even at a much higher dose (19 μM) than its IC_{50} value (0.61 μM) for CE synthesis. Regarding cytotoxic effects on macrophages measured by the MTT assay, cytochalasins D and E induced 10-fold higher IC_{50} values than the doses causing morphological abnormality. These findings indicate that most cytochalasans cause both morphological abnormality and plasma membrane damage on macrophages at similar doses, and certain ones like cytochalasins D and E induce morphological abnormality without plasma membrane damage at lower doses (*3,16*). Intriguingly, among cytochalasans, phenochalasin A has a very unique characteristic of lack ability to cause morphological abnormality and plasma membrane damage even at higher doses. Indeed, phenochalasin A did not show any cytotoxic effects on measurements by the alamar blue (detectable cell viability) and LDH assays (detectable cell membrane damage) in macrophages, and did not inhibit growth of CHO-K1 cells (Figure S1, *http://www.ddtjournal.com/action/getSupplementalData.php?ID=118*). Note that, to date, phenochalasin A is a rare cytochalasan with a phenol moiety in the structure only produced by the marine-derived fungus *Phomopsis* sp. FT-0211.

Cytochalasans are well known to disrupt the actin cytoskeleton (*4-6*) by binding to the barbed end of actin filaments (*17*), causing morphological abnormality and cytotoxic effect on mammalian cells. Therefore, we initially considered that the target molecule of phenochalasin A is not actin. However, phenochalasin A was found to be also bound to G-actin in macrophage lysates and purified G-actin using [^{125}I]phenochalasin A (Figure 3), which showed the same biological activity as phenochalasin A on CE synthesis on macrophages (Figure 2). Furthermore, the binding site of [^{125}I] phenochalasin A in G-actin was the same as that of cytochalasin E (Figure 3), and one phenochalasin A that appeared bound to one G-actin by MS analysis (Figure S2, *http://www.ddtjournal.com/action/getSupplementalData.php?ID=118*). Accordingly, the biological characteristics observed by phenochalasin A appear very mysterious among cytochalasan family. To approach this question, actin filaments in CHO-K1 cells were observed after 1 (or 6)-h treatment of the

drug (phenochalasin A or cytochalasin E) (Figure 4A). Researchers have utilized CHO-K1 cells to investigate actin filament formation because clear actin filaments are observed in the cells. The dose of 2 μM phenochalasin A showed no effects on CHO-K1 cells by MTT assay, whereas 2 μM cytochalasin E caused 50% damage to the cells. The effects on actin filament formation in CHO-K1 cells are in good agreement with morphological changes and cytotoxicity observed in mouse macrophages, suggesting that phenochalasin A ostensibly caused almost no effects on actin filament formation in CHO-K1 cells even though it was bound to the actin. Although actin-cytochalasan complex structures have not been extensively studied, Nair *et al*. reported that cytochalasin D binds the hydrophobic cleft between subdomains 1 and 3 of G-actin based on the crystal structures (*17*). They showed 6 hydrogen bonds between the protein and the ligand, 5 of which were mediated by the isoindolone core and its adjacent cyclohexynol ring. The benzene ring in cytochalasin D structure did not appear to have any interaction with surrounding amino acids nor face outside from actin. According to the 3D structure, it might be that the hydroxy moiety of the phenol in phenochalasin A may be involved in a hydrogen bonding to an amino acid in actin or outside proteins to provide a different function of actin. Intriguingly, detailed analysis of actin filament formation using a confocal microscopy revealed that F-actins disappeared at the apical site of phenochalasin A-treated cells (Figures 4B-g and -H). Actin cytoskeleton interacts with a number of proteins such as actin related proteins (Arp2/3 *etc*) and actin accessory proteins (thymosin, profilin, formin and so on), to have diverse functions and interaction with plasma membranes (*18-20*). Therefore, it is plausible that phenochalasin A binding to G-actin affects a specific function of actin cytoskeleton, leading to blockade of lipid droplet formation in mouse macrophages. Further studies are required to clarify the mechanism of phenochalasin A.

Acknowledgements

We wish to thank Dr. Ichiji Namatame for excellent support with this work.

Funding: This research was supported by JSPS KAKENHI Grant numbers 26253009 (Grant-in-Aid for Scientific Research (A)) to HT.

Conflict of Interest: The authors have no conflicts of interest to disclose.

References

1. Tomoda H, Namatame I, Si S, Kawaguchi K, Masuma R, Namikoshi M, Omura S. Phenochalasins, inhibitors of lipid droplet formation in mouse macrophages, produced by *Phomopsis* sp. FT-0211. J Antibiot. 1999; 52:851-856.
2. Tomoda H, Namatame I, Tabata N, Kawaguchi K, Si S, Omura S. Structure elucidation of fungal phenochalasins, novel inhibitors of lipid droplet formation in mouse macrophages. J Antibiot. 1999; 52:857-861.
3. Namatame I, Tomoda H, Arai M, Omura S. Effect of fungal metabolites cytochalasans on lipid droplet formation in mouse macrophages. J Antibiot. 2000; 53:19-25.
4. Scherlach K, Boettger D, Remme N, Hertweck C. The chemistry and biology of cytochalasans. Nat Prod Rep. 2010; 27:869-886.
5. Skellam E. The biosynthesis of cytochalasans. Nat Prod Rep. 2017; 34:1252-1263.
6. Yahara I, Harada F, Sekita S, Yoshihira K, Natori S. Correlation between effects of 24 different cytochalasins on cellular structures and cellular events and those on actin *in vitro*. J Cell Biol. 1982; 92:69-78.
7. Markwell MA. A new solid-state reagent to iodinate proteins. I. Conditions for the efficient labeling of antiserum. Anal Biochem. 1982; 125:427-432.
8. Cheng H, Rudick MJ. A membrane blotting method for following the time course of protein radioiodination using Iodobeads. Anal Biochem. 1991; 198:191-193.
9. Lee DS, Griffiths BW. Comparative studies of Iodo-bead and chloramine-T methods for the radioiodination of human alpha-fetoprotein. J Immunol Methods. 1984; 74:181-189.
10. Kobayashi K, Ohte S, Ohshiro T, Ugaki N, Tomoda H. A mixture of atropisomers enhances neutral lipid degradation in mammalian cells with autophagy induction. Sci Rep. 2018; 8:12099.
11. Namatame I, Tomoda H, Arai H, Inoue K, Omura S. Complete inhibition of mouse macrophage-derived foam cell formation by triacsin C. J Biochem. 1999; 125:319-327.
12. Bligh EG, Dyer WJ. A rapid method of total lipid extraction and purification. Can J Biochem Physiol. 1959; 37:911-917.
13. Namatame I, Tomoda H, Ishibashi S, Omura S. Antiatherogenic activity of fungal beauveriolides, inhibitors of lipid droplet accumulation in macrophages. Proc Natl Acad Sci U S A. 2004; 101:737-742.
14. Ohshiro T, Kobayashi K, Ohba M, Matsuda D, Rudel LL, Takahashi T, Doi T, Tomoda H. Selective inhibition of sterol *O*-acyltransferase 1 isozyme by beauveriolide III in intact cells. Sci Rep. 2017; 7:4163.
15. Tomoda H, Namatame I, Omura S. Microbial metabolites with inhibitory activity against lipid metabolism. Proc Jpn Acad Ser B Phys Biol Sci. 2002; 78:217-240.
16. Tabas I, Zha X, Beatini N, Myers JN, Maxfield FR. The actin cytoskeleton is important for the stimulation of cholesterol esterification by atherogenic lipoproteins in macrophages. J Biol Chem. 1994; 269:22547-22556.
17. Nair UB, Joel PB, Wan Q, Lowey S, Rould MA, Trybus KM. Crystal structures of monomeric actin bound to cytochalasin D. J Mol Biol. 2008; 384:848-864.
18. Bugyi B, Carlier MF. Control of actin filament treadmilling in cell motility. Annu Rev Biophys. 2010; 39:449-470.
19. Pollard TD. Regulation of actin filament assembly by Arp2/3 complex and formins. Annu Rev Biophys Biomol Struct. 2007; 36:451-477.
20. dos Remedios CG, Chhabra D, Kekic M, Dedova IV,

Tsubakihara M, Berry DA, Nosworthy NJ. Actin binding proteins: regulation of cytoskeletal microfilaments. Physiol Rev. 2003; 83:433-473.

Received July 13, 2022; Revised August 16, 2022; Accepted August 20, 2022.

*Address correspondence to:
Taichi Ohshiro, Department of Microbial Chemistry, Graduate School of Pharmaceutical Sciences, Kitasato University, 5-9-1 Shirokane, Minato-ku, Tokyo 108-8641, Japan.
E-mail: ohshirot@pharm.kitasato-u.ac.jp

Hiroshi Tomoda, Laboratory of Drug Discovery, Graduate School of Pharmaceutical Sciences, Kitasato University, 5-9-1 Shirokane, Minato-ku, Tokyo 108-8641, Japan.
E-mail: tomodah@pharm.kitasato-u.ac.jp

Released online in J-STAGE as advance publication August 25, 2022.

Original Article

DOI: 10.5582/ddt.2022.01026

Effects of eugenol on the behavioral and pathological progression in the MPTP-induced Parkinson's disease mouse model

Urmi Vora[1], Vivek Kumar Vyas[2], Pranay Wal[3], Bhagawati Saxena[1,*]

[1] Department of Pharmacology, Institute of Pharmacy, Nirma University, Ahmedabad, India;
[2] Department of Pharmaceutical Chemistry, Institute of Pharmacy, Nirma University, Ahmedabad, India;
[3] Department of Pharmacology, Pranveer Singh Institute of Technology (Pharmacy), Kanpur, India.

SUMMARY Parkinson's disease (PD) is the world's second most common neurological disorder. Oxidative stress and neuroinflammation play a crucial role in the pathogenesis of PD. Eugenol is a phytochemical with potent antioxidant and anti-inflammatory activity. The present investigation is aimed to study the effect of eugenol in a 1-methyl-4-phenyl-1,2,3,6-tetrahydropyridine (MPTP) induced mouse model of PD and its relationship to antioxidant effect. The effects of seven days of oral pre-treatment and post-treatment with three doses of eugenol (25, 50 and 100 mg/kg/day) were investigated against the MPTP-induced PD mouse model. In addition to the assessment of behavioural parameters using various tests (actophotometer, beam walking test, catalepsy, rearing, rotarod), biochemical parameters including lipid peroxidation and reduced glutathione levels in brain tissues, were also estimated in this study. The binding mode of eugenol in the human myeloid differentiation factor-2 (*h*MD-2) was also studied. Results showed that MPTP administration in mice resulted in the development of motor dysfunction (impaired motor coordination and hypo locomotion) similar to that of PD in different behavioural studies. Pre-treatment with eugenol reversed motor dysfunction caused by MPTP administration while post-treatment with eugenol at a high dose aggravated the symptoms of akinesia associated with MPTP administration. MPTP resulted in increased lipid peroxidation while decreased reduced glutathione levels in the brains of mice. MPTP-induced increased lipid peroxidation and attenuated levels of reduced glutathione were found to be alleviated with eugenol pre-treatment while augmented with eugenol post-treatment. Eugenol showed a binding affinity of -6.897 kcal/mol against the MD2 coreceptor of toll-like receptor-4 (TLR4). Biochemical, as well as neurobehavioral studies, showed that eugenol is having a protective effect, but does not have a curative effect on PD.

Keywords Parkinson's disease, eugenol, MPTP, lipid peroxidation, reduced glutathione

1. Introduction

Parkinson's disease (PD) is the world's second most common neurodegenerative illness, with an estimated frequency of 0.1% to 0.2% (*1*). PD is affecting about 1% of adults older than sixty years of age (*2,3*). PD is mainly characterized by the depletion of dopaminergic neurons in the substantia nigra pars compacta (SNpc) region of the brain (*4,5*). Symptoms of PD involve both motor dysfunctions as well as non-motor symptoms. Motor dysfunctions include tremors, muscle rigidity, postural imbalance, bradykinesia and variable degree of cognitive impairment (*5*). The molecular mechanism for PD is still not clear but the aggregation of the presynaptic protein, α-synuclein leads to the formation of the Lewy body, which is a distinct pathological hallmark of PD (*6*). Apart from the deposition of the Lewy body, the generation of free radicals and oxidative stress plays a crucial role in the pathogenesis of PD (*7*). These generated free radicals can cause the formation of protein carbonyls, DNA damage and lipid peroxidation (*8*). Neural membranes consist of phospholipids with high content of polyunsaturated fatty acids. Lipid peroxidation results in the peroxidation of these polyunsaturated fatty acids and results in the formation of phospholipids and malondialdehyde (MDA). The earlier report shows increased lipid peroxidation activity in the PD patients (*9*).

1-Methyl-4-phenyl-1,2,3,6-tetrahydropyridine (MPTP) is a neurotoxin that causes clinical manifestations that is quite similar to PD, and it is commonly used in experimental animals as a PD model (*10,11*). It has been reported that oxidation of MPTP produces the 1-methyl-4-phenylpyridinium (MPP+) ion,

which blocks the activity of mitochondrial complex I and thus results in the generation of reactive oxygen species (ROS) (*12*).

Current therapies for PD include levodopa, dopaminergic agonists and monoamine oxidase B inhibitors, and combinations of these medications. However, with time these methods become less effective (*13*). This emphasizes the requirement for the development of novel therapeutic strategies for the management and treatment of PD. Phytochemicals having anti-oxidant and anti-inflammatory activities have been presented as a possible treatment for PD (*14*). Eugenol is chemically 4-allyl-2-methoxyphenol and is the main bioactive compound present in herbs and spices like clove, cinnamon, and nutmeg, which has strong anti-oxidants and anti-inflammatory activities (*15*). World health organization (WHO) declared eugenol as a non-mutagenic and generally recognized as a safe (GRAS) substance. Since eugenol is hydrophobic, it may easily penetrate into the brain bypassing the blood-brain barrier when consumed orally. Several *in vivo* and *in vitro* experiments have demonstrated that eugenol exerts a neuroprotective effect in many CNS disorders (*16*). Eugenol is reported to have anti-stress properties (*17*). In previously reported animal studies, eugenol was found to be protective against neurotoxicity induced by acrylamide (*18*), aluminium (*19,20*), chlorpyrifos (*21*), scopolamine (*22*), as well as 6-hydroxydopamine (*23*). In gerbils, it has also been shown to protect against ischemia-induced brain toxicity (*24*). It also prevents amyloid protein aggregation (*25*) and thus prevents symptoms associated with Alzheimer's disease in insulin and Aβ-induced rat models (*26*). Eugenol also aided functional recovery after traumatic brain injury by reducing oxidative stress and neuronal death (*27*) and is also effective against spinal cord injury in rats (*28*). The neuroprotective benefits of eugenol can be attributed in part to its anti-oxidant and anti-inflammatory characteristics. Considering the therapeutic benefits of eugenol in various studies, the objective of this research is to investigate the effect of eugenol in MPTP-induced mouse model of PD and its link to antioxidant function.

2. Materials and Methods

2.1. Chemicals

MPTP was procured by Sterling biologicals, Ahmedabad while Hank's balanced salt solution (HBSS) was obtained from Invitrogen (Thermo Fisher Scientific), Bangalore. Eugenol, 5,5-dithio-bis-(2-nitrobenzoic acid) (DTNB) (Ellman's Reagent) and thiobarbituric acid (TBA) were purchased from Sigma Aldrich (USA). Sodium dodecyl sulphate (SDS), 1,1,3,3-tetraethoxypropane (TEP), trichloroacetic acid, pyridine, n-butanol, glacial acetic acid and all additional solvents and reagents were acquired by HiMedia Laboratories Pvt. Ltd., Mumbai. Eugenol was suspended in 40% propylene glycol in phosphate buffer with pH 6.8 as it is hydrophobic. MPTP is water-soluble so it was dissolved in sterile saline.

2.2. Animals

In the present study, swiss male albino mice were used weighing 30-35 gm. This study was undertaken at the central animal house, Institute of Pharmacy, Nirma University, Ahmedabad, India. All the studies were conducted as per the national institute of health "Guide for the care and use of laboratory animals". All the experimental procedures were approved by the institutional animal ethics committee (IP/PCOL/MPH/25/2019/012).

2.3. Experimental design

This study includes the evaluation of pre-and post-treatment with eugenol (25, 50 and 100 mg/kg) against the MPTP-induced mouse model of PD. A schematic representation of the experimental design is shown in Figure 1. Eight groups of six animals each (n = 6) were formed by randomly assigning the animals to the groups. The list of groups and details of each group is mentioned below: Group I: Control (saline + no MPTP administration); Group II: MPTP; (MPTP (3 mg/kg, *i.p.*) consecutively for five days); Group III: Eug-25 + MPTP (seven days of treatment with eugenol (25 mg/kg, *p.o.*) followed by co-administration of MPTP (3 mg/kg, *i.p.*) for five days from the third day of eugenol treatment); Group IV: Eug-50 + MPTP (seven days of treatment with eugenol (50 mg/kg, *p.o.*) followed by co-administration of MPTP (3 mg/Kg, *i.p.*) for five days from the third day of eugenol treatment); Group V: Eug-100 + MPTP (seven days of treatment with eugenol (100 mg/kg, *p.o.*) followed by co-administration of MPTP (3 mg/kg, *i.p.*) for five days from the third day of eugenol treatment); Group VI: MPTP + Eug-25 (five days of treatment with MPTP (3 mg/kg, *i.p.*) followed by seven days treatment with eugenol (25 mg/kg, *p.o.*)); Group VII: MPTP + Eug-50 (five days of treatment with MPTP (3 mg/kg, *i.p.*) followed by seven days treatment with eugenol (50 mg/kg, *p.o.*)); Group VIII: MPTP + Eug-100 (five days of treatment with MPTP (3 mg/kg, *i.p.*) followed by seven days treatment with eugenol (100 mg/kg, *p.o.*)).

Lastly, behavioural parameters using various tests (actophotometer, narrow beam walking test, catalepsy bar test, cylinder test and rotarod) were estimated and then animals were sacrificed and their brain was isolated, collected and stored in -20°C cold storage. Other biochemical parameters like oxidative stress *i.e.*, lipid peroxidation and endogenous antioxidant i.e., reduced glutathione were estimated.

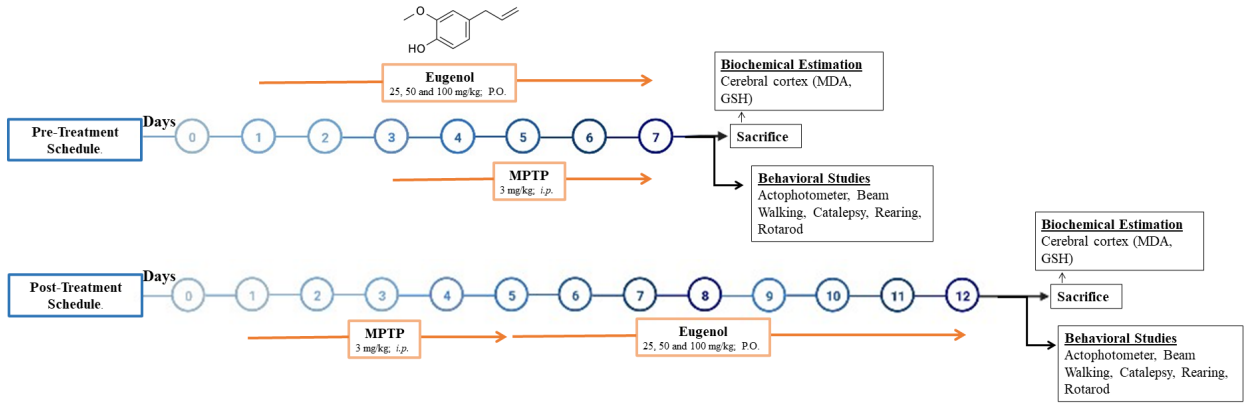

Figure 1. An illustration showing the treatment schedule and design of the study. P.O.: per oral; GSH: reduced glutathione; MDA: malondialdehyde.

2.4. Behavioral parameters

2.4.1. Actophotometer

Actophotometer is mainly used to check the locomotor activity of the rodent. Actophotometer consists of photoelectric cells coupled in a circuit with a counter. When a beam of light strikes the photoelectric cell, the circuit is complete. The animal was placed in the metal box and when it walked through it, the lights of the photocell were being cut off and then a count was recorded. All the animals were initially placed in the apparatus for five minutes for acclimatization. In the main test, mice were kept for five minutes in the apparatus and then the readings were recorded as activity scores (*29*).

2.4.2. Narrow beam-walking test

A narrow beam-walking test is a useful tool for assessing the balance and motor coordination of animals. The main objective of this technique was to monitor the functional recovery of locomotor capacity in rodents following sensorimotor cortex damage (*30,31*). The width, length and thickness of the beam were 12 mm × 50mm × 6mm. For this neurobehavioral test, the mice were placed on one end of the thin beam where they were trained to walk across the elevated beam to reach the platform on the other side of the arm. The time taken in seconds to cross the beam was noted for each animal (*32*).

2.4.3. Catalepsy bar test

Catalepsy is a condition in which an animal maintains an aberrant posture for an extended period. Catalepsy bar test is often performed in laboratory animals to investigate the effects of medications on extrapyramidal symptoms associated with PD (*33*). The catalepsy was measured using a bar test. The front paws of animals were alternately placed on a horizontal bar of 3 cm and 9 cm above and parallel to the base in this bar test. The time was recorded at which the animal removes its paw from the bar. The severity of catatonic response was observed and recorded as follows: Stage I: When a mouse is placed on a table, it moves normally, scoring 0. Stage II. The mouse starts moving only when pushed or touched, scoring 0.5. Stage III. When the front paws of the mouse are alternatively put on a 3 cm high block and the animal fails to straighten its posture after 10 seconds, give it a 0.5 for each paw and a total scoring of 1 for this level. Stage IV. When the front paws of the mouse are alternately put on a 9 cm block, the mouse fails to remove it; give it a 1 for each paw, with a total scoring of 2 for this level. Thus, the highest possible scoring for a single mouse would be 3.5, indicating complete catatonia.

2.4.4. Spontaneous forelimb elevation (cylinder) test

This test was conducted to observe the exploratory behaviour (rearing behaviour) in the subject animal. The animal was placed in a cylindrical jar in such a way that both the hind paws should be in the upright position against the wall of the cylinder. The number of rearing behaviour was observed for each animal for five minutes (*34*).

2.4.5. Rotarod

Rotarod is an apparatus that is used to check motor coordination and balance. In this test, the mice were placed on the horizontal rod that rotates about its long axis. The time taken by each of the mice to fall off was recorded. The normal mouse should remained on the rod for a long time while the mouse treated with MPTP and that showed the Parkinson's-like symptoms were fallen off from the rod as they were not able to maintain their motor coordination and balance (*35*).

2.5. Biochemical parameters

2.5.1. Evaluation of lipid peroxidation

MDA is a byproduct of lipid peroxidation

(polyunsaturated fatty acids) in cells. As a result, MDA level is a good indicator of lipid peroxidation. The amount of MDA in brain tissue was assessed as described before by Draper and Hadley (*36*) with minor modifications. The cortical area of brain tissue was weighed (100 mg). Weighted tissue was homogenized with HBSS buffer (5 mL) at 3,000 rpm in three cycles of 30 seconds each with a 30-second interval in a tube. Centrifugation of the homogenized tissue was done at 3,000 rpm for 10 minutes at 25°C. The supernatant was discarded, and the cell pellet was recovered and then mixed in tubes with 1.5 mL of acetic acid, 1.5 mL of TBA, 0.2 mL of SDS and 0.7 mL of MilliQ water. The control tubes were filled with HBSS (0.1 mL) at the place of homogenate for reference solution. For 1 hour, the tubes were immersed in boiling water. 1 mL Milli Q was added to each tube after it had boiled. Each tube received 5 mL of butanol: pyridine (15:1) solution and then vortexed for 5 minutes. The top organic layer was collected following centrifugation at 3,000 rpm for 10 minutes at 25°C. The amount of MDA generated was determined by measuring the absorbance at 532 nm of the top organic layer. MDA concentration was calculated in µM/mg of brain tissue using standard curves created by TEP.

2.5.2. Assessment of reduced glutathione

The levels of reduced glutathione were measured using Ellman (*37*) method with minor modifications. 100 mg of tissue from the cortical region of the brain was homogenized in ice-cold phosphate buffer (5 mL). The tissue homogenate was treated with 0.1 mL of trichloroacetic acid, followed by a 10 minutes centrifugation at 3,900 g at 25°C. One millilitre of supernatant was collected and then combined with one millilitre each of DTNB and phosphate buffer, vortexed for one minute, and then incubated for five minutes at room temperature. As a blank, 1 mL of DTNB was added to 2 mL of phosphate buffer. At 412 nm, both test samples and blanks were evaluated for absorbance. A standard curve was used to calculate the reduced glutathione levels and expressed as µM/mg of brain tissue.

2.6. *In silico* docking studies

Lipopolysaccharide (LPS) is activating the toll-like receptor 4 (TLR4)/myeloid differentiation factor 2 (MD-2) complex, which then activates an innate immune response. A docking study was carried out using Autodock 4.2 software (*38*). Crystal structures of *human* MD-2 (*h*MD-2) complex with antiendotoxic lipid IVa (PDB ID: 2E59) (*39*) solved at 2.21 Å resolution were downloaded from the protein data bank (PDB). Auto-dock tools (ADT) were used to prepare eugenol and *h*MD-2, all water molecules were deleted, polar hydrogen atoms were added and Kollman United Atoms charges were loaded to perform docking calculations. Co-crystalized lipid IVa was removed from the *h*MD-2 structure. A grid box was constructed at 0.375 Å spacing with grid points in xyz dimensions of 40, 44, and 35, respectively. The Lamarckian genetic algorithm was selected as the search algorithm.

2.7. Statistical analysis

Graph Pad Prism 9 was utilized for the statistical analysis. The data were analyzed by using the one-way ANOVA method followed by Tukey's multiple comparison test. Each bar in the graph represents a mean ± SEM, with each group containing 6 animals. It is statistically significant if the significance value (*p*-value) is less than 0.05.

3. Results

3.1. Eugenol improved the MPTP-induced lowered activity score of the mice in actophotometer

Figure 2 illustrates the effect of pre-and post-treatment with eugenol on the locomotor activity of mice treated with MPTP using an actophotometer. MPTP administration for five consecutive days significantly ($p < 0.05$) reduced the activity score of mice in the actophotometer. Pre-treatment with eugenol (100 mg/kg) significantly ($p < 0.05$) mitigated the MPTP-induced deterioration in the performance of mice in the actophotometer while 25 and 50 mg/kg doses of eugenol were found ineffective. On the contrary, post-treatments with 25 and 50 mg/kg doses of eugenol were not showing any significant protective effect against MPTP-induced deterioration in the locomotor activity of mice in the actophotometer. However, post-treatment

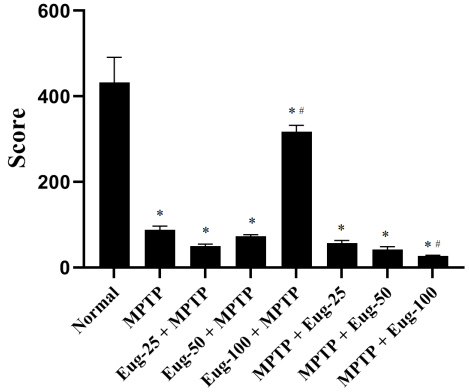

Figure 2. Effect of seven days pre- and post-treatment with eugenol on mean activity score in actophotometer apparatus against mouse model of MPTP-induced PD. Each bar represents data in mean ± SEM ($n = 6$). $^{*}p < 0.05$ compared to control and $^{\#}p < 0.05$ compared to MPTP using one-way ANOVA followed by Tukey's multiple comparisons test.

with eugenol at 100 mg/kg resulted in aggravating significantly ($p < 0.05$) the MPTP-induced deterioration in the locomotor activity of mice in the actophotometer.

3.2. Eugenol improved MPTP-induced deteriorated performance of mice on narrow beam walking test

The effect of pre-and post-treatment with eugenol on the performance of mice treated with MPTP in the narrow beam walking test is shown in Figure 3. MPTP administration for five consecutive days significantly ($p < 0.05$) increase the time taken by mice to cross the narrow beam. The oral pre-treatment with eugenol at all the doses (25, 50 and 100 mg/kg) showed a significant improvement in MPTP-induced deteriorated performance of mice in the beam-walking test. On the contrary, post-treatment with eugenol at all the doses resulted in aggravating significantly ($p < 0.05$) the MPTP-induced deterioration in the performance of mice in the beam walking test.

3.3. Effect of eugenol on motor behaviour of mice in catalepsy bar test

The effect of pre-and post-treatment with eugenol on the performance of mice treated with MPTP in the catalepsy bar test is illustrated in Figure 4. This test was mainly assessed the immobility or muscle rigidity in mice after MPTP administration for five consecutive days. MPTP administration for five consecutive days in mice significantly ($p < 0.05$) increased the catalepsy score. Pretreatment with eugenol at two doses (50 and 100 mg/kg) showed significant alleviation of MPTP-induced augmented catalepsy score while eugenol at the dose of 25 mg/kg was found ineffective. Post treatments with all the doses of eugenol (25, 50 and 100 mg/kg) were not showing any significant protective effect against MPTP-induced increase in catalepsy score in mice.

3.4. Eugenol improved MPTP-induced decreased rearing behaviour in mice

The effect of pre-and post-treatment with eugenol on the rearing behaviour of mice treated with MPTP is shown in Figure 5. This test was mainly performed to evaluate the exploratory behaviour of mice. In this study, MPTP administration for five consecutive days in mice significantly ($p < 0.05$) decreased the rearing behaviour of mice. Pre-treatment with eugenol (50 and 100 mg/kg) showed a significant increase in the MPTP-induced decrease in rearing behaviour while pre-treatment with eugenol at the dose of 25 mg/kg was not showing any improvement. Post treatments with all the doses of eugenol (25, 50 and 100 mg/kg) were not showing any significant alteration in the MPTP-induced decreased rearing behaviour in mice.

3.5. Eugenol alleviates motor incoordination of mice administered with MPTP in rotarod apparatus

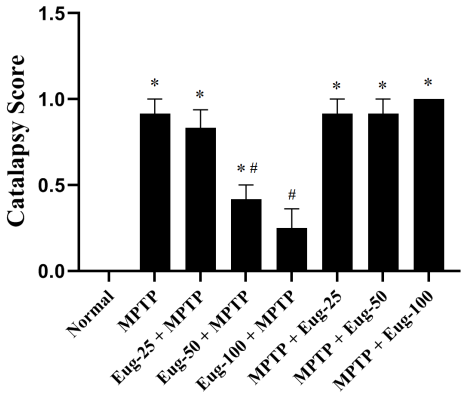

Figure 4. Effect of seven days pre and post treatment with eugenol on catalepsy behaviour against mouse model of MPTP-induced PD. Each bar represents data in mean ± SEM ($n = 6$). $^{*}p < 0.05$ compared to control and $^{\#}p < 0.05$ compared to MPTP using one-way ANOVA followed by Tukey's multiple comparisons test.

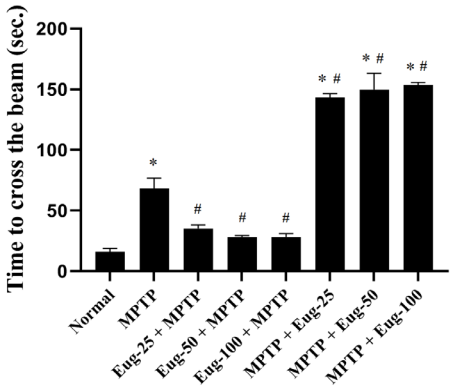

Figure 3. Effect of seven days pre- and post-treatment with eugenol on performance in beam walking test against mouse model of MPTP-induced PD. Each bar represents data in mean ± SEM ($n = 6$). $^{*}p < 0.05$ compared to control and $^{\#}p < 0.05$ compared to MPTP using one-way ANOVA followed by Tukey's multiple comparisons test.

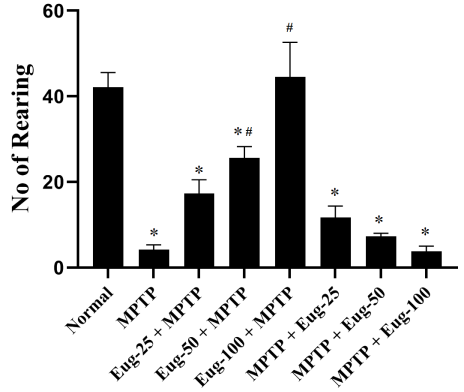

Figure 5. Effect of seven days pre and post treatment with eugenol on rearing activity against mouse model of MPTP-induced PD. Each bar represents data in mean ± SEM ($n = 6$). $^{*}p < 0.05$ compared to control and $^{\#}p < 0.05$ compared to MPTP using one way ANOVA followed by Tukey's multiple comparisons test.

Figure 6 illustrates the effect of pre-and post-treatment with eugenol on the performance of mice treated with MPTP in rotarod apparatus. This test was mainly performed to assess the motor coordination activity. MPTP treatment in mice resulted in a decrease in the fall of time in comparison to control. Thus, MPTP administration in mice caused deterioration in motor coordination. The pre-treatment with a 100 mg/kg of dose of eugenol showed a significant improvement in the motor coordination of mice in rotarod apparatus while the other two doses of eugenol (25 and 50 mg/kg) were found ineffective. On the contrary, post-treatments with the two doses of eugenol (25 and 50 mg/kg) were not showing any significant protective effect against MPTP-induced deterioration in the motor coordination activity of mice in rotarod apparatus. However, post-treatment with eugenol at 100 mg/kg resulted in aggravating significantly ($p < 0.05$) the MPTP-induced deterioration in the motor coordination of mice in rotarod apparatus.

3.6. Eugenol attenuated the MPTP-induced increased lipid peroxidation in the brain of mice

Figure 7 depicts the effect of pre-and post-treatment with eugenol on the lipid peroxidation in the brain of mice treated with MPTP. MDA is the marker of lipid peroxidation. In this study, it was observed that when compared with the control group, MPTP administration in mice augmented the MDA levels in their brain. The pre-treatment with eugenol at all the doses (25, 50 and 100 mg/kg) followed by MPTP administration reduces the MDA level when compared with the MPTP group, which indicates the neuroprotective effect of eugenol. The post-treatment group of eugenol at the dose of 100 mg/kg further increased the MDA levels in the brain of mice treated with MPTP while the two doses of post-treatment of eugenol were not showing any significant alteration.

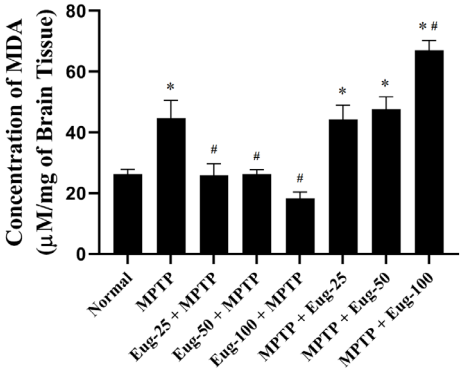

Figure 7. Effect of seven days pre and post treatment with eugenol on MDA levels against mouse model of MPTP-induced PD. Each bar represents data in mean ± SEM ($n = 6$). $^{*}p < 0.05$ compared to control and $^{\#}p < 0.05$ compared to MPTP, using one-way ANOVA followed by Tukey's multiple comparisons test.

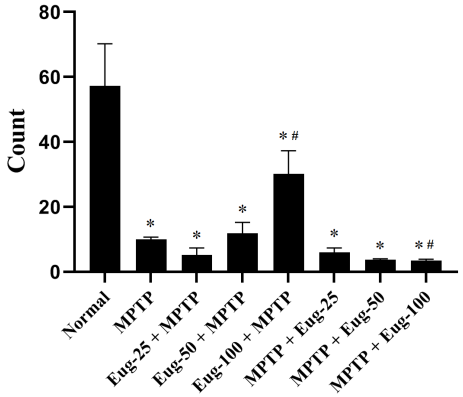

Figure 6. Effect of seven days pre and post treatment with eugenol on motor coordination in rotarod apparatus against mouse model of MPTP-induced PD. Each bar represents data in mean ± SEM ($n = 6$). $^{*}p < 0.05$ compared to control and $^{\#}p < 0.05$ compared to MPTP using one way ANOVA followed by Tukey's multiple comparisons test.

3.7. Eugenol mitigated the MPTP-induced decreased reduced glutathione in the brain of mice

The effect of pre-and post-treatment with eugenol on the reduced glutathione levels in mice treated with MPTP is shown in Figure 8. Reduced glutathione is an endogenous antioxidant. In this study, it was observed that when compared with the control group, MPTP administration in mice decreased the reduced glutathione levels in the brain. The pre-treatment with eugenol (50 and 100 mg/kg) significantly alleviated the MPTP-induced attenuated levels of reduced glutathione in the brain of mice while the dose of 25 mg/kg was found to be ineffective. The post-treatment with all the doses of eugenol were not showing any significant alteration in the MPTP-induced decreased reduced glutathione levels in the brain of mice.

3.8. *In silico* docking interactions of eugenol with TLR4

TLR4/MD-2 heterodimer complex formed *via* transport

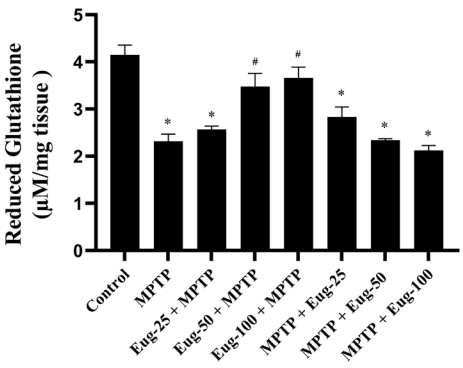

Figure 8. Effect of seven days pre and post treatment with eugenol on reduced glutathione levels against mouse model of MPTP-induced PD. Each bar represents data in mean ± SEM ($n = 6$). $^{*}p < 0.05$ compared to control and $^{\#}p < 0.05$ compared to MPTP, using one-way ANOVA followed by Tukey's multiple comparisons test.

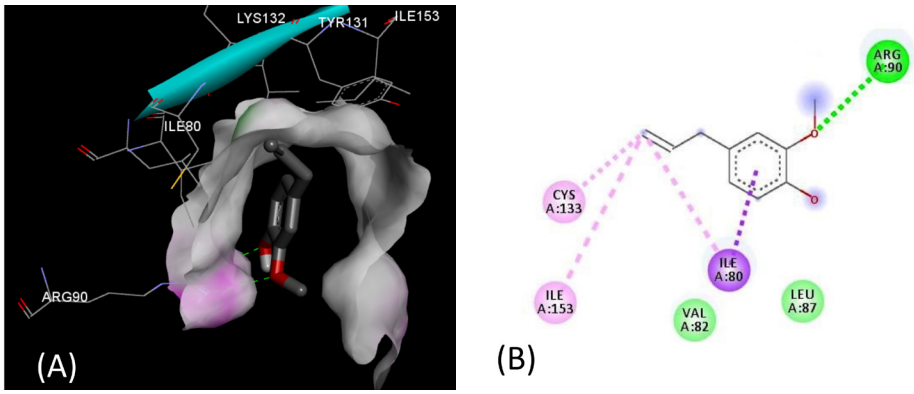

Figure 9. Binding mode of eugenol in the *h*MD-2 proposed by docking studies using AutoDock 4.2. Eugenol is in stick model with colour by atoms and labelled protein residues are capped in wireframe with colour by atom. Hydrogen bonds are shown as green dotted lines **(A)**. 2D view of interacting amino acid residues in the *h*MD-2 with eugenol **(B)**.

of LPS at MD-2 site, which activates TLR4 and its co-receptor MD-2 that will lead to activation of the intracellular signaling. The formation and activation of this complex can be prevented through the binding of an antagonist ligand to the extracellular domain, which will block further intracellular signaling events. In the absence of the X-ray structure of the *h*TLR4, we selected the crystal structure of *h*MD-2 (PDB-ID: 2E59) to study the binding of eugenol in the *h*MD-2. Eugenol showed a binding free energy value (ΔG) of -6.897 kcal/mol. Aromatic ring in eugenol showed pi-sigma interaction with Ile80, One oxygen atom of methoxy group and another oxygen atom of hydroxyl group formed conventional hydrogen bonds with Arg90, which is an important residue for binding of lipid IVa. The methylene group also showed pi-alkyl interaction with Ile153 and van dar Wall interaction with Tyr131. The overall orientation of eugenol in the binding site of *h*MD-2 is shown in Figure 9.

4. Discussion

PD is one of the most idiopathic diseases of neurodegenerative disorders, which is characterized clinically by the presence of tremor, rigidity, postural inability and bradykinesia (*40,41*). MPTP is a neurotoxin that causes clinical manifestations that is quite similar to PD, and it is commonly used in experimental animals as a PD model (*10,11*). The current investigation also reveals that MPTP administration in mice caused the neuromotor impairment in five battery tests (actophotometer, narrow beam walking test, catalepsy bar test, cylinder test and rotarod test). Pre-treatment with eugenol at 50 mg/kg and 100 mg/kg showed a significant reduction in most of the behavioural abnormalities that were observed in the MPTP-induced mouse model of PD. On the contrary, post-treatments with any of the doses of eugenol were not showing any significant protective effect against MPTP-induced Parkinson's symptoms. Moreover, post-treatment with eugenol at 100 mg/kg resulted in aggravating the Parkinson's-like symptoms (Figure 2-6).

In astrocytes, the innocuous MPTP is bio-activated to the dangerous metabolite 1-methyl-4-phenyl-pyridinium ion MPP+ by the synthesis of a dihydropyridinium intermediate by monoamine oxidase (*42*). The dihydropyridinium intermediate passes the cellular membrane easily and performs autoxidation in the extracellular area to produce superoxide anion in addition to MPP+ (*42*). MPP+ stimulates the production of ROS (*43-45*). As a result, oxidative stress is important in the pathogenesis of MPTP-induced PD, as well as the establishment and development of neurobehavioral deficits. The outcomes obtained in this study presented that MPTP administration in mice led to the augmented MDA and attenuated reduced glutathione levels in the brains. MDA is an indicator of lipid peroxidation and oxidative stress, while reduced glutathione is an endogenous antioxidant. Pre-treatment with eugenol at 50 mg/kg and 100 mg/kg significantly alleviated the MPTP-induced altered levels of MDA and reduced glutathione. Thus, pre-treatment with eugenol decreased lipid peroxidation and increased endogenous antioxidants in mice treated with MPTP. However, post-treatment with eugenol with any of the doses did not show any significant effect against MPTP induced augmented levels of MDA, as well as attenuated levels of reduced glutathione in the brain while, post-treatment with eugenol at 100 mg/kg, resulted in aggravating the MPTP-induced augmented levels of MDA in the brain. Similar types of results were depicted in the previously published work (*23,46*). Eugenol has been shown to have direct free radical scavenging properties (*47*). Hence, it appears that the beneficial impact of eugenol pre-treatment on MPTP-induced lipid peroxidation in mice brains was mediated, at least in part, by its free radical scavenging and antioxidant properties (Figure 7). Healthy mice can develop antioxidant systems such as reduced glutathione in response to the oxidative stress induced by MPTP administration. Therefore, pretreatment with eugenol can prevent MPTP-induced neurotoxicity. Damaged mice, on the other hand, have a lower tolerance for oxidative stress and are unable to build up adequate antioxidant systems.

This might make MPTP-induced oxidative stress worsened. These effects are called hormesis (*48*). Taking this statement of result into an account, it shows that the pretreatment of eugenol in a dose-dependent manner shows antioxidant activity and exerts a neuroprotective effect that will ultimately inhibit the oxidative stress while post-treatment at higher dose results in aggravating neurodegeneration. This hormesis is also seen with other phytochemicals such as Zingerone (*46,49*). These findings suggest that following the development of PD symptoms, we should avoid swallowing these spice constituents. However, for further confirmation *in vivo* work needs to be done.

Previous studies indicated that TLR4 is upregulated in the brain of MPTP-treated mice (*50,51*). Several recent pieces of literature report the TLRs as novel disease-modifying therapeutic targets in PD patients (*52-54*). Hence, targeting TLR4 for the management of neurodegenerative diseases including PD has gained a lot of attention around the world. For a better insight into the mechanism behind the anti-inflammatory activity we have docked the eugenol against the MD2 co-receptor of TLR4. Results of the present study elucidated that eugenol had a binding potential against the active site of the MD2 with a binding affinity of -6.897 kcal/mol. The important binding interactions include pi-sigma interaction between the aromatic ring of eugenol with Ile80, conventional hydrogen bonds between one oxygen atom of methoxy group and another oxygen atom of the hydroxyl group with Arg90, which is an important residue for binding of lipid IVa. The methylene group also showed pi-alkyl interaction with Ile153 and van dar Wall interaction with Tyr131 (Figure 9). A previous report showed that eugenol significantly inhibited the gene expression of TLR4 markers (*55*). Eugenol suppressed the expression of LPS-induced pro-inflammatory mediators in human macrophages (*56*) where LPS is the natural agonist of TLR4. Thus, the anti-inflammatory activity of eugenol might be partial because of its antagonistic activity at TLR4. However, this is a very preliminary finding and further *in-vitro*, as well as *in-vivo* studies, are required for confirmation.

5. Conclusion

It can be concluded from all the above-obtained results, that herbal therapy for the approach of various disease treatments can be a novel and most feasible approach. Pre-treatment of eugenol can be proved a novel herbal drug for the treatment of PD. Our *in vivo* study demonstrated that pre-treatment of eugenol can reduce behavioural impairments and improve the oxidative stress parameters as well as antioxidant mechanism. From all these findings, it is revealed that the inclusion of eugenol in the diet reduces the chances of developing Parkinson's symptoms in an elderly individual. These discoveries may encourage the food and pharmaceutical industries to develop safe and effective medicinal goods. However, still further preclinical as well as clinical studies are required to understand its molecular mechanism in detail.

Funding: This work was financially supported by Institute of Pharmacy, Nirma University, Ahmedabad.

Conflict of Interest: The authors have no conflicts of interest to disclose.

References

1. Tysnes OB, Storstein A. Epidemiology of Parkinson's disease. J Neural Transm. 2017; 124:901-905.
2. Samii A, Nutt JG, Ransom BR. Parkinson's disease. Lancet (London, England). 2004; 363:1783-1793.
3. Reeve A, Simcox E, Turnbull D. Ageing and Parkinson's disease: why is advancing age the biggest risk factor? Ageing Res Rev. 2014; 14:19-30.
4. Jankovic J. Parkinson's disease: clinical features and diagnosis. J Neurol Neurosurg psychiatry. 2008; 79:368-376.
5. Wakamatsu M, Ishii A, Iwata S, Sakagami J, Ukai Y, Ono M, Kanbe D, Muramatsu S, Kobayashi K, Iwatsubo T. Selective loss of nigral dopamine neurons induced by overexpression of truncated human α-synuclein in mice. Neurobiol Aging. 2008; 29:574-585.
6. Meade RM, Fairlie DP, Mason JM. Alpha-synuclein structure and Parkinson's disease–lessons and emerging principles. Mol Neurodegener. 2019; 14:29.
7. Bolner A, Micciolo R, Bosello O, Nordera GP. A panel of oxidative stress markers in Parkinson's disease. Clin Lab. 2016; 62:105-112.
8. Giasson BI, Ischiropoulos H, Lee VMY, Trojanowski JQ. The relationship between oxidative/nitrative stress and pathological inclusions in Alzheimer's and Parkinson's diseases. Free Radic Biol Med. 2002; 32:1264-1275.
9. Sharma A, Kaur P, Kumar B, Prabhakar S, Gill KD. Plasma lipid peroxidation and antioxidant status of Parkinson's disease patients in the Indian population. Parkinsonism Relat Disord. 2008; 14:52-57.
10. Hwang DJ, Kwon KC, Song HK, Kim KS, Jung YS, Hwang DY, Cho JY. Comparative analysis of dose-dependent neurotoxic response to 1-methyl-4-phenyl-1, 2, 3, 6-tetrahydropyridine in C57BL/6 N mice derived from three different sources. Lab Anim Res. 2019; 35:1-9.
11. Bloem BR, Irwin I, Buruma OJS, Haan J, Roos RAC, Tetrud JW, Langston JW. The MPTP model: versatile contributions to the treatment of idiopathic Parkinson's disease. J Neurol Sci. 1990; 97:273-293.
12. Gerlach M, Riederer P, Przuntek H, Youdim MBH. MPTP mechanisms of neurotoxicity and their implications for Parkinson's disease. Eur J Pharmacol Mol Pharmacol. 1991; 208:273-286.
13. Suchowersky O. Parkinson's disease: medical treatment of moderate to advanced disease. Curr Neurol Neurosci Rep. 2002; 2:310-316.
14. Koppula S, Kumar H, More SV, Lim HW, Hong SM, Choi DK. Recent updates in redox regulation and free radical scavenging effects by herbal products in experimental models of Parkinson's disease. Molecules. 2012; 17:11391-11420.
15. Barboza JN, da Silva Maia Bezerra Filho C, Silva RO,

Medeiros JVR, de Sousa DP. An overview on the anti-inflammatory potential and antioxidant profile of eugenol. Oxid Med Cell Longev. 2018; 2018:3957262.
16. Nisar MF, Khadim M, Rafiq M, Chen J, Yang Y, Wan CC. Pharmacological properties and health benefits of eugenol: A comprehensive review. Oxid Med Cell Longev. 2021; 2021:2497354.
17. Garabadu D, Shah A, Ahmad A, Joshi VB, Saxena B, Palit G, Krishnamurthy S. Eugenol as an anti-stress agent: modulation of hypothalamic-pituitary-adrenal axis and brain monoaminergic systems in a rat model of stress. Stress. 2011; 14:145-155.
18. Prasad SN. Neuroprotective efficacy of eugenol and isoeugenol in acrylamide-induced neuropathy in rats: behavioral and biochemical evidence. Neurochem Res. 2013; 38:330-345.
19. Said MM, Abd Rabo MM. Neuroprotective effects of eugenol against aluminiuminduced toxicity in the rat brain. Arh Hig Rada Toksikol. 2017; 68:27-36.
20. Mesole SB, Alfred OO, Yusuf UA, Lukubi L, Ndhlovu D. Apoptotic inducement of neuronal cells by aluminium chloride and the neuroprotective effect of eugenol in Wistar rats. Oxid Med Cell Longev. 2020; 2020:8425643.
21. Singh V, Panwar R. *In vivo* antioxidative and neuroprotective effect of 4-Allyl-2-methoxyphenol against chlorpyrifos-induced neurotoxicity in rat brain. Mol Cell Biochem. 2014; 388:61-74.
22. Garabadu D, Sharma M. Eugenol attenuates scopolamine-induced hippocampal cholinergic, glutamatergic, and mitochondrial toxicity in experimental rats. Neurotox Res. 2019; 35:848-859.
23. Kabuto H, Tada M, Kohno M. Eugenol [2-methoxy-4-(2-propenyl) phenol] prevents 6-hydroxydopamine-induced dopamine depression and lipid peroxidation inductivity in mouse striatum. Biol Pharm Bull. 2007; 30:423-427.
24. Won MH, Lee JC, Kim YH, Song DK, Suh HW, Oh YS, Kim JH, kyun Shin T, Lee YJ, Wie MB. Postischemic hypothermia induced by eugenol protects hippocampal neurons from global ischemia in gerbils. Neurosci Lett. 1998; 254:101-104.
25. Dubey K, Anand BG, Shekhawat DS, Kar K. Eugenol prevents amyloid formation of proteins and inhibits amyloid-induced hemolysis. Sci Rep. 2017; 7:40744.
26. Taheri P, Yaghmaei P, Tehrani HS, Ebrahim-Habibi A. Effects of eugenol on alzheimer's disease-like manifestations in insulin-and Aβ-induced rat models. Neurophysiology. 2019; 51:114-119.
27. Barot J, Saxena B. Therapeutic effects of eugenol in a rat model of traumatic brain injury: A behavioral, biochemical, and histological study. J Tradit Complement Med. 2021; 112007:318-327.
28. Ma L, Mu Y, Zhang Z, Sun Q. Eugenol promotes functional recovery and alleviates inflammation, oxidative stress, and neural apoptosis in a rat model of spinal cord injury. Restor Neurol Neurosci. 2018; 36:659-668.
29. Dews PB. The measurement of the influence of drugs on voluntary activity in mice. Br J Pharmacol Chemother. 1953; 8:46-48.
30. Goldstein LB, Davis JN. Beam-walking in rats: studies towards developing an animal model of functional recovery after brain injury. J Neurosci Methods. 1990; 31:101-107.
31. Lad KA, Maheshwari A, Saxena B. Repositioning of an anti-depressant drug, agomelatine as therapy for brain injury induced by craniotomy. Drug Discov Ther. 2019; 13:189-197.
32. Allbutt HN, Henderson JM. Use of the narrow beam test in the rat, 6-hydroxydopamine model of Parkinson's disease. J Neurosci Methods. 2007; 159:195-202.
33. Kulkarni SK. Hand book of experimental pharmacology. Vallabh prakashan, 1987.
34. Schallert T, Fleming SM, Leasure JL, Tillerson JL, Bland ST. CNS plasticity and assessment of forelimb sensorimotor outcome in unilateral rat models of stroke, cortical ablation, parkinsonism and spinal cord injury. Neuropharmacology. 2000; 39:777-787.
35. Shiotsuki H, Yoshimi K, Shimo Y, Funayama M, Takamatsu Y, Ikeda K, Takahashi R, Kitazawa S, Hattori N. A rotarod test for evaluation of motor skill learning. J Neurosci Methods. 2010; 189:180-185.
36. Draper HH, Hadley M. Malondialdehyde determination as index of lipid Peroxidation. Methods Enzymol. 1990; 186:421-431.
37. Ellman GL. Tissue sulfhydryl groups. Arch Biochem Biophys. 1959; 82:70-77.
38. Morris GM, Huey R, Lindstrom W, Sanner MF, Belew RK, Goodsell DS, Olson AJ. AutoDock4 and AutoDockTools4: Automated docking with selective receptor flexibility. J Comput Chem. 2009; 30:2785-2791.
39. Onto U, Fukase K, Miyake K, Satow Y. Crystal structures of human MD-2 and its complex with antiendotoxic lipid IVa. Science. 2007; 316:1632-1634.
40. Dawson TM, Dawson VL. Molecular pathways of neurodegeneration in Parkinson's disease. Science. 2003; 302:819-822.
41. Dauer W, Przedborski S. Parkinson's disease: mechanisms and models. Neuron. 2003; 39:889-909.
42. Di Monte DA, Wu EY, Irwin I, Delanney LE, Langston JW. Production and disposition of 1-methyl-4-phenylpyridinium in primary cultures of mouse astrocytes. Glia. 1992; 5:48-55.
43. Obata T, Chiueh CC. *In vivo* trapping of hydroxyl free radicals in the striatum utilizing intracranial microdialysis perfusion of salicylate: effects of MPTP, MPDP+, and MPP+. J Neural Transm Sect JNT. 1992; 89:139-145.
44. Cassarino DS, Fall CP, Smith TS, Bennett Jr JP. Pramipexole reduces reactive oxygen species production *in vivo* and *in vitro* and inhibits the mitochondrial permeability transition produced by the parkinsonian neurotoxin methylpyridinium ion. J Neurochem. 1998; 71:295-301.
45. Lotharius J, O'Malley KL. The parkinsonism-inducing drug 1-methyl-4-phenylpyridinium triggers intracellular dopamine oxidation: a novel mechanism of toxicity. J Biol Chem. 2000; 275:38581-38588.
46. Kabuto H, Yamanushi TT. Effects of zingerone [4-(4-hydroxy-3-methoxyphenyl)-2-butanone] and eugenol [2-methoxy-4-(2-propenyl) phenol] on the pathological progress in the 6-hydroxydopamine-induced parkinson's disease mouse model. Neurochem Res. 2011; 36:2244-2249.
47. Zhang LL, Zhang LF, Xu JG, Hu QP. Comparison study on antioxidant, DNA damage protective and antibacterial activities of eugenol and isoeugenol against several foodborne pathogens. Food Nutr Res. 2017; 61:1353356.
48. Calabrese V, Cornelius C, Trovato-Salinaro A, Cambria MT, Locascio MS, Rienzo LD, Condorelli DF, Mancuso C, De Lorenzo A, Calabrese EJ. The hormetic role of dietary antioxidants in free radical-related diseases. Curr Pharm

Des. 2010; 16:877-883.
49. Kabuto H, Nishizawa M, Tada M, Higashio C, Shishibori T, Kohno M. Zingerone [4-(4-hydroxy-3-methoxyphenyl)-2-butanone] prevents 6-hydroxydopamine-induced dopamine depression in mouse striatum and increases superoxide scavenging activity in serum. Neurochem Res. 2005; 30:325-332.
50. Noelker C, Morel L, Lescot T, Osterloh A, Alvarez-Fischer D, Breloer M, Henze C, Depboylu C, Skrzydelski D, Michel PP. Toll like receptor 4 mediates cell death in a mouse MPTP model of Parkinson disease. Sci Rep. 2013; 3:1393.
51. Shao Q, Chen Y, Li F, Wang S, Zhang X, Yuan Y, Chen N. TLR4 deficiency has a protective effect in the MPTP/probenecid mouse model of Parkinson's disease. Acta Pharmacol Sin. 2019; 40:1503-1512.
52. Heidari A, Yazdanpanah N, Rezaei N. The role of Toll-like receptors and neuroinflammation in Parkinson's disease. J Neuroinflammation. 2022; 19:135.
53. Chung LY, Lin YT, Liu C, Tai YC, Lin HY, Lin CH, Chen CC. Neuroinflammation upregulated neuronal Toll-like receptors 2 and 4 to drive synucleinopathy in neurodegeneration. Front Pharmacol. 2022; 13:845930.
54. Drouin-Ouellet J, St-Amour I, Saint-Pierre M, Lamontagne-Proulx J, Kriz J, Barker RA, Cicchetti F. Toll-like receptor expression in the blood and brain of patients and a mouse model of Parkinson's disease. Int J Neuropsychopharmacol. 2015; 18:pyu103.
55. Choudhury SS, Bashyam L, Manthapuram N, Bitla P, Kollipara P, Tetali SD. Ocimum sanctum leaf extracts attenuate human monocytic (THP-1) cell activation. J Ethnopharmacol. 2014; 154:148-155.
56. Lee YY, Hung SL, Pai SF, Lee YH, Yang SF. Eugenol suppressed the expression of lipopolysaccharide-induced proinflammatory mediators in human macrophages. J Endod. 2007; 33:698-702.

Received March 26, 2022; Revised July 1, 2022; Accepted August 13, 2022.

Address correspondence to:
Bhagawati Saxena, Department of Pharmacology, Institute of Pharmacy, Nirma University, S.G. Highway, Ahmedabad, 382481, India.
E-mail: bhagawati.saxena@nirmauni.ac.in

Released online in J-STAGE as advance publication August 24, 2022.

Original Article

DOI: 10.5582/ddt.2022.01046

The clinical significance of dupilumab-induced blood eosinophil elevation in Japanese patients with atopic dermatitis

Emi Tosuji, Yutaka Inaba*, Kyoko Muraoka, Kayo Kunimoto, Chikako Kaminaka, Yuki Yamamoto, Masatoshi Jinnin

Department of Dermatology, Wakayama Medical University, Wakayama, Japan.

SUMMARY This study aims to clarify the clinical significance of dupilumab-induced elevation of blood eosinophil in Japanese patients with atopic dermatitis (AD). Eosinophil elevation was defined as ≥ 5% increase of eosinophil percentage within one year after dupilumab initiation. Seven patients (15.7%) were shown to have eosinophil elevation, six of whom developed dupilumab-associated conjunctivitis (DAC) and were accompanied with DAC more frequently than those without eosinophil elevation, with statistically significant difference. Eosinophil percentage resolved spontaneously in all seven patients, including the one without DAC, despite the continuation of dupilumab treatment. None of the patients with eosinophil elevation had cardiac or pulmonary complications attributable to the hypereosinophilia. The patients with eosinophil elevation were all male. Furthermore, none of four patients in whom efficacy of dupilumab was < 25% showed eosinophil elevation. Childhood onset tended to be more common in patients with the elevation of eosinophil. This study suggests that most eosinophil elevation is associated with DAC, and that the eosinophil ratio is a biomarker for DAC.

Keywords Atopic dermatitis, eosinophil, conjunctivitis

1. Introduction

Dupilumab is a fully human monoclonal antibody against the α subunit of the IL-4 receptor (IL-4Rα), which inhibits the IL-4/13 signaling pathway. This pathway is involved in various pathological conditions of atopic dermatitis (AD) including B-cell differentiation, IgE production, activation of eosinophils, basophils, or mast cells, Th2 immune response, goblet cell metaplasia and proliferation, epidermal barrier dysfunction, and inhibition of the production of anti-microbial peptides (*1,2*).

Biologic therapies such as dupilumab inhibit specific cytokine pathways and suppress inflammation in target organs, but sometimes paradoxically induce or increase inflammation in other organs, which are called paradoxical reactions (*3*). Blood eosinophil elevation is a known adverse effect of dupilumab in patients with AD, but it has not yet been the focus of any studies. This study aims to compare the clinical characteristics of patients with AD with and without the eosinophil elevation, and to clarify its clinical significance.

2. Methods

2.1. Patients

This study was approved by the Wakayama Medical University Institutional Review Board (No.3423), and written informed consent was obtained before patients were entered into this study, in accordance with the Declaration of Helsinki.

Medical information was collected from 46 patients with AD (thirty-four males and twelve females) who were treated with dupilumab between May 2018 and February 2022 at our institute. Their clinical features are shown in Table 1.

2.2. Clinical assessment

Patients who met the previously described diagnostic criteria (*4*) and who showed the characteristic features (pruritus, eczema with typical morphology and age-specific patterns and chronic or relapsing history, xerosis, atopic predisposition such as elevated IgE, medical history of allergic diseases, and family history) were defined as having typical AD.

As in a previous study (*5*), moderate, severe, and very severe AD before dupilumab were defined by Eczema Area and Severity Index (EASI) score ≥ 7, ≥ 21.1 and ≥ 50.1, respectively. In this study, efficacy of dupilumab was evaluated by the percentage improvement in EASI scores after the treatment compared to those before the

treatment. Blood eosinophil elevation was defined as ≥ 5% increase of eosinophil percentage within one year after initiation of dupilumab without any other causes.

The diagnosis and severity of conjunctivitis was evaluated based on clinical manifestation and ophthalmologic examination.

2.3. Statistical analysis

Statistical analysis was carried out with Fisher's exact probability test (2 × 2-table) and Pearson's chi-square tests (m × n-table) to compare percentages. Mann-Whitney tests were used to compare medians between the two groups. $p < 0.05$ was considered statistically significant.

3. Results

3.1. Clinical characteristics of patients with AD in the present study

Forty-six patients (34 males and 12 females, average age of 51.3 years), were diagnosed with AD based on previously published guidelines (*4*) (Table 1). Approximately 70% of them showed typical clinical manifestation with erythema, papules, scales, lichenification-based eczema lesions, characteristic rash distribution, atopic predisposition such as elevated IgE, medical history of allergic diseases, and family history. The past history of other allergic diseases was seen in 34.8% of the patients, among which allergic rhinitis (19.6%) and asthma (23.9%) were the most frequent. The childhood onset was in 13.0% of our patients, although the onset was not recorded for 24% patients. In terms of severity of AD before dupilumab initiation, 30.4% were moderate, 54.4% were severe, and 15.2% were very severe. More than 25% efficacy of dupilumab treatment was seen in nearly 90% of the patients. These results are consistent with previous large studies published in 2021(*6*) except for the percentage of childhood onset (13.0% *vs.* 37-39% respectively).

Table 1. Summary of clinical features in AD patients treated by dupilumab (n = 46)

Age at the time of dupilumab initiation (mean years)	51.3
Sex (male)	73.9
Clinical manifestation	
typical	69.6
atypical	30.4
Past history of other allergies	34.8
bronchial asthma	19.6
allergic rhinitis	23.9
Age of onset	
childhood	13.0
adult	63.0
Severity before dupilumab initiation	
moderate	30.4
severe	54.4
very severe	15.2
Mean eosinophilic percentage before dupilumab initiation	9.8
Efficacy of dupilumab	
75-100% improvement	28.3
25-75% improvement	63.0
0-25% improvement	8.7
Adverse effects	43.5
elevation of eosinophil	15.2
conjunctivitis	28.3

Unless indicated, values are percentages.

3.2. Correlation between blood eosinophil elevation and dupilumab-associated conjunctivitis (DAC)

Clinical characteristics were compared between patients with and without blood eosinophil elevation by dupilumab treatment (Table 2). When eosinophil elevation was defined as ≥ 5% increase of eosinophil percentage within one year after dupilumab initiation, seven patients (15.7%) showed the eosinophil elevation. In these patients, there were no evidence of parasitic infections or other hematologic diseases that are known to cause eosinophil elevation.

Six of these seven patients with eosinophil elevation developed DAC, while DAC was seen in only in seven of the 39 patients without eosinophil elevation. Patients with eosinophil elevation were therefore accompanied with DAC more frequently than those without, with statistically significant difference (p = 0.00106, by Fisher's exact test, Table 3). Only one patient with eosinophil elevation did not develop DAC; the patient received chemotherapy for cutaneous squamous cell carcinoma at the same time, but no causes of the eosinophil elevation other than dupilumab treatment could be identified.

When blood eosinophil percentage was compared to severity of conjunctivitis, in three (cases 1, 5, and 6) out of the six patients, the peak of eosinophil percentage mostly coincided with the most serious DAC (Figure 1). In these three cases, the eosinophil percentage decreased and DAC improved at the same time.

Eosinophil percentage resolved spontaneously in all seven patients, including one patient without DAC, despite the continuation of dupilumab treatment. None of the patients with eosinophil elevation had cardiac or pulmonary complications attributable to the hypereosinophilia.

3.3. Correlation of blood eosinophil elevation with other clinical features

There were no significant differences between AD patients with or without eosinophil elevation in mean age, clinical manifestation, past history of other allergies, severity before dupilumab initiation, or efficacy of dupilumab. Mean eosinophil percentage before dupilumab initiation was slightly higher in patients with eosinophil elevation than in patients without elevation.

On the other hand, although not statistically

Table 2. Correlation of clinical features and blood eosinophil elevation in AD patients treated by dupilumab (n = 46)

Items	Patients with elevated eosinophil (n = 7)	Patients without elevated eosinophil (n = 39)	p value
Age at the time of dupilumab initiation	53.3	51.0	0.810
Sex (male)	100	69.2	0.101
Clinical manifestation			1.000
typical	71.4	69.2	
atypical	28.6	30.8	
Past history of other allergies	28.6	35.9	0.479
bronchial asthma	0	23.1	
allergic rhinitis	28.6	23.1	
Age of onset			0.073
childhood	71.4	28.2	
adult	14.3	46.2	
Severity before dupilumab initiation			0.302
moderate	42.8	28.2	
severe	28.6	59.0	
very severe	28.6	12.8	
Mean eosinophilic percentage before dupilumab initiation	10.3	9.7	0.711
Efficacy of dupilumab			0.500
75-100% improvement	42.9	25.6	
25-75% improvement	57.1	64.1	
0-25% improvement	0	10.3	
Adverse effects			0.00106
conjunctivitis	85.7	17.9	

Unless indicated, values are percentages.

Table 3. Comparison of prevalence of conjunctivitis between AD patients with and without blood eosinophil elevation

Items	Conjunctivitis (+)	Conjunctivitis (-)	Total	p value
Elevation (+)	6	1	7	
Elevation (-)	7	32	39	
	13	33	46	0.00106

Eosinophil elevation is defined as ≥ 5% increase of eosinophil percentage within one year after dupilumab initiation. $^{*}p < 0.05$ using Fisher's exact probability test.

significant (p = 0.101 by Fisher's exact test), the patients with eosinophil elevation were all male, while male were only 69.2% of the patients without eosinophil elevation. Furthermore, although insignificant (p = 0.500), none of four patients in whom efficacy of dupilumab was < 25% showed eosinophil elevation.

Additionally, among the patients with eosinophil elevation, the number of patients with childhood onset was five, and adult onset was one (Table 4). Among those without eosinophil elevation, however, 11 had childhood onset and 18 had adult onset. Childhood onset tended to be more common in patients with eosinophil elevation, although without significant difference (p = 0.073).

4. Discussion

Blood eosinophil elevation has been previously reported in patients with AD treated with dupilumab, but the exact percentage of AD patients with the eosinophil elevation is unclear because there is no universally-accepted definition of eosinophilia (*7*).

As the mechanism, blockage of IL-4/13 signaling by the monoclonal antibody in mouse models prevents eosinophils from invading each organ, leading to accumulation of eosinophils in the bloodstream (*8*). Conversely, blood eosinophil elevation is not observed in all AD patients treated with dupilumab, so drug-induced changes of blood eosinophil number may depend on the levels of chemokine suppression by dupilumab and the speed of eosinophil production in each patient (*7*).

In the present study, clinical characteristics were compared between seven patients with (15.2%) and 39 patients without (84.8%) elevation of blood eosinophil. The incidence of DAC was significantly higher in patients with elevation. DAC is one of the most well-known adverse events of dupilumab. The high incidence of DAC by dupilumab is notably seen only in AD, and is less common in other allergic diseases, such as asthma or nasal polyps (*9*). The mechanism of DAC remains unclear, but suppression of goblet cell proliferation and mucin secretion by dupilumab may contribute to its development (*10,11*). Katsuta *et al.* (*12*) also compared the clinical features of AD patients with and those without DAC, and described that blood eosinophil number two month after the dupilumab therapy was significantly higher in those with DAC. Consistently, in the present study, four out of the six patients with DAC also had a peak of eosinophil elevation 2-4 months after administration, and in three out of the four patients, eosinophil percentage was proportional to the activity

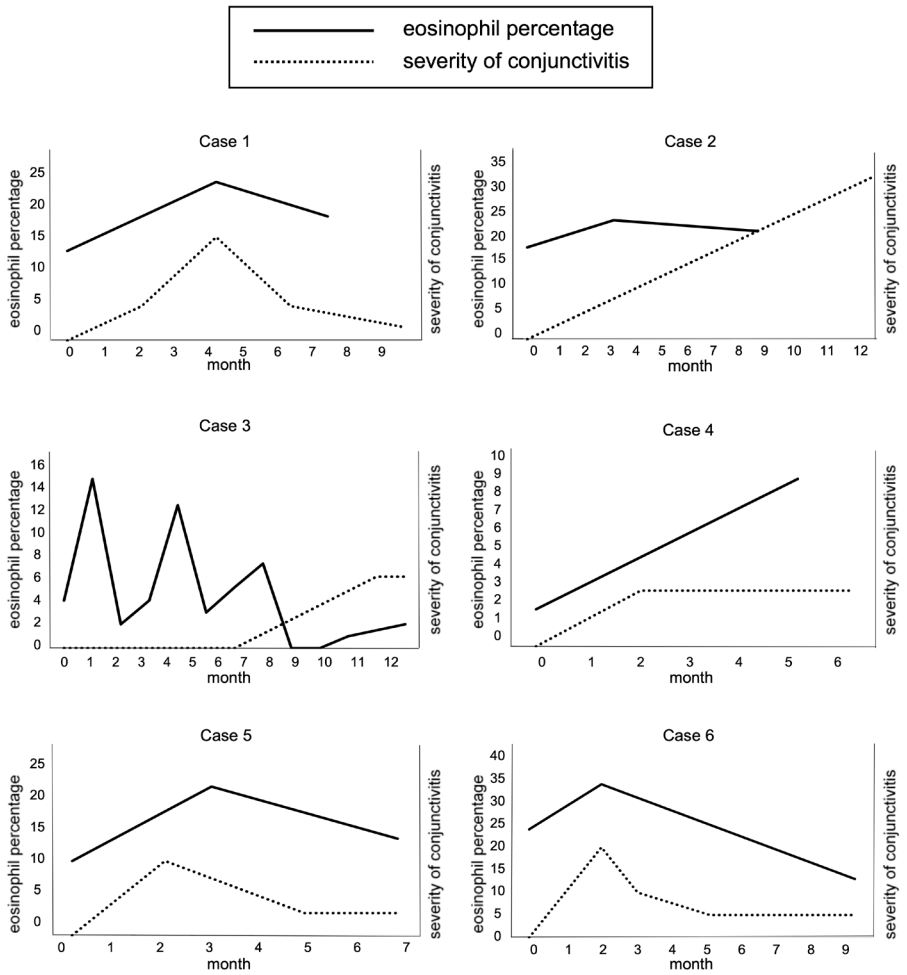

Figure 1. Correlation between eosinophil percentage and severity of conjunctivitis. Vertical axis: severity of conjunctivitis and eosinophil percentage; horizontal axis: month after dupilumab treatment. The solid and dotted lines indicate the eosinophil percentage and the severity of conjunctivitis, respectively. The results were compared for each.

Table 4. Comparison of onset age between patients with and without eosinophil elevation

Items	Childhood	Adult	Total	*p* value
Elevation (+)	5	1	6	
Elevation (-)	11	18	29	
	16	19	35	0.07

of DAC. In these three cases, maximum eosinophil percentage exceeded 20%, which was higher than the other three cases.

Taken together, this is the first report to identify the clinical characteristics of patients with AD with eosinophil elevation, and the results suggest that most eosinophil elevation may be seen in association with DAC. Blood eosinophil percentage can therefore be considered to be a predictive marker for DAC. Moreover, eosinophil elevation by dupilumab does not seem to cause organ damage, and moreover spontaneously disappears, so it is perhaps unnecessary to discontinue dupilumab.

In this study, although not significant, there were no patients showing low efficacy by dupilumab (0-25% improvement) in AD patients with blood eosinophil elevation, while such non-responder was seen only in those without eosinophil elevation. This may also be associated with the action of dupilumab to prevent migration of eosinophils from the bloodstream to the skin. We speculate, for example, that the lack of eosinophil influx into the skin tissue may attenuate the skin inflammation in patients with blood eosinophil elevation.

Similarly, although insignificant, there were more patients with childhood onset among those with eosinophil elevation, perhaps suggesting that the disease duration of AD may correlate with action of dupilumab. Compared with patients with adult-onset, for example, those with childhood onset may tend to have a longer Th2 immune response and increased eosinophil production speed in the bone marrow, resulting in the blood eosinophil elevation after dupilumab therapy. Lack of information of disease duration of several

patients in medical records was a limitation of this comparison.

In conclusion, seven patients (15.7%) among 46 patients with AD were considered to have elevation of blood eosinophil. Those with eosinophil elevation were accompanied with DAC more frequently than those without, with significant difference. Most eosinophil elevation may therefore be seen in association with DAC, and blood eosinophil percentage seems to be a predictive marker for DAC, although further studies with a greater number of patients are required.

Acknowledgements

We acknowledge editing and proofreading by Benjamin Phillis from the Clinical Study Support Center at Wakayama Medical University.

Funding: None.

Conflict of Interest: The authors have no conflicts of interest to disclose.

References

1. Iwaszko M, Biały S, Bogunia-Kubik K. Significance of interleukin (IL)-4 and IL-13 in inflammatory arthritis. Cells. 2021; 10:3000.
2. Paul WE, Zhu J. How are T(H)2-type immune responses initiated and amplified? Nat Rev Immunol. 2010; 10:225-235.
3. Ramos-Casals M, Roberto-Perez-Alvarez, Diaz-Lagares C, Cuadrado MJ, Khamashta MA, Group BS. Autoimmune diseases induced by biological agents: a double-edged sword? Autoimmun Rev. 2010; 9:188-193.
4. Eichenfield LF, Tom WL, Chamlin SL, *et al*. Guidelines of care for the management of atopic dermatitis: section 1. Diagnosis and assessment of atopic dermatitis. J Am Acad Dermatol. 2014; 70:338-351.
5. Leshem YA, Hajar T, Hanifin JM, Simpson EL. What the Eczema Area and Severity Index score tells us about the severity of atopic dermatitis: an interpretability study. Br J Dermatol. 2015; 172:1353-1357.
6. Strober B, Mallya UG, Yang M, Ganguli S, Gadkari A, Wang J, Sierka D, Delevry D, Kimball AB. Treatment outcomes associated with dupilumab use in patients with atopic dermatitis: 1-year results from the RELIEVE-AD study. JAMA Dermatol. 2022; 158:142-150.
7. Wollenberg A, Beck LA, Blauvelt A, *et al.* Laboratory safety of dupilumab in moderate-to-severe atopic dermatitis: results from three phase III trials (LIBERTY AD SOLO 1, LIBERTY AD SOLO 2, LIBERTY AD CHRONOS). Br J Dermatol. 2020; 182:1120-1135.
8. Webb DC, McKenzie AN, Koskinen AM, Yang M, Mattes J, Foster PS. Integrated signals between IL-13, IL-4, and IL-5 regulate airways hyperreactivity. J Immunol. 2000; 165:108-113.
9. Akinlade B, Guttman-Yassky E, de Bruin-Weller M, *et al*. Conjunctivitis in dupilumab clinical trials. Br J Dermatol. 2019; 181:459-473.
10. Bakker DS, Ariens LFM, van Luijk C, van der Schaft J, Thijs JL, Schuttelaar MLA, van Wijk F, Knol EF, Balak DMW, van Dijk MR, de Bruin-Weller MS. Goblet cell scarcity and conjunctival inflammation during treatment with dupilumab in patients with atopic dermatitis. Br J Dermatol. 2019; 180:1248-1249.
11. Voorberg AN, den Dunnen WFA, Wijdh RHJ, de Bruin-Weller MS, Schuttelaar MLA. Recurrence of conjunctival goblet cells after discontinuation of dupilumab in a patient with dupilumab-related conjunctivitis. J Eur Acad Dermatol Venereol. 2020; 34:e64-e66.
12. Katsuta M, Ishiuji Y, Matsuzaki H, Yasuda KI, Kharma B, Nobeyama Y, Hayashi T, Tokura Y, Asahina A. Transient increase in circulating basophils and eosinophils in dupilumab-associated conjunctivitis in patients with atopic dermatitis. Acta Derm Venereol. 2021; 101:adv00483.

Received June 10, 2022; Revised July 28, 2022; Accepted August 16, 2022.

**Address correspondence to:*
Yutaka Inaba, Department of Dermatology, Wakayama Medical University Graduate School of Medicine, 811-1 Kimiidera, Wakayama, Wakayama, 641-0012, Japan.
E-mail: ptfjk298@wakayama-med.ac.jp

Released online in J-STAGE as advance publication August 21, 2022.

Original Article

DOI: 10.5582/ddt.2022.01050

Development of a self-monitoring tool for diabetic foot prevention using smartphone-based thermography: Plantar thermal pattern changes and usability in the home environment

Qi Qin[1], Gojiro Nakagami[1,2], Yumiko Ohashi[3], Misako Dai[4], Hiromi Sanada[1,2], Makoto Oe[5,*]

[1] Department of Gerontological Nursing/Wound Care Management, Graduate School of Medicine, The University of Tokyo, Tokyo, Japan;
[2] Global Nursing Research Center, Graduate School of Medicine, The University of Tokyo, Tokyo, Japan;
[3] Nursing Department, The University of Tokyo Hospital, Tokyo, Japan;
[4] Research Center for Implementation Nursing Science Initiative, Research Promotion Headquarters, Fujita Health University, Aichi, Japan;
[5] Institute of Medical, Pharmaceutical and Health Sciences, Kanazawa University, Kanazawa, Ishikawa, Japan.

SUMMARY Thermography is a well-known risk-assessment tool for diabetic foot ulcers but is not widely used in the home setting due to the influence of the complicated home environment on thermographic images. This study investigated changes in thermographic images in complicated home environments to determine the feasibility of smartphone-based thermography in home settings. Healthy volunteers (age > 20 years) were recruited and required to take plantar thermal images using smartphone-based thermography attached to a selfie stick at different times of the day for 4 days. The thermal images and associated activities and environmental factors were then analyzed using content analysis. Areas with the highest temperature on the plantar thermal images were described and categorized. Device usability was evaluated using 10-point Likert scales, with 10 representing the highest satisfaction. A total of 140 plantar thermal images from 10 participants were analyzed. In 12 classifications, the three commonest patterns based on the highest temperature location were medial arch (42.1%), whole plantar (10.7%), and forefoot and medial arch (7.9%). The medial arch pattern is most frequently seen after awakening (67.5%) compared to other time points. Device usability was rated 7.5 out of 10 on average. This study was the first to investigate the plantar thermal patterns in the home settings, and the medial arch pattern was the most common hot area, which matches previous findings in well-controlled clinical settings. Therefore, smartphone-based thermography may be feasible as a self-assessment tool in the home setting.

Keywords Diabetic foot ulcer, home monitoring, home nursing care, prevention care, self-management

1. Introduction

The diabetic foot ulcer (DFU) is one of the major complications of diabetes. It contributes to high amputation and mortality rates, presenting an enormous economic burden, both on community as well as patients and their families (*1-3*). Interim foot self-management between regular podiatry care sessions could enable timely identification and treatment of pre-ulceration signs (*1,4,5*). Foot skin-temperature monitoring is a recommended self-management tool that has proved effective in preventing DFUs, using identification of inflammation (*6*).

Over the past two decades, many skin-temperature monitoring self-management devices have been developed, including infrared dermal thermometry (*7-12*), remote temperature monitoring systems (*13,14*), and temperature sensor devices (*15-17*). Moreover, to detect problem areas typically masked by sensory neuropathy, thermographic devices can visualize skin temperature as a map, helping patients better understand their condition and thereby improve adherence (*20,21*). However, due to stringent environmental requirements and high cost, thermography is only used for diagnostic assessment in well-controlled clinical settings (*22-24*).

Recent technological advances have facilitated the development of high-quality, clinically validated (*25,26*), inexpensive smartphone-based thermography tools. We proposed a smartphone-linked thermal imaging camera (FLIR ONE Gen 3, Teledyne FLIR LLC, Wilsonville, OR) on a selfie stick as a self-assessment tool for patients at high-risk for DFUs, testing the prototype on two older adults with diabetes. One participant found the tool difficult to use due to unfamiliarity with

smartphones. The other successfully self-assessed his plantar region, but showed no signs of inflammation during the study period (*27*). However, it is unclear as to the extent to which the usability concerns of patient 1 or their complex home environment impacted on the device's feasibility. Factors such as ambient temperature or the patient's daily activities could have affected the thermograms (*28,29*). Because localized areas of increased temperature serve as warning signs for latent inflammation (*30,31*), environmental factors may cause misclassification by creating variance in temperature readings. Therefore, understanding how the home environment could affect thermographs is necessary to better enable its use. Although previous studies classified plantar thermal patterns based on plantar angiosome types (*24,32*), and variations of plantar temperatures in post-exercise thermograms in a clinical setting (*33*), no study has investigated plantar thermal patterns in a home environment.

This study aimed to investigate thermographic changes in plantar temperature distributions in healthy participants to control for pathological variance, to determine whether the home environment affects the thermal images, to assess the feasibility of the use of the novel device, and to identify the minimal environment prerequisites for the use of thermography in the home environment. Furthermore, we investigated the usability of the modified device set.

2. Methods

2.1. Study design and participants

This study, conducted from February to March 2021, recruited healthy adult volunteers (age > 20 years) using the snowball sampling method. Individuals with a diagnosis of angiopathy or with an existing foot wound were excluded.

2.2. Study variables and measurements

The main outcomes were changes to the participants' plantar thermographs, self-obtained by using smartphone thermography devices in their home. Data on participants' baseline characteristics, thermography-related variables, and usability-related variables were collected *via* a customized self-reported questionnaire. Participant-related characteristics included age, sex, body mass index (BMI), presence of callus(es), callus site, presence of dry skin, foot deformity, foot photos, and smoking. Thermography-related variables included the characteristics of the home environment, including ambient temperature, humidity, type of floor, use of heating devices, shoe type. This also included activities undertaken immediately before thermography such as smoking, drinking, standing, sitting, and exercising. The timing of the thermographs was determined, such as after waking, after returning home, after showering or bathing, and before bed, along with main daily activities and daily steps.

Device usability was evaluated using a questionnaire for obtaining information regarding usability-related variables, such as ease of use, adherence, and their main problems with the device, on a 10-point Likert scale (score range: 0-10, with 10 indicating the highest satisfaction with the provided device set).

This study used a modified prototype set, which included an extension cord to connect the smartphone to FLIR ONE (*27*) that enabled easier control and angle adjustment during thermography (Figure 1); FLIR ONE Gen 3-IOS thermal imaging camera [FLIR® Systems, Inc.] attached to a 100-cm selfie stick [Elecom P-SSB01RWH, Elecom Co., Ltd., Osaka, Japan] and connected to a smartphone [iPhone SE 2nd generation, Apple Inc., CA, USA] with an extension cord [F.Wave concept, F.Wave Corp., Tokyo, Japan]).

Photographs of feet were taken with a digital camera (Panasonic DMC-FX70, Panasonic Corp., Osaka, Japan). Ambient temperature and humidity were measured with Tanita TT-558 GY Thermo-Hygrometer (TANITA Corp., Tokyo, Japan). Daily steps were measured with

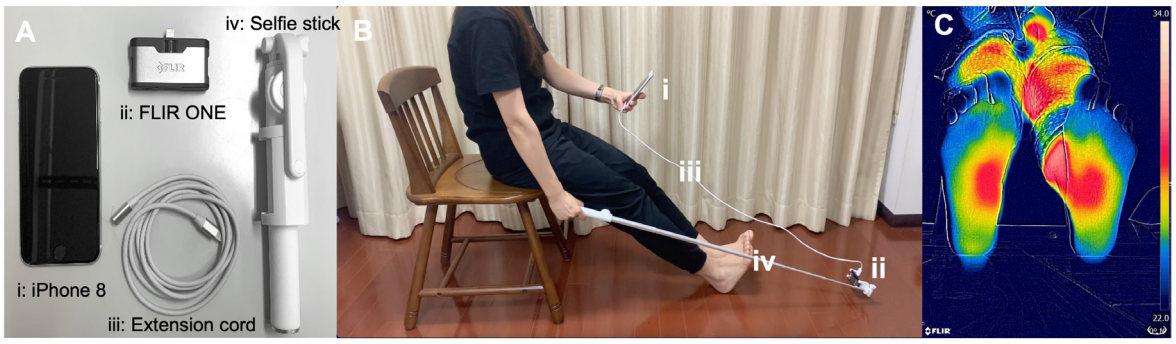

Figure 1. Demonstration of the use of the self-monitoring thermography set. The components of the set are show in picture **A**, including a smartphone (iPhone 8) (i), a smartphone-based thermography FLIR ONE (ii), an extension cord (iii) to connect the phone and the thermography, and a selfie stick (iv) to control the angle of the thermography. Picture **B** shows the demonstration of the use of the set, and the taken thermographic image (**C**).

a pedometer (OMRON HJ-325-W, Omron Co., LTD, Osaka, Japan).

2.3. Procedures

On the initial day of recruitment, all participants were given the device set and followed the researcher's instructions to practice obtaining thermographs. The researcher adjusted the distance between FLIR ONE and the plantar surface and marked the distance on the selfie sticker for participants to use as a reference when obtaining thermographs at home. Photographs of the participants' feet were taken, and the participants took the device set and instructions home for 1 week. Participants were required to use the device to take thermographs of their foot sole at home for 4 days, at least twice per day, including before going to bed and after waking up. Furthermore, they were required to fill out questionnaires that included items such as thermal image-associated home-environment and activities. After 4 days participants were asked to fill out another questionnaire on usability of the device.

2.4. Data analyses

Participant characteristics were summarized, and responses to the questionnaire on device usability were described as numbers and percentages. The acquired thermographic images were analyzed qualitatively as follows. Thermographic images were arranged on the time axis, including the home environment and physical activities, characteristics of thermographic patterns as descriptions of the plantar area with the highest temperature, activity-related events, and the home environment before obtaining the thermographic images were independently converted sequentially into text by two researchers. The content summarized by the two researchers was compared, and consensus was reached in cases of any disagreement. Then, content analysis was conducted to determine the relationship between the thermographic images and related variables. The core phrases were extracted as meaning units from the descriptive texts for each participant and summarized in a cross table. Thermographic patterns were then classified based on the connected phrases before them – namely, the time of thermography. Each connected phrase became a category of thermographic patterns. Thereafter, the frequency of each thermographic pattern was determined as numbers and percentages. The most frequently described thermographic patterns, overall and in each category, were counted as common patterns. Next, rare patterns were identified, and other environmental characteristics in addition to the aforementioned categories were searched in the raw data, summarized, and then qualitatively described as the environment to be avoided during thermography.

2.5. Ethical consideration

This study was approved by the Research Ethics Committee of the Graduate School of Medicine, The University of Tokyo, Tokyo, Japan (No. 2020275NI). Written informed consent was obtained from all participants before their enrolment in this study.

3. Results

3.1. Participant characteristics

Participant characteristics and information related to the home environment are shown in Table 1. Among the 10 participants (age 30.3 ± 5.6 years [mean ± SD]; BMI 21.06 ± 1.9 kg/m^2), four were male and six were female.

3.2. Representative case description

The changes in participants' thermal patterns over time during the survey period were verbally described as follows, with the thermographic pictures arranged on a

Table 1. Participants' characteristics and home settings

ID	Age	Sex	BMI (kg/m^2)	Presence of callus(es)	Pain on callus	Dry skin (Sole)	Foot deformity	Smoking behavior	Floor type	Indoor shoes
01	36	F	21.9	5th MTH on both feet	Painless	No	No	No	Wood	Socks or barefoot
02	23	M	19.6	1st toe, 2nd MTH on both feet	Painless	No	Hallux valgus on both feet	No	Wood	Barefoot
03	30	M	24.7	No	/	No	No	No	Wood	Barefoot
04	29	M	22.7	No	/	No	No	No	Carpet	Barefoot
05	27	M	19.8	No	/	No	No	No	Carpet	Barefoot
06	40	F	21.7	No	/	No	No	No	Wood	Barefoot
07	35	F	22.5	2nd MTH on both feet	Painless	No	Hallux valgus on left feet	No	Wood	Fluffy indoor boots
08	24	F	18.6	2nd MTH on both feet	Painless	No	No	No	Wood with heating	Barefoot
09	33	F	19.6	2nd MTH on both feet	Painless	No	Hallux valgus on both feet	No	Wood	Slippers
10	26		19.5	No	/	No	No	No	Wood	Socks and slippers

M, Male; F, Female; BMI, body mass index; MTH, metatarsal head.

time axis (Figure 2).

Case 1 was a 36-year-old female participant (BMI 21.9 kg/m^2). She had painless calluses on the lateral first toe and the 5th metatarsal head (MTH) on both feet. Her home had wooden flooring; she walked barefoot at home most of the time; and kneeled on the floor sometimes. On the first day of survey, she stayed home for remote work and mostly did desk work. She arose at 6:30 in the morning, assumed Seiza (a formal position of sitting in Japan) for 18 minutes, and then took one thermograph of her feet when she experiences feet numbness. The temperature was 13.7℃, and the humidity was 36%. Thermographs showed the highest temperatures on the midfoot and heel in both feet. She then started her day of remote work, with a daylong seminar until 5:30 pm. Most of the time, she sat on the floor with a blanket to warm her legs; ambient temperature was 16.6℃, and the humidity was 36%. The thermograph obtained after sitting the whole day showed the highest temperature in the midfoot region. She took a 15-minute bath. After the bath, the highest temperature shifted from the midfoot to forefoot region; ambient temperature was 17.0℃, and the humidity was 39%. She did some stretches after the shower and went to bed, before which she felt cold; the room temperature was 17.5℃, and the humidity was 40%. The temperature on the forefoot decreased, and the midfoot region regained the highest temperature again. She walked 1,513 steps from the time she got up until she went to sleep.

3.3. Classifications of change in thermographic images

Based on the description of highest temperature of the foot plantar aspect on the thermal images, the sites of highest temperature were separated into five areas: forefoot (toe and MTH), toe, MTH, arch, and heel; 12 types of thermal patterns were classified. The representative thermal images for each thermal pattern and the illustration for each pattern are shown in Figure 3. The patterns were named based on the combination of the highest temperature areas.

The overall pattern distributions and those at different times of the day are shown in Table 2. The top three common patterns were medial arch (42.1%), whole plantar (10.7%), and forefoot and medial arch

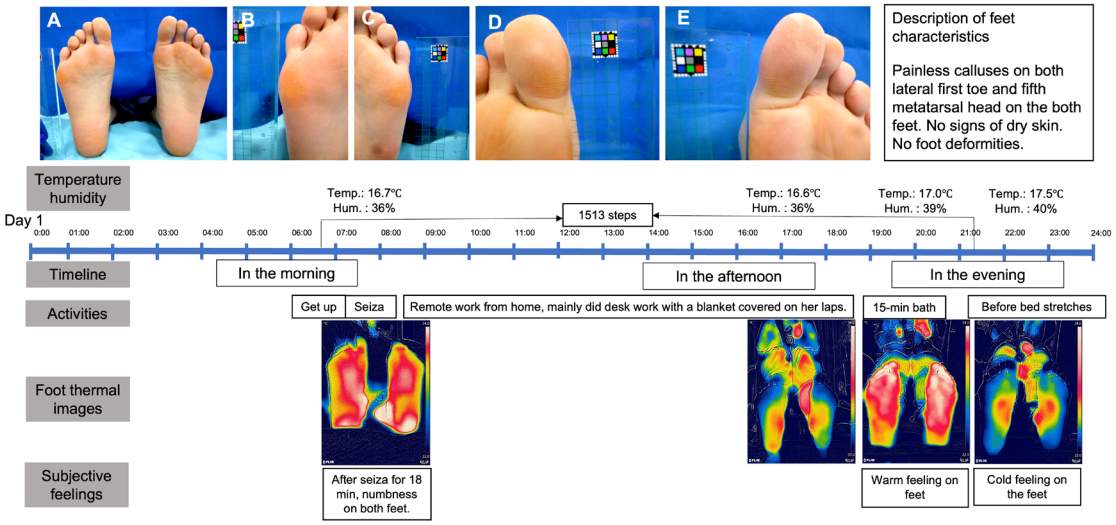

Figure 2. One example of case summary from ID1. Photos of foot plantar (**A**) and foot calluses (**B, C, D, E**) were taken before starting the survey. The descriptions of feet are shown on the right side of the foot photos. Information including temperature, time, activities before taking thermal images and subjective feelings while taking thermal images are displayed under the photos.

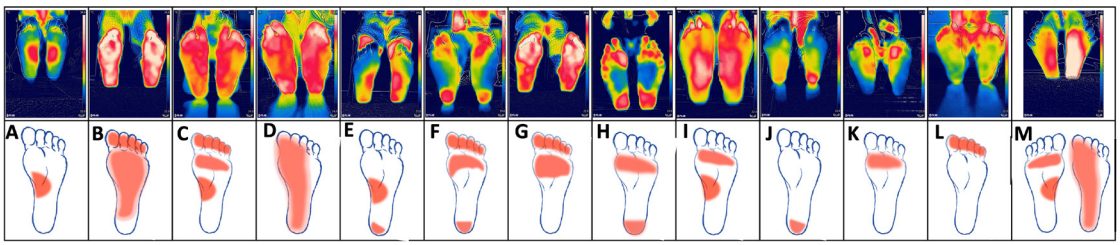

Figure 3. Representative images of thermal patterns. Patterns were named based on the highest temperature area of the plantar on the thermal images. The images on the top are representative images for each pattern, and the images on the bottoms are conceptual images where orange color indicates higher temperature. Pattern **A**: medial arch; Pattern **B**: whole plantar; Pattern **C**: forefoot and medial arch; Pattern **D**: medial plantar; Pattern **E**: medial arch and heel; Pattern **F**: forefoot and heel; Pattern **G**: forefoot; Pattern **H**: MTH (metatarsal head) and heel; Pattern **I**: MTH and medial arch; Pattern **J**: heel; Pattern **K**: MTH; Pattern **L**: toe; Pattern **M**: asymmetric.

(7.9%). Medical arch pattern was most frequently seen in the morning after getting up and staying indoors. Thermal patterns in the afternoon varied by activities. After walking, increased forefoot and medial arch (18.5%) and medial plantar (18.5) patterns were noted, whereas when remaining indoors, the medial arch had the highest temperature. In the evening, after bathing and before bed showed an increased number of whole plantar pattern (21.4%) and asymmetric patterns (22.9%).

Most of the patterns were symmetric; however, there were 16 (11.4%) asymmetric thermal images (Table 3). Half of the asymmetric thermal images were taken before bed, 18.8% were after getting up, 18% were after outdoor walking, and 12.5% were after taking a bath.

Some atypical patterns were found in different participants. A few representative thermal images are shown in Figure 4. Two were taken before bed, and one was obtained after getting up.

3.4. Results of usability evaluation

The results of questionnaires related to usability are shown in Table 4. The main problem in the use of the device set concerned the selfie stick and extension cord. One participant wrote "the selfie stick was difficult to extend". Two participants wrote "bluetooth control would be better than an extension cord". To improve adherence for self-monitoring, participants wrote "one measurement per day is preferrable", "it would be better if you can set the camera angle still because sometimes the camera angle changes easily", "having an alarm reminder would be helpful", "instead of using a selfie stick, a tripod might be better for older adults". In other suggestions, one participant wrote "being able to check on the photo prior to taking the thermograph to make sure my feet were in frame was easier. It

Table 2. Thermal pattern distribution at different times of the day

Pattern	Total	Morning N (%)	Afternoon N (%)			Evening N (%)	
		After getting up	Indoor	After outdoor walking	After biking	After bathing	Before bed
Medial arch	59 (42.1)	27 (67.5)	4 (80.0)	10 (37.0)	2 (40.0)	7 (25.0)	9 (25.7)
Whole plantar	15 (10.7)	2 (5.0)	0 (0.0)	1 (3.7)	0 (0.0)	6 (21.4)	6 (17.1)
Forefoot and medial arch	11 (7.9)	1 (2.5)	0 (0.0)	5 (18.5)	0 (0.0)	4 (14.3)	2 (5.7)
Medial plantar	8 (5.7)	3 (7.5)	0 (0.0)	5 (18.5)	0 (0.0)	0 (0.0)	0 (0.0)
Medial arch and heel	8 (5.7)	3 (7.5)	0 (0.0)	1 (3.7)	0 (0.0)	0 (0.0)	4 (11.4)
Forefoot and heel	7 (5.0)	0 (0.0)	0 (0.0)	1 (3.7)	0 (0.0)	3 (10.7)	3 (8.6)
Forefoot	6 (4.3)	0 (0.0)	0 (0.0)	1 (3.7)	2 (40.0)	3 (10.7)	0 (0.0)
MTH and heel	3 (2.1)	0 (0.0)	0 (0.0)	0 (0.0)	1 (20.0)	1 (3.6)	1 (2.9)
MTH and medial arch	2 (1.4)	1 (2.5)	0 (0.0)	0 (0.0)	0 (0.0)	1 (3.6)	0 (0.0)
Heel	2 (1.4)	0 (0.0)	0 (0.0)	0 (0.0)	0 (0.0)	0 (0.0)	2 (5.7)
MTH	2 (1.4)	0 (0.0)	0 (0.0)	0 (0.0)	0 (0.0)	1 (3.6)	0 (0.0)
Toe	1 (0.7)	0 (0.0)	1 (20.0)	0 (0.0)	0 (0.0)	0 (0.0)	0 (0.0)
Asymmetric	16 (11.4)	3 (7.5)	0 (0.0)	3 (11.1)	0 (0.0)	2 (7.1)	8 (22.9)
Total images	140 (100.0)	40 (100.0)	5 (100.0)	27 (100.0)	5 (100.0)	28 (100.0)	35(100.0)

*Number of images varies between participants. **N (%): Number (percentage of the total images). MTH: metatarsal head

Table 3. Asymmetric thermal pattern distribution at different times of the day

Items	Total	Morning N (%)	Afternoon N (%)	Evening N (%)	
		After getting up	After outdoor walking	After bathing	Before bed
Asymmetric patterns in total	16	3 (18.8)	3 (18.8)	2 (12.5)	8 (50.0)
Right medial arch and left medial arch and heel	2			1 (50)	1 (50)
Right toe and medial arch and heel and left toe and medial arch	2				2 (100)
Right medial plantar and left medial arch	1		1 (100)		
Left medial plantar	1			1 (100)	
Left medial arch and heel	1				1 (100)
Right forefoot and heel and left heel	1	1 (100)			
Left 5th MTH	1				1 (100)
Right forefoot and heel and left whole plantar	1				1 (100)
Right MTH and left medial arch	1	1 (100)			
Right forefoot and left medial arch	1	1 (100)			
Right heel	1				1 (100)
Right forefoot and left lateral plantar	1		1 (100)		
Left foot medial arch	1		1 (100)		
Right medial arch and left whole plantar	1				1 (100)

*Number of images varies between participants. **N (%): Number (percentage of the total pattern number).

Table 4. Results of questionnaires related to usability

Questions	Scores* N (%)**								
	0–2	3	4	5	6	7	8	9	10
How easy do you find this device set to use?					2 (20)	3 (30)	3 (30)	2 (20)	
Do you think you can use this device to assess your feet every day?		2 (20)	2 (20)	2 (20)	2 (20)			2 (20)	

*Scale from 0 to 10, and 10 is the highest level in satisfaction and agreement. **N (%): Number and percentage of all answers.

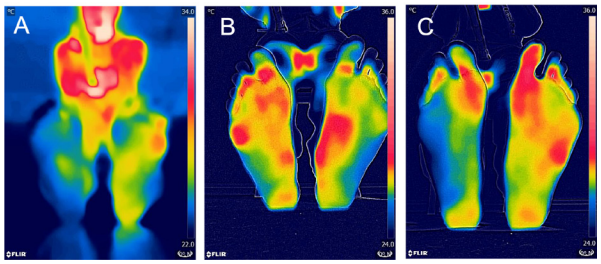

Figure 4. Atypical thermal patterns. A. thermal pattern before bed; **B.** thermal pattern after getting up; **C.** thermal pattern before bed. Thermal images are from different participants.

might be helpful for people with vision problems". All participants could use the device at least once per day during the survey (data not shown).

4. Discussion

This study is the first to investigate thermographic patterns at different times of the day in a home environment to provide information for the use of a novel self-assessment tool for people with diabetes. Thermal images from healthy participants were summarized into mainly 12 symmetric and 16 asymmetric patterns. The commonest pattern, the medial arch pattern, is mostly like to be seen immediately after getting up and indicates that the morning might be the best time for plantar self-assessment.

Thermal patterns at different times of the day and activities prior to the thermal imaging were recorded. We found that the change of thermal patterns is less likely to be affected by activities rather than the time that the thermal images were taken, and thermal patterns in the morning are most consistent compared with those at other times of the day, possibly because of skin blood-flow changes caused by activities (*28*). Skin blood flow is sufficiently relevant as one of the primary factors influencing thermography. Skin blood flow is related to the autonomic nervous system, which controls vasoconstriction and vasodilatation of the capillary vessels to maintain homeostasis. Therefore, other factors such as physical activity may directly correlate with skin blood flow (*29*). In the clinical settings, acclimation time is usually set before taking the thermal images (*31*). However, it could be difficult when considering thermography as a daily assessment tool. Therefore, thermography after getting up is associated with minimal activities, which could provide the most stable and consistent images for the evaluation of the risk of diabetic foot ulcers.

The medial arch pattern is the commonest thermal pattern, with a 42.1% of the thermographic images belonging to this category and was most frequently seen after getting up (67.5%) and staying indoors (80%). This pattern has previously been called the bilateral butterfly pattern and is considered a normal pattern that indicates an overlapping area supplied by the medial plantar and lateral plantar arteries (*34*). This butterfly pattern has been confirmed in 50% (*34*) and 46.9% (*32*) of healthy participants in two studies that investigated plantar thermographic patterns in well-controlled environments. The results suggest that thermal images obtained in the morning can obtain the same information as in a well-controlled environment (*33*).

Nonetheless, 11.4% of thermal patterns from different healthy participants were asymmetric. Asymmetric or low temperature on one side of the foot is usually an indicator of peripheral artery disease in people with diabetes (*36*). However, it was found in healthy participants in this study, which suggested that assessment based on a single thermal image is insufficient to judge the risk of DFUs; thus, assessment of plantar thermal images on a regular basis is more reliable. Assessment of a single foot might generate information bias.

Atypical thermal patterns showed a hotspot on the MTH and heel areas with asymmetric patterns. Hotspot is a sign of early inflammation, and most previous studies used algorithms that relied on a comparison between temperatures in the same region of interest, *e.g.*, MTH, on both feet (*10-13*). This study showed that, in the home environment, many patterns could be mistaken as danger signs, since they also exist in healthy participants. Certain situations should be avoided before taking a thermographic image of the soles such as immediately after waking and showering. Moreover, the algorithm for studies used thermometry, temperature sensors, and thermal mats that could not be applied to smartphone-thermography and which are easily mistaken and cause unnecessary concerns (*23*). Normal patterns are usually restored in the morning, suggesting that if a suspicious hotspot shows on the thermographic image, another one should be obtained the following morning to check whether the hotspot has disappeared. If it does disappear, then it may likely have resulted from activities rather than inflammation. If it does not disappear, then patients

could then contact health care professionals or visit them for further examination.

All participants gave a high score on the ease of using the thermography set. However, some improvement is required. Most relate to remembering to use daily and how to take a clear thermographic image. For people who do not have an ulcer, the requirement of taking daily plantar thermal images may be a burden (*37*). To improve adherence, a daily reminder seems to be an easy approach. To improve the user friendliness, personalized adjustment is needed for the use of the thermography set.

This study had several noticeable limitations. First, only 10 participants from a younger healthy population with a low BMI were included. Older adults with diabetes or higher BMI might show different thermal patterns (*24*). Second, all participants had a similar lifestyle of limited home environments and activities; accordingly, it is unclear whether people with more complicated lifestyles would have similar results; this needs to be further investigated. Finally, this study was conducted over a short time period. Therefore, the seasonal effect on the results of this study should be confirmed.

In conclusion, this study provided information for the feasibility of a novel self-assessment tool using smartphone-based thermography in the home setting. When using thermography for foot assessment in a home setting, assessment immediately after waking is the most preferred for reliable evaluation. To avoid false positives and unnecessary concerns, daily self-assessments and communication with trained healthcare professionals on abnormal patterns on consecutive days are recommended. This easy-to-use and relatively inexpensive tool may have high clinical value and help empower people with diabetes for foot self-care.

Funding: This work was supported by JSPS KAKENHI Grant Number JP 20K10780.

Conflict of Interest: The authors have no conflicts of interest to disclose.

References

1. Schaper NC, Netten JJ, Apelqvist J, Bus SA, Hinchliffe RJ, Lipsky BA. Practical guidelines on the prevention and management of diabetic foot disease (IWGDF 2019 update). Diabetes Metab Res Rev. 2020; 36:e3266.
2. Boulton AJ, Vileikyte L, Ragnarson-Tennvall G, Apelqvist J. The global burden of diabetic foot disease. Lancet. 2005; 366:1719-1724.
3. Armstrong DG, Swerdlow MA, Armstrong AA, Conte MS, Padula WV, Bus SA. Five-year mortality and direct costs of care for people with diabetic foot complications are comparable to cancer. J Foot Ankle Res. 2020; 13:2-5.
4. Rogers LC, Lavery LA, Joseph WS, Armstrong DG. All feet on deck – The role of podiatry during the COVID-19 pandemic. J Am Podiatr Med Assoc. 2020; 97:17-18.
5. Golledge J, Fernando M, Lazzarini P, Najafi B, G Armstrong D. The potential role of sensors, wearables and telehealth in the remote management of diabetes-related foot disease. Sensors (Basel). 2020; 20:4527.
6. Ena J, Carretero-Gomez J, Arevalo-Lorido JC, Sanchez-Ardila C, Zapatero-Gaviria A, Gómez-Huelgas R. The association between elevated foot skin temperature and the incidence of diabetic foot ulcers: A meta-analysis. Int J Low Extrem Wounds. 2021; 20:111-118.
7. Armstrong DG, Lavery LA. Monitoring neuropathic ulcer healing with infrared dermal thermometry. J Foot Ankle Surg. 1996; 35:335-338.
8. Armstrong DG, Lavery LA, Liswood PJ, Todd WF, Tredwell JA. Infrared dermal thermometry for the high-risk diabetic foot. Phys Ther. 1997; 77:169-177.
9. Lavery LA, Armstrong DG. Temperature monitoring to assess, predict, and prevent diabetic foot complications. Curr Diab Rep. 2007; 7:416-419.
10. Armstrong DG, Holtz-Neiderer K, Wendel C, Mohler MJ, Kimbriel HR, Lavery LA. Skin temperature monitoring reduces the risk for diabetic foot ulceration in high-risk patients. Am J Med. 2007; 120:1042-1046.
11. Skafjeld A, Iversen MM, Holme I, Ribu L, Hvaal K, Kilhovd BK. A pilot study testing the feasibility of skin temperature monitoring to reduce recurrent foot ulcers in patients with diabetes--a randomized controlled trial. BMC Endocr Disord. 2015; 15:55.
12. Lavery LA, Higgins KR, Lanctot DR, Constantinides GP, Zamorano RG, Armstrong DG, Athanasiou KA, Agrawal CM. Home monitoring of foot skin temperatures to prevent ulceration. Diabetes Care. 2004; 27:2642-2647.
13. Frykberg RG, Gordon IL, Reyzelman AM, Cazzell SM, Fitzgerald RH, Rothenberg GM, Bloom JD, Petersen BJ, Linders DR, Nouvong A, Najafi B. Feasibility and efficacy of a smart mat technology to predict development of diabetic plantar ulcers. Diabetes Care. 2017; 40:973-980.
14. Killeen AL, Brock KM, Dancho JF, Walters JL. Remote temperature monitoring in patients with visual impairment due to diabetes mellitus: A proposed improvement to current standard of care for prevention of diabetic foot ulcers. J Diabetes Sci Technol. 2020; 14:37-45.
15. Najafi B, Mohseni H, Grewal GS, Talal TK, Menzies RA, Armstrong DG. An Optical-Fiber-Based Smart Textile (Smart Socks) to manage biomechanical risk factors associated with diabetic foot amputation. J Diabetes Sci Technol. 2017; 11:668-677.
16. Reyzelman AM, Koelewyn K, Murphy M, Shen X, Yu E, Pillai R, Fu J, Scholten HJ, Ma R. Continuous temperature-monitoring socks for home use in patients with diabetes: Observational study. J Med Internet Res. 2018; 20:e12460.
17. Ming A, Walter I, Alhajjar A, Leuckert M, Mertens PR. Study protocol for a randomized controlled trial to test for preventive effects of diabetic foot ulceration by telemedicine that includes sensor-equipped insoles combined with photo documentation. Trials. 2019; 20:521.
18. Liu C, van Netten JJ, van Baal JG, Bus SA, van der Heijden F. Automatic detection of diabetic foot complications with infrared thermography by asymmetric analysis. J Biomed Opt. 2015; 20:26003.
19. Saminathan J, Sasikala M, Narayanamurthy VB, Rajesh K, Arvind R. Computer aided detection of diabetic foot ulcer using asymmetry analysis of texture and temperature

features. Infrared Phys Technol. 2020; 105:103219.
20. Shneiderman B, Plaisant C, Hesse BW. Improving healthcare with interactive visualization. Computer. 2013; 46:58-66.
21. Hazenberg CEVB, Aan de Stegge WB, Van Baal SG, Moll FL, Bus SA. Telehealth and telemedicine applications for the diabetic foot: A systematic review. Diabetes Metab Res Rev. 2020; 36:e3247.
22. Qin Q, Oe M, Ohashi Y, Shimojima Y, Imafuku M, Dai M, Nakagami G, Yamauchi T, Yeo S, Sanada H. Factors associated with the local increase of skin temperature, 'Hotspot,' of callus in diabetic foot: A cross-sectional study. J Diabetes Sci Technol. 2021:19322968211011181.
23. van Netten JJ, Prijs M, van Baal JG, Liu C, van der Heijden F, Bus SA. Diagnostic values for skin temperature assessment to detect diabetes-related foot complications. Diabetes Technol Ther. 2014; 16:714-721.
24. Renero-C FJ. The thermoregulation of healthy individuals, overweight-obese, and diabetic from the plantar skin thermogram: a clue to predict the diabetic foot. Diabet Foot Ankle. 2017; 8:1361298.
25. van Doremalen RFM, van Netten JJ, van Baal JG, Vollenbroek-Hutten MMR, van der Heijden F. Validation of low-cost smartphone-based thermal camera for diabetic foot assessment. Diabetes Res Clin Pract. 2019; 149:132-139.
26. Kanazawa T, Nakagami G, Goto T, Noguchi H, Oe M, Miyagaki T, Hayashi A, Sasaki S, Sanada H. Use of smartphone attached mobile thermography assessing subclinical inflammation: A pilot study. J Wound Care. 2016; 25:177-182.
27. Oe M, Tsuruoka K, Ohashi Y, Takehara K, Noguchi H, Mori T, Yamauchi Oe, M, Tsuruoku K, Ohash Y, Takehara K, Noguch H, Mori T, Yamauchi T, Sanada H. Prevention of diabetic foot ulcers using a smartphone and mobile thermography: a case study. J Wound Care. 2021; 30:116-119.
28. Fernández-Cuevas I, Bouzas Marins JC, Arnáiz Lastras J, Gómez Carmona PM, Piñonosa Cano S, García-Concepción MÁ, Sillero-Quintana M. Classification of factors influencing the use of infrared thermography in humans: A review. Infrared Phys Tech. 2015; 71:28-55.
29. Charkoudian N. Skin blood flow in adult human thermoregulation: How it works, when it does not, and why. Mayo Clin Proc. 2003; 78:603-612.
30. Nishide K, Nagase T, Oba M, Oe M, Ohashi Y, Iizaka S, Nakagami G, Kadowaki T, Sanada H. Ultrasonographic and thermographic screening for latent inflammation in diabetic foot callus. Diabetes Res Clin Pract. 2009; 85:304-309.
31. Oe M, Takehara K, Noguchi H, Ohashi Y, Amemiya A, Sakoda H, Suzuki R, Yamauchi T, Ueki K, Kadowaki T, Sanada H. Thermographic findings in a case of type 2 diabetes with foot ulcer due to callus deterioration. Diabetol Int. 2017; 8:328-333.
32. Nagase T, Sanada H, Takehara K, Oe M, Iizaka S, Ohashi Y, Oba M, Kadowaki T, Nakagami G. Variations of plantar thermographic patterns in normal controls and non-ulcer diabetic patients: Novel classification using angiosome concept. J Plast Reconstr Aesthet Surg. 2011; 64:860-866.
33. Wang M, Song Y, Fekete G, Gu Y. The variation of plantar temperature and plantar pressure during shod running with socks or not. J Biomim, Biomater Biomed Eng. 2018; 35:1-8.
34. Sun PC, Jao SHE, Cheng CK. Assessing foot temperature using infrared thermography. Foot Ankle Int. 2005; 26:847-853.
35. Stess RM, Sisney PC, Moss KM, Graf PM, Louie KS, Gooding GA, Grunfeld C. Use of liquid crystal thermography in the evaluation of the diabetic foot. Diabetes Care. 1986; 9:267-272.
36. Ilo A, Romsi P, Mäkelä J. Infrared thermography as a diagnostic tool for peripheral artery disease. Adv Skin Wound Care. 2020; 33:482-488.
37. Lavery LA, Higgins KR, Lanctot DR, Constantinides GP, Zamorano RG, Athanasiou KA, Armstrong DG, Agrawal CM. Preventing diabetic foot ulcer recurrence in high-risk patients: Use of temperature monitoring as a self-assessment tool. Diabetes Care. 2007; 30:14-20.

Received June 23, 2022; Revised August 1, 2022; Accepted August 19, 2022.

*Address correspondence to:
Makoto Oe, Institute of Medical, Pharmaceutical and Health Sciences, Kanazawa University, 5-11-80 Kodatsuno, Kanazawa, Ishikawa 920-0942, Japan.
E-mail: makotooe@staff.kanazawa-u.ac.jp

Released online in J-STAGE as advance publication August 25, 2022.

Original Article

DOI: 10.5582/ddt.2022.01020

Trimetazidine improves left ventricular global longitudinal strain value in patients with heart failure with reduced ejection fraction due to ischemic heart disease

Rille Puspitoadhi Harjoko[1], Mochamad Ali Sobirin[1,2,*], Ilham Uddin[1], Udin Bahrudin[1], Nani Maharani[2], Susi Herminingsih[1], Hiroyuki Tsutsui[3]

[1] Department of Cardiology and Vascular Medicine, Faculty of Medicine, Universitas Diponegoro - Dr. Kariadi General Hospital, Semarang, Indonesia;
[2] Department of Pharmacology and Therapeutics, Faculty of Medicine, Universitas Diponegoro, Indonesia;
[3] Department of Cardiovascular Medicine, Graduate School of Medical Sciences, Kyushu University, Japan.

SUMMARY Heart failure with reduced ejection fraction (HFrEF) due to ischemic heart disease (IHD) showed a progressive decline in left ventricular contractile function. However, no previous study has examined the left ventricular global longitudinal strain (LV GLS) parameter that represents LV contractile function. We investigated whether trimetazidine could improve the LV GLS value in patients with HFrEF due to IHD. We performed a double-blind, randomized controlled trial (RCT) including 26 patients with HFrEF due to stable IHD who were given modified-release trimetazidine 35 mg twice per day (n = 13) or placebo (n = 13) for 3 months in addition to standard medication. Left ventricular systolic function including GLS values was assessed at baseline and after 3 months using echocardiography. A total of 25 participants (13 control and 12 trimetazidine groups) were recruited with a baseline average age of 57.1 ± 10 years, and LV ejection fraction (LVEF) value of 34.6% ± 4.4%, and a GLS value of 7.4% ± 2.1%. Baseline clinical characteristics and echocardiogram were similar between the two groups. There was significant GLS improvement in the trimetazidine group (−6.9% ± 2.4% to −8.4% ± 2.6%, p = 0.000), but no significant differences were noted in the control group. The GLS improvement was significantly higher in the trimetazidine group than the control (1.5% + 0.9% *vs.* −0.7% + 1.7%, p = 0.001). No adverse drug reactions from the administration of trimetazidine in this study. Trimetazidine may improve GLS values in patients with HFrEF due to IHD.

Keywords Heart failure with reduced ejection fraction, ischemic heart disease, trimetazidine, global longitudinal strain, LV contractile

1. Introduction

Over the last four decades, the prevalence of heart failure with reduced ejection fraction (HFrEF) related to ischemic heart disease (IHD) has increased by 26% in men and 48% in women (*1*). Despite significant improvements in clinical symptoms and a reduced pace of clinical decline, heart failure progression has remained due to diminished contractile function. Furthermore, it is still the world's greatest cause of morbidity and mortality (*2*). Over the past few years, many studies have established metabolic remodeling as another pathophysiological mechanism of heart failure (HF) that is not widely known (*3,4*). Trimetazidine ([2,3,4-trimethoxybenzyl piperazine dihydrochloride; TMZ) is a metabolic modulator that is useful in treating HF with angina due to IHD. In addition to the treatment of angina, there is growing evidence that TMZ improves cardiac contractile function in heart failure (*5-9*). However, no study has used the global longitudinal strain (GLS) parameter to describe a better left ventricular (LV) contractile function yet. GLS is a strong predictor of mortality and morbidity of HFrEF in various etiologies including IHD and can detect improvement or decrease in contractility function earlier than other conventional echocardiographic parameters (*10-13*). This study aimed to determine whether TMZ administration can increase LV GLS values in patients with HFrEF due to IHD.

2. Materials and Methods

2.1. Research design

This study was an experimental clinical study with a

double-blind, randomized, placebo-controlled trial design conducted at Dr. Kariadi General Hospital Semarang from January to July 2020.

2.2. Research subjects

The subjects were stable patients with HFrEF due to IHD from an outpatient cardiac clinic of Dr. Kariadi General Hospital Semarang who met the inclusion and exclusion criteria and agreed to participate by signing informed consent. The study inclusion criteria were patients with functional class New York Heart Association (NYHA) I–II HFrEF with LV ejection fraction (LVEF) 20-40% of echocardiography, significant IHD evidence from previous coronary angiography examination, and/or a history of the acute coronary syndrome and/or revascularization, who received established standard medical therapy for 4 weeks before randomization. Exclusion criteria were patients who were over 75 years of age; have atrial fibrillation and severe arrhythmias, revascularization history within 60 days, primary heart valve abnormalities, Parkinson's disease, or symptoms, routinely used monoamine oxidase inhibitor drugs, and stage 4 chronic kidney disease (CKD) history; were undergoing dialysis (hemodialysis), and have inadequate echocardiographic image quality (poor echo window). The research protocol has received ethical clearance from the Ethics Commission for Health and Medical Research, Faculty of Medicine, Diponegoro University, and Dr. Kariadi General Hospital Semarang (No. 433/EC/KEPK-RSDK/2020) and a permit to conduct research from the Diklit section of Dr. Kariadi General Hospital Semarang.

2.3. TMZ drug administration

Trizedon modified-release® (MR; PT. Servier Indonesia, Tower of Kadin Indonesia 18th Floor: HR Rasuna Said Road Block X-5 Kav. 2-3, Jakarta 12950, Indonesia) was administered at a dose of 35 mg/12 h for 12 weeks (*14*). It was given with food, swallowed whole, and not chewed (*15*). TMZ adherence rate was defined as the number of doses taken during the study protocol period (12 weeks) of 85% of all TMZ treatment protocols (*16*).

2.4. Echocardiography and GLS examination of the left ventricle

Echocardiography was performed according to the standard procedure of transthoracic echocardiography examination. GLS examination was assessed using the two-dimensional (2D) speckle-tracking method by taking apical views of two, three, and four chambers at a frame rate of 40-90/s and focusing on the left ventricle. The GLS analysis was aggregated into a bull's eye pattern (17 segments), and a mean value was calculated. LV GLS was processed offline using IntelliSpace Cardiovascular version 1.2 B.V with Qlab version 11 (Phillips Medical System, Netherland). GLS was measured twice; at the beginning and end of the study at 12- week intervals, in percentage (%). The change in GLS is obtained by subtracting the final GLS value from the initial GLS value.

2.5. Statistical analysis

Data analysis includes descriptive analysis and hypothesis testing. Descriptive data will be displayed in the form of mean ± standard deviation, frequency, and percentage. The groups were compared using a two-tailed unpaired Student's *t*-test for variables with normal distribution and Wilcoxon test for variables without normal distribution. *P* values < 0.05 were considered statistically significant.

3. Results

Thirty-six subjects met the inclusion criteria. Ten patients were excluded because three had atrial fibrillation, three had CKD stage IV/V, and four underwent a revascularization procedure within 60 days. Twenty-six subjects were randomized using a random sample generator application. Subjects were divided into two groups as follows: the TMZ group with 13 subjects who received standard therapy plus TMZ 35 mg/12 h and the placebo group with 13 subjects who received standard therapy plus placebo. One patient from the TMZ group dropped out 1 week after initial treatment due to stroke, widespread infarction, decreased consciousness, severe lung infection, and sepsis in a private hospital (Figure 1).

3.1. Baseline demographics and clinical characteristics

There were no statistically significant differences in demographic characteristics between the two groups examined by gender, age, and body mass index (BMI). The median age of the participants was 54 (43-68) years old in the TMZ group and about 60 (41-66) years old in the control group ($p = 0.241$). Most subjects from both groups were men, with 11 (91.7%) samples in the TMZ group and 11 (84.6%) samples in the control group ($p = 1.000$). The mean BMIs of the participants were 25.3 ± 4.1 and 23.3 ± 3.5 kg/m^2 in the TMZ and placebo groups, respectively (Table 1).

The clinical characteristics were similar between groups as shown in Table 1. The median serum creatinine levels in the TMZ and control groups were 1.1 (0.5-1.9) and 1.1 (0.7-1.5) mg/dL ($p = 0.324$), respectively, with estimated glomerular filtration rates of 76.2 ± 38.4 and 77.7 ± 30.6 mL/min/1.73 m^2, respectively ($p = 0.914$). Most samples from both groups (76%) had a history of multivessel disease due to coronary angiography, and no substantial difference was found between the two groups. Four respondents (30.8%) in

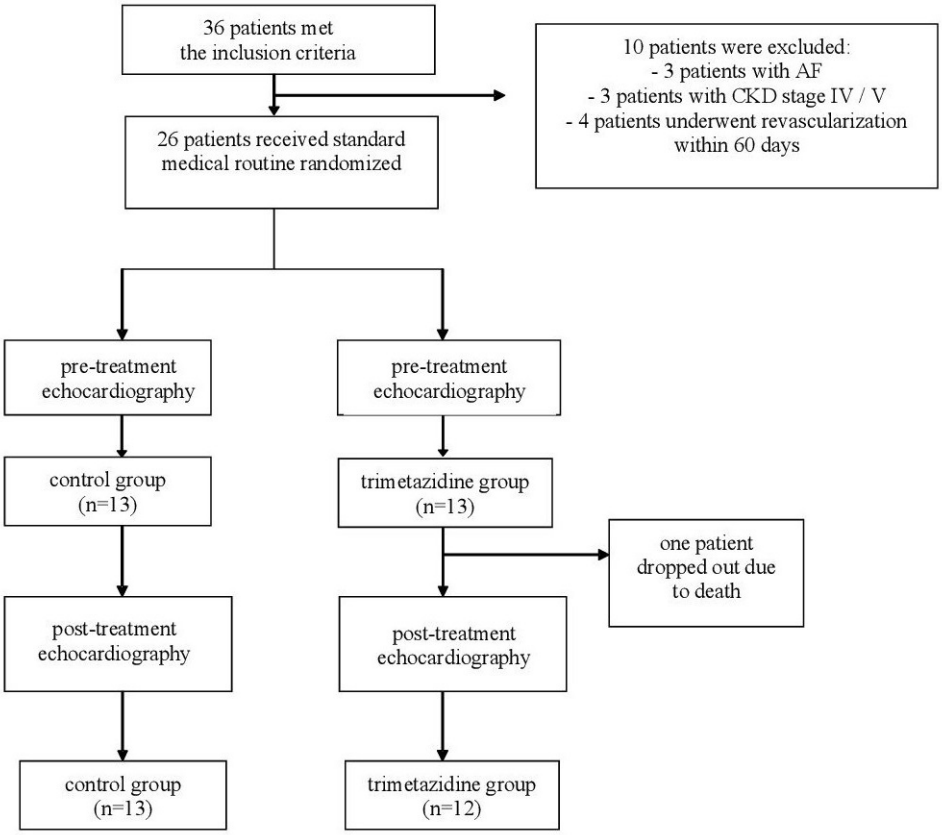

Figure 1. Participant flow. AF, atrial fibrillation; CKD, chronic kidney disease.

the control group and four respondents (33.3%) in the TMZ group underwent a complete revascularization procedure. All patients received angiotensin-converting enzyme inhibitors or angiotensin receptor blockers, beta-blockers, mineralocorticoid receptor antagonists, antiplatelets, and statins as part of the medical treatment. Other medications were calcium channel blockers (4.0%), nitrate (68%), diuretics (20%), and antidiabetic drugs (28%). There was no significant difference in medical treatment between the groups. The TMZ group received standard medical therapy plus TMZ 35 mg/12 h for 88.5 (88-90) days with an adherence rate of 99.3%. The control subjects received standard medical therapy plus a placebo for 89 (87-90) days with an adherence rate of 99.2%.

3.2. Baseline echocardiogram characteristics

Baseline echocardiographic findings were comparable between groups in 2D values and systolic and diastolic functions of the left ventricle. There were no differences in LVEF using the biplane method (LVEF Biplane; 33.3% ± 4.9% *vs.* 35.8% ± 3.5%, $p = 0.150$), GLS (−7.8% ± 1.7% *vs.* −6.9% ± 2.4%, $p = 0.280$), and LV global circumferential strain (GCS) values (−11.9% ± 4.0% *vs.* −14.4% ± 4.5%, $p = 0.150$) between the TMZ and control groups. In LV diastolic function, the E/e′ ratios of the TMZ and control groups were 16 (8.9-29.2) and 13.4 (7.0-10.2, $p = 0.355$), respectively. Left atrial volume index (LAVi) was also comparable between groups (33.7 ± 14.9 *vs.* 35.7 ± 16.1 mL/m^2, respectively; $p = 0.758$; Table 2).

3.3. Comparison of Pre- and Post-echocardiographic findings between groups

There was a significant increase in the parameters of early and late systolic functions in the TMZ group, which included LVEF, GLS, and LV GCS, whereas there was no significant difference in the control group. In the TMZ group, there were significant increases in the LV GLS (from − 6.9% ± 2.4% to − 8.4% ± 2.6%, $p = 0.001$) and GCS values (from −11.6% [−5.9% to −19.4%] to 13.9% [−8.3% to –19.7%], $p = 0.028$). The mean LVEF values increased significantly from the pre-value of 33.3% ± 4.9% to 40.3% ± 5.5% ($p = 0.000$) in the TMZ group but not significantly from a median of 36.7% (29.7%-40.0%) to 37.1% (29.5%-45.2%, $p = 0.542$) in the control group (Table 3).

There were significant differences between the initial and final diastolic function parameters in the TMZ group (E/e' ratio and LAVi), whereas there was no significant difference in the control group. The mean E/e' ratio decreased significantly in the TMZ group from 16.8 ± 6.1 to 13.5 ± 6.6 ($p = 0.046$), whereas it also decreased but not significantly in the control group from a median of

Table 1. Baseline demographic and clinical characteristics

Variables	Groups		*p*-value
	Trimetazidine (*n* = 12)	Control (*n* = 13)	
Age (years)*	54 (43-68)	60 (41–66)	0.241[a]
Sex**			
Male	11 (91.7%)	11 (84.6%)	1.000[b]
Female	1 (8.3%)	2 (15.4%)	
Body Mass Index (kg/m^2)*	25.3 ± 4.1	23.3 ± 3.5	0.195[a]
Systolic Blood Pressure (mmHg)	111.5 ± 13.5	119.4 ± 16.4	0.197[a]
Heart Rate (times/min)	71.5 ± 1.5	73.9 ± 10.8	0.634[a]
QRS complex duration (ms)	111 (96–177)	115.5 (91–140)	0.703[a]
History of Disease**			
DM	4 (33.3%)	5 (38.5%)	1.000[b]
Hypertension	5 (41.7%)	7 (53.8%)	0.551[c]
Obesity	2 (16.7%)	0 (00.0%)	0.220[b]
Acute Coronary Syndrome	7 (41.7%)	5 (38.5%)	1.000[b]
Multivessel Disease	9 (75.0%)	10 (76.9%)	1.000[b]
CTO lession	1 (8.3%)	3 (23.1%)	0.593[b]
Complete Revascularization	4 (33.3%)	4 (30.8%)	1.000[b]
Medical treatment**			
Diuretic	3 (25.0%)	2 (15.4%)	0.645[b]
ACEi/ARB	12 (100%)	13 (100%)	0.842[c]
Beta blocker	12 (100%)	13 (100%)	0.842[c]
MRA	12 (100%)	13 (100%)	0.842[c]
Nitrate	9 (75.0%)	8 (61.5%)	0.673[b]
CCB	0 (0.0%)	1 (7.7%)	1.000[b]
Ivabradine	0 (0.0%)	1 (7.7%)	1.000[b]
Digoxin	1 (8.3%)	0 (0.0%)	0.480[b]
Antiplatelet	12 (100%)	13 (100%)	0.842[c]
Statin	12 (100%)	13 (100%)	0.842[c]
Diabetes Mellitus Drugs	4 (33.3%)	3 (23.1%)	0.576[c]
Renal Function*			
Creatinine (mg/dL)	1.1 (0.5–1.9)	1.1 (0.7–1.5)	0.324[a]
eGFR (mL/min/1.73 m^2)	76.2 ± 38.4	77.7 ± 30.6	0.914[a]

*Described as mean ± standard deviation and median (min-max). **Described in *n* (%). The value is significant if $p < 0.05$. [a]Unpaired *t*-test with the alternative Mann–Whitney *U* test. [b]Fischer exact test. [c]Chi-square test. DM, diabetes mellitus; CTO, chronic total occlusion; ACEi, angiotensin-converting enzyme inhibitor; ARB, angiotensin receptor blocker; MRA, mineralocorticoid receptor antagonist; eGFR, estimated glomerular filtration rate; CCB, calcium channel blocker.

Table 2. Baseline echocardiogram characteristics

Variables	Groups		*p*-value
	Trimetazidine (*n* = 12)	Control (*n* = 13)	
Echocardiographic measurements Left ventricle dimension*			
EDV (mL)	177.0 ± 42.6	149.5 ± 37.7	0.100[a]
ESV (mL)	118.9 ± 34.2	96.9 ± 29.3	0.096[a]
EDVi (mL/m^2)	102.8 ± 26.3	95.3 ± 27.8	0.456[a]
ESVi (mL/m^2)	69.1 ± 21.0	61.8 ± 18.1	0.359[a]
Left Ventricular Systolic Function*			
LVEF (%)	33.3 ± 4.9	35.8 ± 3.5	0.150[a]
GLS (%)	– 6.9 ± 2.4	–7.8 ± 1.7	0.280[a]
GCS (%)	–11.9 ± 4.0	–14.4 ± 4.5	0.150[a]
Left Ventricular Diastolic Function*			
E/A	1.2 (0.5–3.2)	0.8 (0.6–3.6)	0.742[a]
E/e'	16 (8.9–29.2)	13.4 (7.0–10.2)	0.355[a]
LAVi (mL/m^2)	33.7 ± 14.9	35.7 ± 16.1	0.758[a]
Diastolic Dysfunction**			
Grade I	4 (33.3%)	8 (61.5%)	0.347[b]
Grade II	5 (41.7%)	2 (15.4%)	
Grade III	3 (25.0%)	3 (23.1%)	

*Described as mean ± standard deviation (intersection of deviation) and median (min-max). **Described as *n* (%). The value is significant if $p < 0.05$. [a]Unpaired *t*-test with the alternative Mann-Whitney *U* test. [b]Chi-square test. EDV, End-Diastolic Volume; ESV, End-Systolic Volume; EDVi, End-Diastolic Volume index; ESVi, End-Systolic Volume index; GLS, Global Longitudinal Strain; GCS, Global Circumferential Strain; LAVi, Left Atrial Volume index.

13.4 (7.1-30.2) to 12.6 (5.4-21.9, $p = 0.301$). There was a significant decrease in the mean LAVi value in the TMZ group from 33.7 ± 14.9 to 25.5 ± 12.2 mL/m^2 ($p = 0.049$), whereas there was no significant difference in the control group from 35.7 ± 16.1 to 36.3 ± 13.1 mL/m^2 ($p = 0.889$). There was no significant difference between the mean E/A ratio's initial and final values in the two groups (Table 3). There were significant differences between the initial and final diastolic function parameters in the TMZ group (E/e' ratio and LAVi), whereas there was no significant difference in the control group. The mean E/e' ratio decreased significantly in the TMZ group from 16.8 ± 6.1 to 13.5 ± 6.6 ($p = 0.046$), whereas it also decreased but not significantly in the control group from a median of 13.4 (7.1-30.2) to 12.6 (5.4-21.9, $p = 0.301$). There was a significant decrease in the mean LAVi value in the TMZ group from 33.7 ± 14.9 to 25.5 ± 12.2 mL/m^2 ($p = 0.049$), whereas there was no significant difference in the control group from 35.7 ± 16.1 to 36.3 ± 13.1 mL/m^2 ($p = 0.889$). There was no significant difference between the mean E/A ratio′s initial and final values in the two groups (Table 3).

3.4. Δ Changes in LV GLS and others chocardiographic parameters between TMZ and Control Group

After 3 months intervention, there were no differences in LV GLS (−8.4% ± 2.6% *vs.* −7.1% ± 1.8%, $p = 0.170$), and LV GCS (−13.8% ± 3.9% *vs.* −13.3% ± 5.5%, $p = 0.828$) and LVEF using the biplane method (40.3% ± 5.5% *vs.* 37.0% ± 5.5%, $p = 0.142$), between the TMZ and control groups as shown in Table 3.

A significant difference was noted in the change (Δ) in GLS values between the TMZ and control groups (1.5% + 0.9% *vs.* −0.7% + 1.7%, $p = 0.001$). TMZ also increased the mean LV GCS by 1.9% ($p = 0.024$) and there was a significant difference (Δ) in the mean GCS value between the TMZ and control groups (Δ 1.9 *vs.* −1.1, respectively; $p = 0.005$). Using the biplane method, significant increases were noted in the mean LVEF values of the TMZ (7.0%, $p = 0.000$) and there was a significant difference in the increase (Δ) of the mean LVEF value between the TMZ and control groups (Δ 7.0 *vs.* 1.1, respectively; $p = 0.001$) (Table 3).

There was no significant difference between TMZ and control groups in the change (Δ) of diastolic function,

Table 3. Pre-Post Echocardiographic and Δ Changes between Trimetazidine and Control groups

Variables	Mean ± SD; Median (min–max)		*p*-value
	Trimetazidine (*n* = 12)	Control (*n* = 13)	
Left Ventricular Dimension			
EDV (mL) Pre	177.0 ± 42.6	149.5 ± 37.7	0.100[d]
EDV (mL) Post	159.8 + 41.6	151.1 ± 39.2	0.594[d]
P	0.075[c]	0.824[c]	
Δ EDV	–17.2 ± 30.2	1.6 ± 26.1	0.108[d]
ESV (mL) Pre	118.9 ± 34.2	96.9 ± 29.3	0.096[d]
ESV (mL) Post	96.5 ± 30.8	96.8 ± 32.2	0.983[d]
P	0.005[c]	0.991[c]	
Δ ESV	–22.4 ± 22.4	–0.1 ± 18.2	0.012[d]
EDVi (mL/m^2) Pre	102.8 ± 26.3	95.3 ± 27.8 89 (68–142)	0.456[d]
EDVi (mL/m^2) Post	91.7 ± 21.4	97.1 ± 26.6 89 (62–143)	0.586[d]
P	0.056[c]	0,946[b]	
Δ EDVi	–11.0 ± 17.9	1.8 ± 17.9	0.008[d]
ESVi (mL/m^2) Pre	69.1 ± 21.0	61.8 ± 18.1	0.359[d]
ESVi (mL/m^2) Post	55.3 ± 16.4	62.2 ± 21.3	0.379[d]
P	0.005[c]	0.901[c]	
Δ ESVi	–13.8 ± 13.6	–0.4 ± 12.2	0.012[d]
Left Ventricular Systolic Function*			
LVEF (%) Pre	33.3 ± 4.9	35.8 ± 3.5 36.7 (29.7–40)	0.150[d]
LVEF (%) Post	40.3 ± 5.5	37.0 ± 5.5 37.1 (29.5–45.2)	0.142[d]
P	0.000[c]	0.542[b]	
Δ LVEF	7.0 ± 4.5	1.1 ± 3.1	0.001[d]
GLS (%) Pre	–6.9 ± 2.4	–7.8 ± 1.7	0.280[d]
GLS (%) Post	–8.4 ± 2.6	–7.1 ± 1.8	0.170[d]
P	0.000[c]	0.162[c]	
Δ GLS	1.5 ± 0.9	–0.7 ± 1.7	0.001[d]
GCS (%) Pre	–11.9 ± 4.0 11.6 (5.9–19.4)	–14.4 ± 4.5 13.9 (9.8–22.1)	0.150[a]
GCS (%) Post	–13.8 ± 3.9 13.9 (8.3–19.7)	–13.3 ± 5.5 10.3 (7.9–20.2)	0.828[a]
P	0.024[b]	0.175[b]	
Δ GCS	1.9 ± 2.6	–1.1 ± 2.1	0.005[a]
Left Ventricular Diastolic Function*			
E/A Pre	1.4 ± 0.9 1.2 (0.5–3.2)	1.5 ± 1.0 0.8 (0.6–3.6)	0.742[a]
E/A Post	1.4 ± 1.1	1.2 ± 0.7	0.935[d]
P	0.760[c]	0.877[c]	
Δ E/A	0.04 ± 0.5 0.1 (–0.9 to 1.0)	–0.3 ± 0.7 –0.1 (0.7 to–2.1)	0.299[a]
E/e' Pre	16.8 ± 6.1 16.1 (8.9–29.2)	14.8 ± 6.6 13.4 (7.1–30.2)	0.355[a]
E/e' Post	13.5 ± 6.6 10.0 (7.1–26.0)	13.2 ± 5.1 12.6 (5.4–21.9)	0.907[a]
P	0.046[b]	0.301[c]	
Δ E/e'	–3.3 ± 5.0 –2.2 (–13.8 to 5.6)	–1.6 ± 5.8 –1.7 (–17.6 to 7.8)	0.264[a]
LAVi (mL/m^2) Pre	33.7 ± 14.9 32.3 (9.4–56.4)	35.7 ± 16.1 33.9 (12.7–67.3)	0.758[a]
LAVi (mL/m^2) Post	25.5 ± 12.2 24.8 (12.5–50.9)	36.3 ± 13.1 33.9 (19.4–68.2)	0.041[a]
P	0.049[b]	0.889[b]	
Δ LAVi	–8.2 ± 12.9	0.6 ± 16.0	0.144[d]

Statistical analysis was performed using the [a]Mann–Whitney *U* test, [b]Wilcoxon test, [c]paired *t*-test and [d]unpaired *t*-tests. The value is significant if $p < 0.05$. SD, standard deviation; EDV, End-Diastolic Volume; ESV, End-Systolic Volume; EDVi, End-Diastolic Volume index; ESVi, End-Systolic Volume index; GLS, Global Longitudinal Strain; GCS, Global Circumferential Strain; LAVi, Left Atrial Volume index.

although in the TMZ group there were improvements in E/e' and LAVi parameters as shown in Table 3.

3.5. Intrarater and Interrater variability

Intrarater and interrater reliability of the GLS examination were analyzed by calculating the intraclass and interclass correlation coefficients. Intraclass and interclass correlation coefficients and 95% CI were

calculated using MedCalc Statistical Software version 19.1 based on the mean-rating (k = 2), absolute-agreement, and two-way mixed-effect model. Intraclass correlation coefficient = 0.991 with 95% CI = 0.978-0.997 for interrater reliability and interclass correlation coefficient = 0.982 with 95% CI = 0.954-0.993 for interrater reliability were obtained. Thus, it can be said that the interrater and interrater reliability of the GLS examination in this study is excellent.

3.6. TMZ safety

Two subjects from the control group experienced gastrointestinal side effects, including nausea, stomach pain, and vomiting. The subjects who experienced digestive system disorders had the same complaints before they participated in the study; thus, these complaints could not be ascertained to be related to the intervention conducted in this study. The patients well-tolerated this indigestion complaint. Meanwhile, in the TMZ group, no subjects complained of any side effects. There were no subjects who stopped treatment because of the complaints they felt.

4. Discussion

4.1. Effect of TMZ on the LV GLS values

The results of this study showed that administration of TMZ MR 35 mg/12 h for 3 months can improve LV contractile function with an LV GLS value parameter of 1.5% ± 0.9% (p = 0.001), followed by an increase in other contractility function parameters, including LV GCS (1.9% ± 2.6%, p = 0.005) and LVEF values (7.0 ± 4.5, p = 0.000).

Improvement of LVEF with the addition of TMZ to the standard medical procedure has been shown by previous studies. For instance, the meta-analysis of Gao *et al*. (*2*) (17 randomized clinical trials [RCTs]/n = 955) that reported that the addition of TMZ can increase weighted mean difference LVEF + 7.37% ($p < 0.01$) on IHD-induced HFrEF and the meta-analysis of Zhang *et al.* (*17*) (16 RCTs/n = 884) showed that TMZ could increase LVEF + 6.46% ($p < 0.01$).

Most studies used the LVEF parameter to represent the LV contractility function. This technique has limitations, including the determination of suboptimal endocardial margins and extensive wall motion abnormalities. Other technical challenges include geometric assumptions related to using two axes to assess LV function globally, optimal apical display alignment without foreshortening, arrhythmias, and loading-dependent factor influence on the ventricular function assessment (*10*). Given the limitations of this routine parameter, the complexity of LV's contractile function is unlikely to be comprehensively represented by the LVEF assessment method alone. GLS with 2D-speckle-tracking echocardiography is a new noninvasive method of ultrasound imaging with quantitative and objective capabilities to assess the global and regional functions of the cardiac myocardium. This modality is semi-automatic and capable of analyzing a complex cardiac mechanical system and a reproducible, angle-independent examination with no geometric assumptions and less load-dependent and of detecting early changes in myocardial contractile function and predictors of mortality and morbidity of HFrEF due to IHD (*18-20*).

Inhibition of metabolic remodeling, which includes mitochondrial dysfunction, energetic disturbances, oxidative stress, and EC coupling disorders in the myocardium, is the mechanism underlying the increase in GLS values in TMZ administration. The four components of metabolic remodeling are interrelated with structural remodeling, which underlie decreased contractility function in HFrEF. Administration of TMZ induces partial β-FA (β-ox) oxidation inhibition, increases pyruvate dehydrogenase and glucose oxidation, which is energetically beneficial in IHD (*21*), limits the accumulation of sodium, Ca^{2+}, and intracellular acidosis, reduces induced cell damage reactive oxygen species (ROS), inhibits cardiac fibrosis and inflammation through the ROS/connective tissue growth factor pathway, prevents cell apoptosis through the mitogen-activated protein kinase/ATK pathway, reduces uncoupling protein, and increases the creatinine phosphate (PCr)/adenosine triphosphate (ATP) ratio. ATP and its final effects are decreased cellular damage and repair of HF (*2*).

The TMZ mechanism improves contractility using GLS through improved mitochondrial and energetic functions. In Fragasso *et al*. study (*22*), which involved 12 patients with HFrEF due to IHD, TMZ increased the functional grade and LV function in patients with HF and increased the PCr/ATP ratio, indicating preservation of levels of noninvasive myocardial high-energy phosphate, as viewed using *in vivo* 31P magnetic resonance spectroscopy. On TMZ, the NYHA grade decreased from 3.04 ± 0.26 to 2.45 ± 0.52 ($p < 0.005$), whereas EF (34 ± 10 *vs.* 39% ± 10%, $p \leq 0.03$) and METS (from 7.44 ± 1.84 to 8.78 ± 2.72, $p < 0.03$) increased. The mean cardiac PCr/ATP ratio was 1.35 ± 0.33 with placebo but increased 33% to 1.80 ± 0.50 ($p < 0.03$) with TMZ.

The TMZ mechanism to improve LV contractility through inhibition of oxidative stress was demonstrated in the study of Belardinelli *et al.* (23). The research involved 51 patients (mean age 51.4 ± 6 years) with cardiac HF secondary to ischemic cardiomyopathy (EF 32.5% ± 4.5%), decreased plasma malondialdehyde levels (from 3.98 ± 0.69 to 2.15 ± 0.59 mmol/L), and decreased lipid hydroperoxides (from 3.72 ± 0.9 to 2.06 ± 0.6 mmol/L) versus the placebo group ($p < 0.01$), demonstrating the antioxidant properties of TMZ after 4 weeks of treatment with oral TMZ (20 mg TID). Similarly, the study of Di Napoli *et al.* (*6*), involving 61 patients with dilated ischemic cardiomyopathy, showed

that the 18-month administration of TMZ increased the mean C-reactive protein of the control group than the TMZ group ($p < 0.001$) and showed an increase in LVEF + 11% ($p < 0.001$), an improvement in NYHA, and a decrease in mean LVESV and LVEDV ($p < 0.001$) in the TMZ group ($p < 0.001$).

Another mechanism for enhancing LV contractility with TMZ was also shown in the study of Belardinelli *et al.* (*14*), which included 49 patients with ischemic cardiomyopathy and multivessel disease who received TMZ with standard HF therapy for 2 months. The sample was tested for low-dose contractile response to dobutamine, with an improvement in mean LVEF + 5.6%. This improvement is also consistent with this study in which TMZ administration of 35 mg/12 h for 3 months significantly increased GLS values in HFrF by 1.5% ± 0.9% ($p = 0.001$) due to IHD for 3 months.

Another finding of this study, besides the improvement in LV systolic function, is the increase in diastolic function after 3 months of TMZ administration. IHD and severe LV dysfunction altered the diastolic function and progressively decreased LV compliance and increased left atrial pressure and LV filling pressure at the diastolic as assessed by the parameters recommended by the 2016 American Society of Echocardiography guidelines for diastolic dysfunction assessment (*24*). This effect on TMZ's LV diastolic function may also be related to TMZ's metabolic anti-ischemic effect in the myocardium undergoing chronic hypoperfusion. Improvements in diastolic function due to the addition of TMZ in ischemic cardiomyopathy have been shown in the study of Vitale *et al.* (*25*), which showed that adding TMZ to standard therapy for 6 months improved diastolic function as assessed by mitral flow doppler analysis with echocardiography, in addition to improving LVEF.

The clinical importance of GLS improvement after TMZ administration to HFrEF was demonstrated in the study of Sengeløv *et al*. (*13*), which involved 1,065 HFrEF patients and showed that GLS remains an independent predictor of all-cause mortality in a multivariable model after adjusting for age, sex, BMI, total cholesterol, mean arterial pressure, heart rate, ischemic cardiomyopathy, percutaneous transluminal coronary angioplasty, Cardiac bypass surgery, noninsulin-dependent diabetes mellitus, and conventional echocardiographic parameters (hazard ratio [HR]: 1.15; 95% CI 1.04-1.27, $p = 0.008$ per 1% decrease). No other echocardiographic parameters remained independent predictors after adjusting for these variables. This study is the first double-blind RCT that evaluated the effect of TMZ on LV contractile function with the GLS value parameter in patients with HFrEF due to IHD. The results of this study indicate that TMZ can improve LV systolic function as assessed by the LV GLS value and is clinically significant because each reduction in GLS value is 1% (HR: 1.15; 95% CI 1.04-1.27, $p = 0.008$).

4.2. Adherence to drugs and side effects of TMZ

In this study, TMZ was relatively safe and well-tolerated in patients with HFrEF, which can be seen from the compliance level, with 99.3% TMZ at a median of 88.5 (88-90) days of taking medication. During the study period, no allergies or serious side effects were reported by the TMZ administration. None of the patients discontinued the TMZ drug. This safety is relevant to various previous studies, which also stated that TMZ is safe enough to be given to HFrEF sufferers due to IHD even for a longer period (*2,26-27*).

4.3. Research limitations

This study assessed the short-term effect (3 months) of TMZ on echocardiographic parameters alone and did not assess other clinical outcome parameters such as exercise capacity, major cardiovascular events, and HF hospitalization incidence. Additionally, most standard HF treatments of the subjects could not achieve the maximum recommended daily dose target guidelines for HF.

5. Conclusion

TMZ may improve the LV contractile function in patients with HFrEF due to IHD using the LV GLS value.

Funding: This work was supported by a grant from Universitas Diponegoro in International Publication Research Scheme No: 474-72/UN7.P4.3/PP/2019.

Conflict of Interest: The authors have no conflicts of interest to disclose.

References

1. Čelutkienė J, Balčiūnas M, Kablučko D, Vaitkevičiūtė L, Blaščiuk J, Danila E. Challenges of treating acute heart failure in patients with chronic obstructive pulmonary disease. Card Fail Rev. 2017; 3:56-1.
2. Gao D, Ning N, Niu X, Hao G, Meng Z. Trimetazidine: A meta-analysis of randomized controlled trials in heart failure. Heart.2011; 97:278-86.
3. Nickel A, Löffler J, Maack C. Myocardial energetics in heart failure. Basic Res Cardiol. 2013; 108:358.
4. Bertero E, Maack C. Metabolic remodelling in heart failure. Nat Rev Cardiol. 2018; 15:457-470.
5. Knuuti J, Wijns W, Saraste A, *et al*. ESC Guidelines for the diagnosis and management of chronic coronary syndromes. Eur Heart J. 2019; 2019:1-71.
6. Di Napoli P, Taccardi AA, Barsotti A. Long term cardioprotective action of trimetazidine and potential effect on the inflammatory process in patients with ischaemic dilated cardiomyopathy. Heart. 2005; 91:161-165.
7. Tuunanen H, Engblom E, Naum A, Någren K, Scheinin M, Hesse B, Juhani Airaksinen KE, Nuutila P, Iozzo P, Ukkonen H, Opie LH, Knuuti J. Trimetazidine, a

metabolic modulator, has cardiac and extracardiac benefits in idiopathic dilated cardiomyopathy. Circulation. 2008; 118:1250-1258.
8. Lopatin YM, Rosano GM, Fragasso G, Lopaschuk GD, Seferovic PM, Gowdak LH, Vinereanu D, Hamid MA, Jourdain P, Ponikowski P. Rationale and benefits of trimetazidine by acting on cardiac metabolism in heart failure. Int J Cardiol. 2016; 203:909-915.
9. Fragasso G, Palloshi A, Puccetti P, Silipigni C, Rossodivita A, Pala M, Calori G, Alfieri O, Margonato A. A randomized clinical trial of trimetazidine, a partial free fatty acid oxidation inhibitor, in patients with heart failure. A randomized clinical trial of trimetazidine, a partial free fatty acid oxidation inhibitor, in patients with heart failure. J Am Coll Cardiol. 2006; 48:992-998.
10. Luis SA, Chan J, Pellikka PA. Echocardiographic assessment of left ventricular systolic function: An overview of contemporary techniques, including speckle-tracking echocardiography. Mayo Clin Proc. 2019; 94:125-138.
11. Stanton T, Leano R, Marwick TH. Prediction of all-cause mortality from global longitudinal speckle strain: Comparison with ejection fraction and wall motion scoring. Circ Cardiovasc Imaging. 2009; 2:356-364.
12. Cho GY, Marwick TH, Kim HS, Kim MK, Hong KS, Oh DJ. Global 2-Dimensional strain as a New Prognosticator in Patients With Heart Failure. J Am Coll Cardiol. 2009; 54:618-624.
13. Sengeløv M, Jørgensen PG, Jensen JS, Bruun NE, Olsen FJ, Fritz-Hansen T, Nochioka K, Biering-Sørensen T. Global longitudinal strain is a superior predictor of all-cause mortality in heart failure with reduced ejection fraction. JACC Cardiovasc Imaging. 2015; 8:1351-1359.
14. Belardinelli R, Purcaro A. Effects of trimetazidine on the contractile response of chronically dysfunctional myocardium to low-dose dobutamine in ischaemic cardiomyopathy. Eur Heart J. 2001; 22:2164-2170.
15. Ozbay L, Unal DO, Erol D. Food effect on bioavailability of modified-release trimetazidine tablets. J Clin Pharmacol. 2012; 52:1535-1539.
16. Cramer JA, Roy A, Burrell A, Fairchild CJ, Fuldeore MJ, Ollendorf DA, Wong PK. Medication compliance and persistence: Terminology and definitions. Value Health. 2008; 11:44-47.
17. Zhang L, Lu Y, Jiang H, Zhang L, Sun A, Zou Y, Ge J. Additional use of trimetazidine in patients with chronic heart failure: A meta-analysis. Ration Pharmacother Cardiol. 2012; 8:242-250.
18. Mondillo S, Galderisi M, Mele D, Cameli M, Lomoriello VS, Zacà V, Ballo P, D'Andrea A, Muraru D, Losi M, Agricola E, D'Errico A, Buralli S, Sciomer S, Nistri S, Badano L. Speckle-tracking echocardiography: A new technique for assessing myocardial function. J Ultrasound Med. 2011; 30:71-83.
19. Motoki H, Borowski AG, Shrestha K, Troughton RW, Tang WHW, Thomas JD, Klein AL. Incremental prognostic value of assessing left ventricular myocardial mechanics in patients with chronic systolic heart failure. J Am Coll Cardiol. 2012; 60:2074-2081.
20. Takigiku K, Takeuchi M, Izumi C, Yuda S, Sakata K, Ohte N, Tanabe K, Nakatani S. Normal range of left ventricular 2-dimensional strain - Japanese ultrasound speckle tracking of the left ventricle (JUSTICE) study. Circ J. 2012; 76:2623-2632.
21. Psotka MA, Gottlieb SS, Francis GS, Allen LA, Teerlink JR, Adams KF Jr, Rosano GMC, Lancellotti P. Cardiac calcitropes, myotropes, and mitotropes: JACC review topic of the week. J Am Coll Cardiol. 2019; 73:2345-2353.
22. Fragasso G, Perseghin G, De Cobelli F, Esposito A, Palloshi A, Lattuada G, Scifo P, Calori G, Del Maschio A, Margonato A. Effects of metabolic modulation by trimetazidine on left ventricular function and phosphocreatine/adenosine triphosphate ratio in patients with heart failure. Eur Heart J. 2006; 27:942-948.
23. Belardinelli R, Solenghi M, Volpe L, Purcaro A. Trimetazidine improves endothelial dysfunction in chronic heart failure: An antioxidant effect. Eur Heart J. 2007; 28:1102-1108.
24. Nagueh SF, Smiseth OA, Appleton CP, Byrd BF 3rd, Dokainish H, Edvardsen T, Flachskampf FA, Gillebert TC, Klein AL, Lancellotti P, Marino P, Oh JK, Popescu BA, Waggoner AD. Recommendations for the evaluation of left ventricular diastolic function by echocardiography: An update from the American Society of Echocardiography and the European Association of Cardiovascular Imaging. J Am Soc Echocardiogr. 2016; 29:277-314.
25. Vitale C, Wajngaten M, Sposato B, Gebara O, Rossini P, Fini M, Volterrani M, Rosano GM. Trimetazidine improves left ventricular function and quality of life in elderly patients with coronary artery disease. Eur Heart J. 2004; 25:1814-1821.
26. Fragasso G, Rosano G, Baek SH, Sisakian H, Di Napoli P, Alberti L, Calori G, Kang SM, Sahakyan L, Sanosyan A, Vitale C, Marazzi G, Margonato A, Belardinelli R. Effect of partial fatty acid oxidation inhibition with trimetazidine on mortality and morbidity in heart failure: Results from an international multicentre retrospective cohort study. Int J Cardiol. 2013; 163:320-325.
27. Huang CQ, Dong BR. Effect of trimetazidine for congestive heart failure: A systematic review. Chin J Evid Based Med. 2007; 7:37-44.

Received March 5, 2022; Revised June 28, 2022; Accepted August 11, 2022.

Address correspondence to:
Mochamad Ali Sobirin, Department of Cardiology and Vascular Medicine, Faculty of Medicine, Diponegoro University - Dr. Kariadi General Hospital, Jl. Dr. Sutomo No. 16 Semarang, Jawa Tengah - Indonesia 50244.
E-mail: dr_alibirin@fk.undip.ac.id

Released online in J-STAGE as advance publication August 24, 2022.

Brief Report

DOI: 10.5582/ddt.2022.01048

Prevalence of SARS-CoV-2 antibodies among university athletic club members: A cross-sectional survey

Yukihiro Mori[1,2], Mamoru Tanaka[3], Hana Kozai[3], Kiyoshi Hotta[2], Yuka Aoyama[4], Yukihiro Shigeno[5,6], Makoto Aoike[1], Hatsumi Kawamura[1], Masato Tsurudome[1,7], Morihiro Ito[1,7,*]

[1] Graduate School of Life and Health Sciences, Chubu University, Aichi, Japan;
[2] Center for Nursing Practicum Support, Chubu University, Aichi, Japan;
[3] Department of Food and Nutritional Sciences, College of Bioscience and Biotechnology, Chubu University, Aichi, Japan;
[4] Department of Clinical Engineering, College of Life and Health Sciences, Chubu University, Aichi, Japan;
[5] Center for Emergency Medical Technician Practicum Support, Chubu University, Aichi, Japan;
[6] The Fire Department Headquarters in Kasugai-City, Aichi, Japan;
[7] Department of Biomedical Sciences, College of Life and Health Science, Chubu University, Aichi, Japan.

SUMMARY School-based coronavirus disease 2019 (COVID-19) testing is an important part of a comprehensive prevention strategy in public health. To assess the prevalence of severe acute respiratory syndrome coronavirus 2 (SARS-CoV-2) antibodies in a university athletic club community with repeated occurrences of SARS-CoV-2 infections, we conducted a cross-sectional survey for asymptomatic antibody prevalence using a SARS-CoV-2 rapid antibody test kit. On January 26, 2021 we administered questionnaires to determine their history of contact with infected individuals and took blood samples from 129 undergraduates. The prevalence of SARS-CoV-2 antibodies among the subjects was 3.9%. Only 6.2% of the participants reported close contact with infected individuals. In this study, we clarified the prevalence of asymptomatic SARS-CoV-2 antibodies in university athletic clubs where SARS-CoV-2 infections had repeatedly occurred, which will be helpful in discussing how to identify and prevent the transmission of infections within university athletic club communities.

Keywords SARS-CoV-2 antibodies, university athletic club, COVID-19, asymptomatic antibody prevalence, SARS-CoV-2 rapid antibody test

1. Introduction

The appearance of severe acute respiratory syndrome coronavirus 2 (SARS-CoV-2) in late 2019 led to the pandemic of coronavirus disease 2019 (COVID-19). As of June 2022, the pandemic has resulted in more than 530 million infected cases and over 6.3 million deaths worldwide. This has had the most serious global consequences on society, the economy, health systems, and human health since the 1918 influenza pandemic, which killed more than 50 million people.

In August 2020, a study in the United States reported a widespread outbreak of SARS-CoV-2 infection in a large university (*1*), and another study, in the next month, reported a rapid increase in SARS-CoV-2 infections in adults aged 18-22 years (*2*). With the increasing number of COVID-19 cases in college students, continuous preventive efforts, including strong testing regimes, were implemented to prevent outbreaks on or near university campuses. The need for quarantine was emphasized to protect the wider community (*3*). School closures were imposed in many countries to prevent the spread of the disease to young people and their surroundings. In previous studies, school closures were associated with a temporary reduction in COVID-19 incidence and mortality (*4*).

COVID-19 mortality rates rise with age, with death being relatively rare among young adults (*5*). In general, the perception that young people have lower morbidity, severity, and mortality than older people can result in reduced awareness of infection control. When college students are infected with SARS-CoV-2, the potential for the rapid spread of the virus in the university environment is a significant concern, considering that students tend to have wider social networks than the general population.

Cluster infections of COVID-19 can occur in any population, including within families (*6*), communities

(*7*), and nursing homes (*8*). Educational institutions can be one such example (*9*). Therefore school-based COVID-19 testing is considered an important part of a comprehensive prevention strategy for identifying SARS-CoV-2 infections in schools and for maintaining face-to-face instruction and extra-curricular activities (*10*). Therefore, we conducted a cross-sectional screening survey of SARS-CoV-2 antibody prevalence in a university community. We also retrospectively investigated the contact history of the members of this community. This university community comprised students belonging to two athletic clubs. Many of the students at this university live in dormitories. We chose this community to study because of the elevated risk of outbreaks of not only COVID-19, but also other infectious diseases in these populations. The inclusion criterion was a lack of obvious symptoms of infection among the participants.

In this study, the primary objective was to assess the prevalence of asymptomatic SARS-CoV-2 antibodies among the students in university athletic clubs where COVID-19 had occurred repeatedly. The secondary objective was to observe the infection dynamics that can occur within university athletic clubs. Finally, to our knowledge, this is the first study to provide the prevalence of SARS-COV2 asymptomatic infections in athletic clubs of universities. We believe that these results could help identify and prevent the transmission of COVID-19 within university athletic club communities.

2. Materials and Methods

2.1. Participants

The flowchart of this study is shown in Figure 1. The participants were undergraduates belonging to either of the two athletic clubs at a private university in Japan. This university has an enrollment of approximately 12,000 students. The first confirmed COVID-19 infection in these athletic clubs was identified on July 14, 2020. Subsequently, 11 infections were confirmed from late November 2020 to mid-January 2021. This population was operationally defined in the present study as "the university athletic club with repeated occurrences of COVID-19 infection". A total of 129 students from these clubs without obvious symptoms of infection were included in the study; the COVID-19-infected students mentioned above were excluded. In Japan, vaccination with the COVID-19 mRNA vaccine began in early February 2021, therefore, none of the study populations had received the COVID-19 mRNA vaccine at the time we conducted our survey in January 2021.

2.2. SARS-CoV-2 antibody testing

SARS-CoV-2 antibody testing was performed on January 26, 2021, after the outbreak of infections in this club had ended. This period of blood collection was the first COVID-19 epidemics in Japan. We collected blood from the fingertips of the participants using safety lancets,

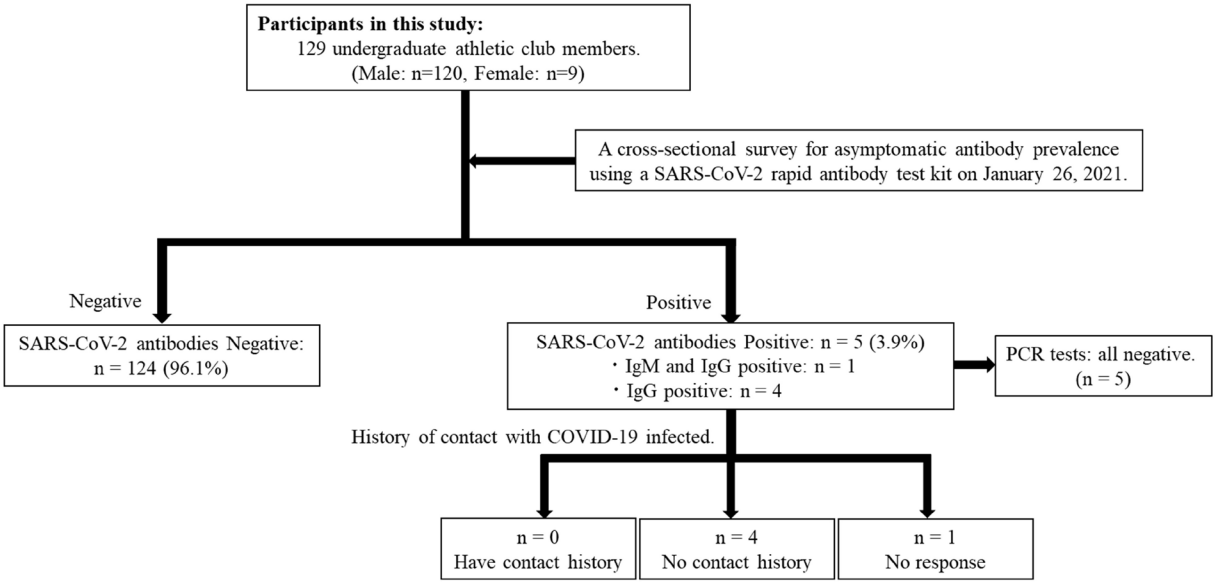

Figure 1. Study flow-chart. The first confirmed COVID-19 infection in this communities were identified on July 14, 2020. Subsequently, 11 infections were confirmed consecutively from late November 2020 to mid-January 2021. SARS-CoV-2 antibody testing was performed on January 26, 2021, after the outbreak of infections in this club had ended. We tested the participants (n = 129) for SARS-CoV-2 IgM and IgG antibodies using rapid antibody test kits. However, the selection criteria for the 129 subjects were those without obvious symptoms of infection, and COVID-19 patients were not included. Five blood samples (3.9%) tested positive for IgG antibodies, among which one sample was also positive for IgM antibodies. COVID-19, coronavirus disease 2019; SARS-CoV-2, severe acute respiratory syndrome coronavirus 2; IgM/G, Immunoglobulin M/G; PCR, polymerase chain reaction.

paying close attention to hygiene and infection control. The blood samples were tested using the SARS-CoV-2 Rapid Antibody Test RUO (Roche Diagnostics KK, Tokyo, Japan) by following the procedure on the package insert. This kit simultaneously detects SARS-CoV-2 IgG and IgM antibodies using immunochromatography. The procedure is as follows: the collected blood is placed into the sample drop hole of the test device, 3 drops (90 μL) of buffer solution are added into the sample drop hole of the test device, and the results are read after 15 minutes. This test kit indicates that the patient may not be infected with SARS-CoV-2 if the line appears only on C (Control). The appearance of a line at G or M, together with C, indicates positivity for IgG or IgM antibodies specific for SARS-CoV-2, suggesting possible previous SARS-CoV-2 infection.

2.3. Reverse transcription-polymerase chain reaction (RT-PCR) testing

Saliva samples were collected from those who were positive for IgM and IgG antibodies in the SARS-CoV-2 antibody testing to perform real-time RT-PCR to check for SARS-CoV-2 infection. The Light Cycler 96 (Roche, Basel, Switzerland) and SARS-CoV-2 Direct Detection RT-qPCR Kit (TaKaRa, Siga, Japan) were used, and assessments were made by following the protocols. This kit uses the primer and probe sequence described in the "2019-Novel Coronavirus (2019-nCoV) Real-time RT-PCR Panel Primers and Probes" (Effective: Jan 24, 2020) published by the U.S. Centers for Disease Control and Prevention.

2.4. Survey

We surveyed the participants' attributes (age, sex), lifestyle habits (smoking and alcohol consumption), and medical history using a questionnaire. Participants were asked about contacts with individuals infected with SARS-CoV-2 in the last 6 months. The yes or no questions were: "Have any close relatives or anyone else around you been infected with COVID-19?" and for close contact, "I was in contact with a COVID-19 patient closer than 1 meter for 15 min or more without any infection prevention measures (mask, *etc.*)".

2.5. Statistical analysis

Microsoft Excel 2019 was used to aggregate the data collected and to calculate descriptive statistics. The data were primarily for exploratory purposes and are thus expressed as numbers and percentages.

2.6. Ethics

This study was approved by the ethics committee of the Chubu University (Approval No. 20200039). The study was performed in accordance with the principles of the Declaration of Helsinki. The participants provided their written informed consent to participate in this study.

3. Results and Discussion

The participants included 120 men (93.0%) and 9 women (7.0%) with a mean age of 19.3 ± 1.0 years. Table 1 shows the participants' attributes, habits (smoking and alcohol consumption), and medical history. Six of the participants (4.7%) smoked and 21 (16.3%) drank alcohol. The most common medical complaint was asthma (17 participants, 13.2%), followed by pneumonia (5 participants, 3.9%), meningitis and heart disease (one each, 0.8%). Although we surveyed the participants' smoking and drinking habits and their medical history, there was no significant relationship between these factors and the prevalence of SARS-CoV-2 antibodies.

Results of the questionnaires revealed that 103 (80.6%) participants were aware of contacts infected with SARS CoV-2 and 26 (19.4%) were not. Among the 103 participants who answered "Yes", 94 (92.2%), did not have close contact with the infected person, eight (6.2%) had close contact and one (1.6%) did not respond. Participants were allowed to choose more than one option for relationship to infected contact, and the results showed that the vast majority (102, 99.0%) reported "a fellow club member" as the infected contact, one said "a friend outside the club," and one did not provide a response (Table 2).

We tested the participants (n = 129) for SARS-CoV-2 IgM and IgG antibodies. Five blood samples (3.9%) tested positive for IgG antibodies, of which one was also positive for IgM antibodies (Table 2). These antibody-positive samples were all from men (20.4 ± 0.8 years) and none of them reported any clinical symptoms associated with COVID-19. The PCR test results of

Table 1. Background characteristics of the study participants

Items	*n* (%)
Sex	
Male	120 (93.0)
Female	9 (7.0)
Smoking status	
Non-smoker	123 (95.3)
Former smoker	0 (0.0)
Current smoker	6 (4.7)
Alcohol	
Non-drinker	108 (83.7)
Drinker	21 (16.3)
Medical history*	
None	112 (86.8)
Asthma	17 (13.2)
Pneumonia	5 (3.9)
Meningitis	1 (0.8)
Heart disease	1 (0.8)

*Multiple responses were allowed.

saliva samples were negative in all five samples (100%) (Table 3).

All participants who tested positive for SARS-CoV-2 antibody (5 participants, 100%) were aware of the infected contacts, however four (80%) said that they had no history of close contact with the infected person, one (20%) did not respond. In addition, four (80%) said that they were fellow members of the same club for relationship to infected, one (20%) did not respond (Table 4).

We were inspired to conduct this study, because we wanted to determine the prevalence of asymptomatic COVID-19 infections and infection dynamics in one university athletic club with repeated COVID-19 infections. To the best of our knowledge, there have been no studies on the prevalence of asymptomatic COVID-19 infections in university athletic club communities where SARS-CoV-2 infections occurred. Our study revealed that the prevalence of asymptomatic COVID-19 infections was 3.9% in the university athletic club community where COVID-19 infections had repeatedly occurred. This result is consistent with previous studies of university students and staff that reported SARS-CoV-2 antibody-positive rates of approximately 1-4% (*11,12*). However, a similar study conducted in Japan reported a rate of 1.23% (*13*). Our results were well above this value.

The first COVID-19 infection in this population was confirmed in mid-July 2020. Subsequently, 11 infections were confirmed from late November 2020 to mid-January 2021. To retrospectively track the contact history of this community, we conducted a questionnaire survey along with SARS-CoV-2 antibody testing of serum samples. The results showed that about 80% of the participants were aware of an infected person nearby, and only about 6% had close contact with the infected individual. Because of the lack of a comparison group, it is unclear whether this contact rate is higher than that in other communities.

In Japan, priority vaccination with the COVID-19 mRNA vaccine began in early February 2021 for approximately 4.8 million healthcare workers, therefore, none of the study populations had received the COVID-19 mRNA vaccine at the time we conducted our survey in January 2021. Therefore, the data obtained here provide valuable information on the prevalence of asymptomatic SARS-CoV-2 antibodies among members of athletic clubs prior to the widespread use of the COVID-19 mRNA vaccine.

In addition, since the club activities continued during

Table 2. SARS-CoV-2 antibody test results, presence or absence of infected individuals in the vicinity; contact history and relationship with infected individuals

Items		*n* (%)
SARS-CoV-2 antibodies		
IgM	Negative	128 (99.2)
	Positive	1 (0.8)
IgG	Negative	124 (96.1)
	Positive	5 (3.9)
Awareness of infected individuals in the vicinity		
Yes		103 (80.6)
No		26 (19.4)
Contact history[†]		
Yes		8 (6.2)
No		94 (92.2)
No response		1 (1.6)
Relationship[††]		
Fellow club member		102 (99.0)
Friend outside club		1 (1.0)
No response		1 (1.0)

SARS-CoV-2, severe acute respiratory syndrome coronavirus 2; IgM/G, Immunoglobulin M/G. [†]Contact history and Relationships, $n = 103$. [††]The relationship question allowed for multiple responses.

Table 4. Presence/absence of infected individuals in the vicinity of SARS-CoV-2 antibody-positive individuals, contact history, and relationship

Items	*n* (%)
Awareness of infected individuals in the vicinity	
Yes	5 (100)
No	0 (0)
Contact history	
Yes	0 (0)
No	4 (80.0)
No response	1 (20.0)
Relationship	
Fellow club member	4 (80.0)
Friend outside club	0 (0)
No response	1 (20.0)

SARS-CoV-2, severe acute respiratory syndrome coronavirus 2.

Table 3. Attributes of SARS-CoV-2 antibody-positive individuals, detection of SARS-CoV-2 IgM and IgG antibodies

Case No.	Age	Sex	Medical history	SARS-CoV-2 PCR	COVID-19 Symptoms	SARS-CoV-2 Antibodies	
						IgM	IgG
1	21	Male	Asthma	Negative	None	+	+
2	21	Male	-	Negative	None	-	+
3	20	Male	-	Negative	None	-	+
4	20	Male	-	Negative	None	-	+
5	19	Male	Asthma, pneumonia	Negative	None	-	+

+, positive; -, negative; COVID-19, coronavirus disease 2019; SARS-CoV-2, severe acute respiratory syndrome coronavirus 2; PCR, polymerase chain reaction; IgM/G, Immunoglobulin M/G.

the COVID-19 pandemic, university administrators and coaches must implement preventive measures, such as encouraging appropriate social distancing, conducting daily health checks, and measuring body temperature (*14*). Furthermore, many members of these athletic clubs live in student dormitories which are places where crowded situations can occur easily. The risk of spreading COVID-19 infections in shared living environments, such as dormitories, has long been pointed out (*15*).

Club activities are an essential element of university life, the suspension of club activities during the COVID-19 pandemic can affect the members' progress and be a source of serious anxiety. Moreover, it has been pointed out that exercising during a pandemic has a positive effect on mental health (*16*). Therefore, university administrators and club coaches should try to maintain opportunities for exercise in order to maintain the students' physical and mental health. As such, strategies to prevent the spread of COVID-19 in club communities, in addition to robust infection control measures, must involve the creation of an environment that enables monitoring of SARS-CoV-2 antibody prevalence through continuous testing.

This study had several limitations. 1) The specificity declared by the manufacturer of the SARS-CoV-2 rapid antibody test kit used in this study was 98.65%, with a sensitivity of 99.03% for cases after 14 days of illness. However, SARS-CoV-2 antibody tests can produce contradictory results depending on the assay used (*17,18*). 2) Differences in the positive rates of SARS-CoV-2 antibodies can arise due to factors, such as country, region, community, race (*19*), socioeconomic environment (*20*), and cultural background (*21*). 3) Due to the limited number of samples we were able to collect, the sample size for this study was not large, so caution should be exercised when generalizing the results. In addition, the male-female ratio in this population was 40:3 and the age group was 19.3 ± 1.0 years, which makes our results difficult to compare with those of previous studies (*22*), which have observed age- and sex-based differences in SARS-CoV-2 antibody responses. A variety of other potential biases were not addressed, such as participation in social activities outside of the club activities and district of residence. 4) In the questionnaire survey, it should be noted that the participants' knowledge or awareness of infected people nearby and their contact history were based on self-reports. Regarding the operational definition of contact history, in particular, there is limited evidence supporting its accuracy. In addition, although a low percentage of participants had a history of contact with infected people, the results of this study do not necessarily mean that it was more likely that exposure came from outside the community. Multiple previous studies that investigated contact history through questionnaires and interviews have also designated operational definition (*23,24*). In discussing the relationship between SARS-CoV-2 antibody prevalence within communities, it is important to carefully consider how to devise tracking methods, set operational definitions, and consider the subjective bias of the participants with regard to the contact history data obtained from questionnaires and interviews. 5) Because this was a cross-sectional study, we did not follow up on the prevalence of SARS-CoV-2 antibodies in the participants' community. 6) Finally, this study represents provisional results as of January 2021, and results may change due to future epidemics, changes in the state of control, and the impact of new variants.

In summary, the present study provides novel and unique data on the prevalence of asymptomatic COVID-19 infections within a community of university athletic clubs where infections had repeatedly occurred. This is a strength of this study. These findings could be useful for comparative data for future studies involving athletic club communities.

Acknowledgements

The authors thank Atsuo Iiyoshi, PhD (Chancellor, Chubu University Educational Corporation), for his full support in promoting this study. We greatly appreciate all university students for their participation in this study.

Funding: None

Conflict of Interest: The authors have no conflicts of interest to disclose.

References

1. Wilson E, Donovan CV, Campbell M, Chai T, Pittman K, Seña AC, Pettifor A, Weber DJ, Mallick A, Cope A, Porterfield DS, Pettigrew E, Moore Z. Multiple COVID-19 clusters on a university campus - North Carolina, August 2020. MMWR Morb Mortal Wkly Rep. 2020; 69:1416-1418.
2. Salvatore PP, Sula E, Coyle JP, Caruso E, Smith AR, Levine RS, Baack BN, Mir R, Lockhart ER, Tiwari TSP, Dee DL, Boehmer TK, Jackson BR, Bhattarai A. Recent increase in COVID-19 cases reported among adults aged 18-22 years - United States, May 31-September 5, 2020. MMWR Morb Mortal Wkly Rep. 2020; 69:1419-1424.
3. Walke HT, Honein MA, Redfield RR. Preventing and responding to COVID-19 on college campuses. JAMA. 2020; 324:1727-1728.
4. Auger KA, Shah SS, Richardson T, Hartley D, Hall M, Warniment A, Timmons K, Bosse D, Ferris SA, Brady PW, Schondelmeyer AC, Thomson JE. Association between statewide school closure and COVID-19 incidence and mortality in the US. JAMA. 2020; 324:859-870.
5. Levin AT, Hanage WP, Owusu-Boaitey N, Cochran KB, Walsh SP, Meyerowitz-Katz G. Assessing the age

specificity of infection fatality rates for COVID-19: systematic review, meta-analysis, and public policy implications. Eur J Epidemiol. 2020; 35:1123-1138.
6. Chan JF, Yuan S, Kok KH, *et al.* A familial cluster of pneumonia associated with the 2019 novel coronavirus indicating person-to-person transmission: a study of a family cluster. Lancet. 2020; 395:514-523.
7. Kim NJ, Choe PG, Park SJ, Lim J, Lee WJ, Kang CK, Park WB, Seong MW, Oh MD. A cluster of tertiary transmissions of 2019 novel coronavirus (SARS-CoV-2) in the community from infectors with common cold symptoms. Korean J Intern Med. 2020; 35:758-764.
8. Arons MM, Hatfield KM, Reddy SC*, et al.* Presymptomatic SARS-CoV-2 Infections and Transmission in a Skilled Nursing Facility. N Engl J Med. 2020; 382:2081-2090.
9. Ismail SA, Saliba V, Lopez Bernal J, Ramsay ME, Ladhani SN. SARS-CoV-2 infection and transmission in educational settings: a prospective, cross-sectional analysis of infection clusters and outbreaks in England. Lancet Infect Dis. 2021; 21:344-353.
10. Lanier WA, Babitz KD, Collingwood A, Graul MF, Dickson S, Cunningham L, Dunn AC, Mackellar D, Hersh AL. COVID-19 testing to sustain in-person instruction and extracurricular activities in high schools — Utah, November 2020–March 2021. MMWR Morb Mortal Wkly Rep. 2021; 70:785-791.
11. Tilley K, Ayvazyan V, Martinez L, Nanda N, Kawaguchi ES, O'Gorman M, Conti D, Gauderman WJ, Van Orman S. A cross-sectional study examining the seroprevalence of severe acute respiratory syndrome coronavirus 2 antibodies in a university student population. J Adolesc Health. 2020; 67:763-768.
12. Tsitsilonis OE, Paraskevis D, Lianidou E*, et al.* Seroprevalence of antibodies against SARS-CoV-2 among the personnel and students of the National and Kapodistrian University of Athens, Greece: A preliminary report. Life. 2020; 10:214.
13. Nawa N, Kuramochi J, Sonoda S, Yamaoka Y, Nukui Y, Miyazaki Y, Fujiwara T. Seroprevalence of SARS-CoV-2 IgG antibodies in Utsunomiya City, Greater Tokyo, after first pandemic in 2020 (U-CORONA): a household- and population-based study. Cold Spring Harbor Laboratory, 2020.
14. Chen P, Mao L, Nassis GP, Harmer P, Ainsworth BE, Li F. Returning Chinese school-aged children and adolescents to physical activity in the wake of COVID-19: Actions and precautions. J Sport Health Sci. 2020; 9:322-324.
15. Gorny AW, Bagdasarian N, Koh AHK*, et al.* SARS-CoV-2 in migrant worker dormitories: Geospatial epidemiology supporting outbreak management. Int J Infect Dis. 2021; 103:389-394.
16. Zhang Y, Zhang H, Ma X, Di Q. Mental health problems during the COVID-19 pandemics and the mitigation effects of exercise: A longitudinal study of college students in China. Int J Environ Res Public Health. 2020; 17:3722.
17. Merrill AE, Jackson JB, Ehlers A, Voss D, Krasowski MD. Head-to-head comparison of two SARS-CoV-2 serology assays. J Appl Lab Med. 2020; 5:1351-1357.
18. Mitsunaga T, Seki Y, Yoshioka M, Suzuki I, Akita K, Mashiko S, Uzura M, Takeda S, Sekine A, Mashiko K. Comparison of the diagnostic value of immunochromatography kits in corona virus disease 2019 patients: A prospective pilot study. JMA J. 2021; 4:32-40.
19. Vahidy FS, Nicolas JC, Meeks JR, Khan O, Pan A, Jones SL, Masud F, Sostman HD, Phillips R, Andrieni JD, Kash BA, Nasir K. Racial and ethnic disparities in SARS-CoV-2 pandemic: analysis of a COVID-19 observational registry for a diverse US metropolitan population. BMJ Open. 2020; 10:e039849.
20. Goyal MK, Simpson JN, Boyle MD, Badolato GM, Delaney M, Mccarter R, Cora-Bramble D. Racial and/or ethnic and socioeconomic disparities of SARS-CoV-2 infection among children. Pediatrics. 2020; 146:e2020009951.
21. Abuelgasim E, Saw LJ, Shirke M, Zeinah M, Harky A. COVID-19: Unique public health issues facing Black, Asian and minority ethnic communities. Curr Probl Cardiol. 2020; 45:100621.
22. Klein SL, Pekosz A, Park H-S*, et al.* Sex, age, and hospitalization drive antibody responses in a COVID-19 convalescent plasma donor population. J Clin Invest. 2020; 130:6141-6150.
23. Chirathaworn C, Sripramote M, Chalongviriyalert P*, et al.* SARS-CoV-2 RNA shedding in recovered COVID-19 cases and the presence of antibodies against SARS-CoV-2 in recovered COVID-19 cases and close contacts, Thailand, April-June 2020. PLoS One. 2020; 15:e0236905.
24. Dimcheff DE, Schildhouse RJ, Hausman MS, Vincent BM, Markovitz E, Chensue SW, Deng J, McLeod M, Hagan D, Russell J, Bradley SF. Seroprevalence of severe acute respiratory syndrome coronavirus-2 (SARS-CoV-2) infection among Veterans Affairs healthcare system employees suggests higher risk of infection when exposed to SARS-CoV-2 outside the work environment. Infect Control Hosp Epidemiol. 2021; 42:392-398.

Received June 14, 2022; Revised June 22, 2022; Accepted August 17, 2022.

**Address correspondence to:*
Morihiro Ito, Department of Biomedical Sciences, College of Life and Health Sciences, Chubu University, 1200 Matsumoto-cho, Kasugai, Aichi 487-8501, Japan.
E-mail: m-ito@isc.chubu.ac.jp

Released online in J-STAGE as advance publication August 21, 2022.

Brief Report

DOI: 10.5582/ddt.2022.01045

Electrolyzed water produced using carbon electrodes promotes the proliferation of normal cells while inhibiting cancer cells

Kyoko Nakamura*

Pharmaceutical Research and Technology Institute, Kindai University, Osaka, Japan.

SUMMARY We previously developed electrolyzed water (EW) using carbon electrodes and estimated its ability to inhibit the proliferation of human cervical carcinoma HeLa cells. In this study, we found that EW-containing media could not only inhibit HeLa cell proliferation, but were also capable of promoting the proliferation of normal human dermal fibroblasts (NHDF). In addition, the developed EW could reduce cytochrome *c*, as demonstrated by the cytochrome *c* reduction assay. Interestingly, EW with a greater pH, which was unable to inhibit HeLa cell proliferation, completely lost the ability to reduce cytochrome *c*. Our results indicate that EW has opposite effects on cancer and normal cell proliferation and has the ability to reduce cytochrome *c*. Based on our findings, we suggest the possibility that the reducing capacity of our developed EW may be involved in the significant inhibition of HeLa cell proliferation.

Keywords electrolyzed water, cell proliferation, reducing ability, normal cells, cancer cells

1. Introduction

Electrolyzed water (EW) is usually produced using an electrolytic cell with a separation baffle between the anode and cathode. The produced water from the anode side is called electrochemically oxidized water (EOW) or acidic water and is characterized by low pH values. On the other hand, electrochemically reduced water (ERW) is characterized by high pH values and is also known as alkaline water. The particular EOW generated by electrolysis of sodium chloride solution has a strong bactericidal effect and can disinfect viruses, such as hepatitis B virus (*1,2*). There have been many reports on ERW, which has been suggested to have many health benefits in humans (*3*). With regard to the inhibition of cell proliferation, ERW inhibited the growth of human lung adenocarcinoma A549 and HeLa cells as well as the growth of human normal fibroblast TIG-1 cells (*4,5*). A recent study showed that ERW treatment of MCF-7 and MDA-MB-453 human breast cancer cells or a TUBO cloned cell line derived from a mammary carcinoma of Her2-neu transgenic mice inhibited cell survival and induced apoptosis (*6*). This study also showed that ERW treatment delayed the development of mammary tumors in transgenic mice (*6*). Thus, although ERW inhibits the proliferation of cancer cells and shows anticancer potential, it also inhibits the proliferation of normal cells. Recently, we showed that EW produced without a separation baffle using carbon electrodes exhibited acidic pH (pH ≤ 3.5) and inhibited human HeLa cancer cell proliferation (*7*). Several researchers have reported that EW produced without a separation baffle is neutral (pH 6.6 to 7.8) (*8*) and slightly acidic (pH 5.0 to 6.5) (*9-10*). Therefore, it is interesting to note that our developed EW without a separation baffle exhibits an acidic pH. There have been very few studies on the effect of acidic EW on cell proliferation. Nakamura *et al*. examined the effect of slightly acidic EW, which inhibited adult human gingival fibroblasts and normal human dermal fibroblasts (NHDF) (*9*). However, there are no reports on the effects of acidic EW on cancer cell proliferation. Therefore, we first reported the potential ability of acidic EW produced using carbon electrodes to inhibit the proliferation of cancer cells (*7*). We have yet to examine the effect of our developed acidic EW on normal cell proliferation.

Reactive oxygen species (ROS) play an important role in cell proliferation, and cancer cells are characterized by elevated levels of ROS compared to normal cells (*11*). A previous study showed that increased cell number by mammary carcinogens is mediated through ROS generation (*12*). Hence, ROS have been implicated in anticancer drug mechanisms (*13*). Furthermore, ERW acts as a scavenger of ROS-induced oxidative stress and is useful for treating various diseases caused by ROS. Kim *et al*. showed that ERW consumption in diabetic *db/db* mice reduces blood glucose concentration and

prevents the loss of β-cell mass by oxidative stress (*14*). Moreover, ROS have been shown to be associated with cisplatin toxicity, including nephrotoxicity, and ERW has been reported to exert a nephroprotective effect against cisplatin-induced kidney toxicity and oxidative damage in mice (*15*). Shirahata *et al*. and Huang *et al*. reported that ERW can scavenge ROS with a high reducing ability (*16,17*). Thus, ERW is an antioxidant that scavenges ROS. However, we do not know whether our developed EW has a reducing ability.

The goal of the present study was to evaluate the reducing ability of our developed EW and its effect on NHDF cell proliferation. We first examined whether the developed EW affected the cell proliferation of the normal cell line NHDF and then, using a cytochrome *c* reduction assay, investigated whether it had a reducing ability. Our results demonstrate that our developed EW promotes the proliferation of NHDF while inhibiting that of cancer cells is associated with its reducing ability.

2. Materials and Methods

2.1. Preparation of electrolyzed water (EW) -containing media

The EW production method used in our study has been described in detail elsewhere (*7*). To investigate the effects of EW on the proliferation of cancer and normal cells, media was prepared using EW or tap water (W) (control). The EW had a pH of 3-3.5. Dulbecco's modified Eagle medium (DMEM) powder (Nissui Pharmaceutical Co., Ltd., Tokyo, Japan) was dissolved in W or EW (①-W or ①-EW, respectively) according to the manufacturer's instructions. We observed differently sized black dots in the ①-EW medium under the microscope in a previous study (data not shown) (*7*). Then, these media were filtered through a 0.2-μm filter (cellulose acetate membrane) to remove relatively large fragments that had broken off a piece of carbon electrodes (②-W and ②-EW). W-medium and EW-medium were sterilized by autoclaving at 121°C and then supplemented with 10% fetal bovine serum (FBS) (Nichirei Biosciences Inc., Tokyo, Japan), 0.584 g/L glutamine (Wako Pure Chemical Industries, Ltd., Osaka, Japan), 100 μg/mL streptomycin (Nacalai Tesque, Kyoto, Japan), 100 U/mL penicillin (Nacalai Tesque), and 10% sodium hydrogen carbonate (Wako). Finally, the W-culture medium had a pH of about 8.3 and the EW-culture medium a pH of about 8.1.

2.2. Cell culture

In this study, a human cancer cell line (HeLa) and a normal cell line (NHDF) were used. HeLa and NHDF cells were maintained in low-glucose DMEM (Sigma, St. Louis, MO, USA) supplemented with 10% FBS, 100 μg/mL streptomycin, and 100 U/mL penicillin. The cells were grown in culture dishes under standard conditions at 37°C and 5% CO_2. To study the effects of EW on the proliferation of HeLa and NHDF cells, these cells were cultured in EW or W (control) media.

2.3. Cell proliferation assay

Cell proliferation assays were performed on HeLa and NHDF cells as described previously (*7*). Briefly, cultured cells were trypsinized and collected by centrifugation at 800× g for 5 min. Subsequently, the cells were resuspended in EW or W control culture media, and 8 × 10^4 cells were seeded in culture flasks, followed by incubation for 3 d at 37°C in a humidified atmosphere containing 5% CO_2 and 95% air. The effects of EW on cell proliferation were assessed by counting the number of viable cells. HeLa and NHDF cells were trypsinized, stained with trypan blue, and counted using a hemocytometer daily for 3 days.

2.4. Cytochrome *c* reduction assay

Cytochrome *c* reduction was monitored by measuring the increase in absorbance at 550 nm at 37°C using a spectrophotometer. Cytochrome *c* was soluble in 0.15 M NaCl 20 mM Tris-HCl, pH 7.4 (1 mM cytochrome *c* solution). The assay was carried out in a 1 cm cuvette, and the reaction mixture consisted of 50 μL Tris-HCl pH 7.5 (1 M), 20 μL cytochrome *c* solution (1 mM), and 830 μL distilled water. To initiate the reaction, 100 μL of EW test samples were added to the reaction mixture in a cuvette. The activity was expressed as the change in absorbance at 550 nm and was monitored for a period of 7200 sec (2 h).

3. Results and Discussion

Our previous experiments showed that EW generated using a special carbon electrode and exhibited acidic pH (pH ≤ 3.5) inhibits the proliferation of human cervical carcinoma HeLa cells (*7*). The EW-containing medium used in this study inhibited HeLa cell proliferation (Figure 1A). Although it is known that EW-containing medium affects the proliferation of cancer cells, the effect of EW-containing medium on the proliferation of normal cells remains unknown. To investigate the effect of the EW-containing medium on the proliferation of normal cells, we utilized the NHDF cell line. Surprisingly, the proliferation of NHDF was remarkably upregulated by the EW-containing medium, whereas the proliferation of NHDF cultured in the W control medium exhibited slower proliferation for 3 days (Figure 1B). The growth of NHDF cells in the W control or the EW-containing medium was also observed as shown in Figure 1C. Our developed EW was containing carbon compounds observed very small black dots (Figure 1C) and we found that these carbon compounds are associated with

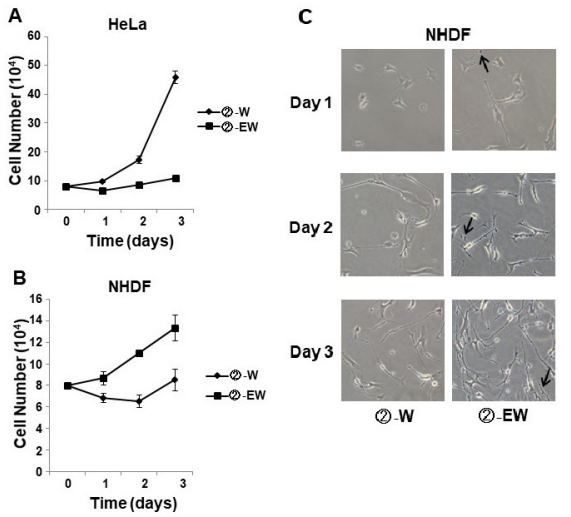

Figure 1. The effect of W and EW media on the proliferation of human cancer cell line HeLa and human normal cell line NHDF. Each ②-W and ②-EW was prepared by filtration (0.2 μm) of ①-W or ①-EW, respectively. Cells were seeded at a density of 8×10^4 cells in flasks containing each culture medium. Cells were counted daily for 3 d (**A**; HeLa cells, **B**; NHDF cells). NHDF cells were photographed for 3 days at ×10 (**C**). The arrow indicates very small black dots. Data are expressed as the mean ± SD of three independent experiments.

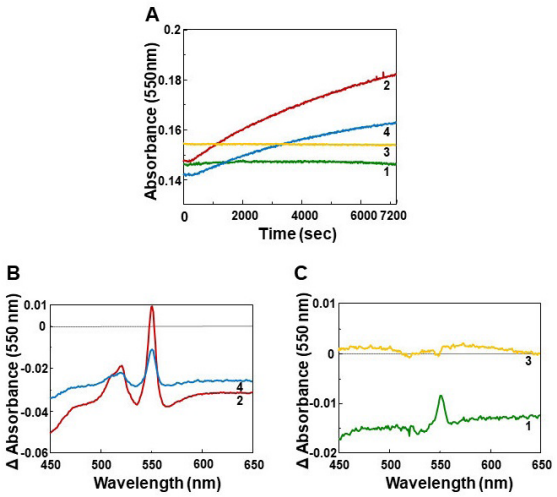

Figure 2. Reduction of cytochrome *c* by EW. Cytochrome *c* reduction by EW 17 h (1), EW 72 h (2), EW high pH (3), and frozen EW (4) (**A**). Each EW 17 h and EW 17 h was prepared by electrolysis of tap water for 17 h and 72 h, respectively. EW high pH meant that EW had a pH of 6.21. Number 4 denotes that EW was stored at − 20°C. Time difference absorption spectra (2 h aged spectra minus the corresponding 1 min aged ones) of four EW samples (**B**) and (**C**). Up to 2 h of incubation, EW 72 h evidenced increases in absorbance at 550 nm.

the inhibition of HeLa cell proliferation in our previous study (*7*). These results indicate that EW inhibits cancer cell proliferation and promotes normal cell proliferation. Although few studies on the effect of EW on normal cell proliferation have been reported, Shirahata *et al*. reported the anti-proliferative effects of ERW on normal cells (*4,5*). On the other hand, Satoh *et al*. reported that neutral pH hydrogen-enriched EW exerted repressive effects against both colony formation and cell proliferation in human tongue carcinoma HSC-4 cells, but not in normal human tongue epithelial-like cells DOK (*8*). Moreover, Tsai *et al*. reported that treatment with a combination of ERW and glutathione had no inhibitory effect on the viability of normal peripheral blood mononuclear cells, whereas cytotoxic effects were observed in leukemia cells (HL-60) (*18*). This phenomenon of promotion of normal cell proliferation in EW-containing culture medium has never been reported before. Thus, it is noteworthy that our developed EW stimulates normal cell proliferation while inhibiting that of cancer cells.

While ERW is considered to play a potentially beneficial role in inhibiting cancer cell proliferation, several findings have also indicated that ERW has the ability to scavenge ROS such as hydrogen peroxide (H_2O_2), with has a high reducing ability (*16,17*). ROS scavengers are a group of antioxidant substances that can be considered reducing agents (*19*). Furthermore, Komatsu *et al*. reported that scavenging ROS by ERW is associated with the suppressive effect of ERW on the growth of cancer cells (*20*). Satoh *et al*. reported that neutral pH hydrogen-enriched EW caused growth inhibition of cancer cells, together with scavenging of intracellular oxidants (*8*). Thus, the reducing ability may contribute to the inhibitory effect of ERW on cancer cell proliferation. Since our developed EW could inhibit the proliferation of cancer cells, we investigated whether it possessed a reducing ability. To evaluate the potential activity of EW as a reducing agent, a cytochrome *c* reduction assay was performed with EW electrolyzed for 17 h (EW 17 h) and 72 h (EW 72 h). EW used in our study of cell proliferation was electrolyzed for 72 h and has a pH of 3-3.5 (*7*). EW 17 h has a pH of less than 4; however, it remains unknown whether EW 17 h inhibits the proliferation of HeLa cells. A reduction in cytochrome *c* level was observed at 550 nm (*21*). As shown in Figure 2A and 2B, EW 72 h was able to reduce cytochrome *c*. On the other hand, EW 17 h barely reduced cytochrome *c* (Figure 2A), and a slight reducing ability of EW was observed (Figure 2C). These results suggest that the EW developed in this study has reducing ability and that 72 h of electrolysis may be required to gain this reducing ability. Furthermore, we evaluated the reducing ability of EW at a pH greater than 3.5. In a previous study, we found that EW with at a pH greater than 3.5 was unable to inhibit HeLa cell proliferation (*7*). EW with a pH of 6.21 had no reducing ability (Figure 2A and 2C). Thus, our findings indicate that the reducing ability of EW contributes to the inhibition of HeLa cell proliferation.

ROS also plays an important role in the control of cellular senescence. Cellular senescence was first reported by Hayflick and Moorhead (1961). They discovered that cultured normal human fibroblasts had a slow proliferative rate and a finite proliferative capacity,

now termed cellular senescence (*22*). Increased ROS levels in normal cells cause oxidative stress, resulting in cellular senescence (*23*). Thus, cultured normal cells are limited in the number of times they can divide and exhibit a process termed cellular senescence or cellular aging (*24*). However, cancer cells generally have higher levels of ROS than normal cells, and the increase in ROS levels contributes to the promoting of cancer cell proliferation (*25,26*). Hence, as shown in Figure 1, it could be speculated that ROS levels are associated with the proliferative rate of normal (NHDF) or cancer (HeLa) cells cultured in a W control medium. Conversely, normal (NHDF) or cancer (HeLa) cell proliferation was enhanced or inhibited in the EW-containing medium when compared with that in the W control medium (Figure 1). It is thought that one of the reasons for these results may be the reduced ability of the EW-containing medium to lower cellular ROS levels.

Although EW was stored at 4°C in our previous study, it was dispensed into 50 mL tubes and stored at −20°C in this study. We also assessed the reducing ability of the frozen EW. Surprisingly, the reducing ability of EW was decreased upon freezing (Figure 2A and 2B). In a previous study, we found that carbon compounds present in EW were associated with inhibition of HeLa cell proliferation (*7*). Therefore, it is possible that carbon compounds have a reducing ability, which is affected by frozen storage, whereas storage at 4°C has no effect. We hope to investigate these possibilities in future studies.

In conclusion, we found that the developed EW not only inhibited tumor cell proliferation, but also stimulated normal cell proliferation. We also show that EW has the ability to reduce cytochrome *c*, suggesting that the reducing ability of EW may contribute to the inhibition of cancer cell proliferation in an EW-containing medium. Thus, our results indicate that the developed EW has dual functions in inhibiting cancer cell proliferation and promoting normal cell proliferation. Previous studies have shown that the inhibitory effect of carbon compounds in EW on tumor cell proliferation can be removed by washing cultured cells with PBS. We then suggested that carbon compounds predicted to be associated with cell growth inhibition are reversibly attached to the cell surface. Therefore, as a treatment for cancer, particularly gastric cancer, carbon compounds in EW may be better administered orally than injected into patients. We hope that EW with reducing ability will be useful for developing anti-cancer agents.

Acknowledgements

The authors thank Mr. Yoshihiro Kojima and Mr. Masashi Zenki (Toyo Tanso Co., Ltd., Osaka, Japan) for providing special carbon electrodes and for performing the cytochrome *c* reduction assay and data analysis.

Funding: None.

Conflict of Interest: The authors have no conflicts of interest to disclose.

References

1. Okuda R, Sasazaki H, Kanehira M, Okabe T, Abe S, Tagami A, Iwamatsu Y, Miya Y, Shimizu Y. Bactericidal effect of high oxidation potential water viewed from a morphological change. Jpn J Conserv Dent. 1994; 37:755-765. (in Japanese)
2. Hati S, Mandal S, Minz PS, Vij S, Khetra Y, Singh BP. Electrolyzed oxidized water (EOW): Non-thermal approach for decontamination of food borne microorganisms in food industry. Food Nutr Sci. 2012; 3:760-768.
3. Shirahata S, Hamasaki T, Teruya K. Advanced research on the health benefit of reduced water. Trends Food Sci Technol. 2012; 23:124-131.
4. Shirahata S, Kabayama S, Kusumoto K, Goto M, Teruya K, Otsubo K, Morisawa S, Hayashi H, Katakura K. Electrolyzed reduced water which can scavenge active oxygen species suppresses cell growth and regulates gene expression of animal calls. In: New Development and New Applications in Animal Cell Technology (Merten OW *et al*., eds.). Kluwer Academic Publishers, the Netherlands, 1998; pp. 93-96.
5. Shirahata S, Murakami E, Kusumoto K-I, amashita M, Oda M, Teruya K, Kabayama S, Otubo K, Morisawa S, Hayashi H, Katakura Y. Telomere shortening in cancer cells by electrolyzed-reduced water. In: Animal Cell Technology: Challenges for the 21st Century (Ikura K, ed.). Kluwer Academic Publishers, Dordecht, 1999; pp. 355-359.
6. Frajese GV, Benvenuto M, Mattera R, Giampaoli S, Ambrosin E, Bernardini R, Giganti MG, Albonici L, Dus I, Manzari V, Modesti A, Mattei M, Bei R. Electrochemically reduced water delays mammary tumors growth in mice and inhibits breast cancer cells survival *in vitro*. Evid Based Complement Alternat Med. 2018; 2018, 4753507.
7. Nakamura K, Muraoka O. Effect of electrolyzed water produced using carbon electrodes on HeLa cell proliferation. Biosci Trends. 2018; 11:688-693.
8. Saitoh Y, Okayasu H, Xiao L, Harata Y, Niwa N. Neutral pH hydrogen-enriched electrolyzed water achieves tumor-preferential clonal growth inhibition over normal cells and tumor invasion inhibition concurrently with intracellular oxidant repression. Oncol Res. 2008; 17:247-255.
9. Nakamura T, Oda H, Sato S. Effects of slightly acidic electrolyzed water on oral pathogens and human gingival fibroblasts. Jpn J Conserv Dent. 2010; 53:570-578. (in Japanese)
10. Ye Z, Wang S, Chen T, Gao W, Zhu S, He J, Han Z. Inactivation mechanism of Escherichia coli induced by slightly acidic electrolyzed water. Sci Rep. 2017; 7:6279.
11. Stzatrowski TP, Nathan CF. Production of large amounts of hydrogen peroxide by human tumor cells. Cancer Res. 1991; 51:794-798.
12. Burdick AD, Davis JW 2nd, Liu KJ, Hudson LG, Shi H, Monske ML, Burchiel SW. Benzo(a)pyrene quinones increase cell proliferation, generate reactive oxygen species, and transactivate the epidermal growth factor

receptor in breast epithelial cells. Cancer Res. 2003; 63:7825-7833.
13. Trachootham D, Alexandre J, Huang P. Targeting cancer cells by ROS-mediated mechanisms: a radical therapeutic approach? Nat Rev Drug Discov. 2009; 8:579-591.
14. Kim MJ, Jung KH, Uhm YK, Leem KH, Kim HK. Preservative effect of electrolyzed reduced water on pancreatic beta-cell mass in diabetic *db/db* mice. Biol Pharm Bull. 2007; 30:234-236.
15. Cheng TC, Hsu YW, Lu FJ, Chen YY, Tsai NM, Chen WK, Tsai CF. Nephroprotective effect of electrolyzed reduced water against cisplatin-induced kidney toxicity and oxidative damage in mice. J Chin Med Assoc. 2018; 81:119-126.
16. Shirahata S, Kabayama S, Nakano M, Miura T, Kusumoto K, Gotoh M, Hayashi H, Otsubo K, Morisawa S, Katakura Y. Electrolyzed-reduced water scavenges active oxygen species and protects DNA from oxidative damage. Biochem Biophys Res Commun. 1997; 234:269-274.
17. Huang KC, Yang CC, Lee KT, Chien CT. Reduced hemodialysis-induced oxidative stress in end-stage renal disease patients by electrolyzed reduced water. Kidney Int. 2003; 64:704-714.
18. Tsai CF, Hsu YW, Chen WK, Ho YC, Lu FJ. Enhanced induction of mitochondrial damage and apoptosis in human leukemia HL-60 cells due to electrolyzed-reduced water and glutathione. Biosci Biotechnol Biochem. 2009; 73:280-287.
19. V Rajeswer Rao. Advances in structure and activity relationship of coumarin derivatives. Academic Press-Elsevier, Amsterdam, the Netherlands, 2016; pp. 47-76.
20. Komatsu T, Kabayama S, Hayashida A, Nogami H, Teruya K, Katakura Y, Otsubo K, Morisawa S, Shirahata S. Suppressive effect of electrolyzed-reduced water on the growth of cancer cells and microorganisms. In: Animal Cell Technology: From target to market. Kluwer Academic Publishers, Dordrecht, 2001; pp.220-223.
21. Massey V. The microestimation of succinate and the extinction coefficient of cytochrome *c*. Biochim Biophys Acta. 1959; 34:255-256.
22. Hayflick L, Moorhead PS. The serial cultivation of human diploid cell strains. Exp Cell Res. 1961; 25:585-621.
23. Kondoh H, Lleonart ME, Bernard D, Gil J. Histol Histopathol. 2007; 22:85-90.
24. Hayflick L. The cell biology of human aging. N Engl J Med. 1976; 295:1302-1308.
25. Snezhkina AV, Kudryavtseva AV, Kardymon OL, Savvateeva MV, Melnikova NV, Krasnov GS, Dmitriev AA. ROS generation and antioxidant defense systems in normal and malignant cells. Oxid Med Cell Longev. 2019; 2019:6175804.
26. Perillo B, Donato MD, Pezone A, Zazzo ED, Giovannelli P, Galasso G, Castoria G, Migliaccio A. ROS in cancer therapy: the bright side of the moon. Exp Mol Med. 2020; 52:192-203.

Received June 10, 2022; Revised July 22, 2022; Accepted August 16, 2022.

**Address correspondence to:*
Kyoko Nakamura, Pharmaceutical Research and Technology Institute, Kindai University, 3-4-1 Kowakae, Higashiosaka, Osaka 577-8502, Japan.
E-mail: kyoko@phar.kindai.ac.jp

Released online in J-STAGE as advance publication August 21, 2022.

Commentary

DOI: 10.5582/ddt.2022.01055

Listing of the neutralizing antibodies amubarvimab and romlusevimab in China: Hopes and impediments

Miaona Liu, Wei Li, Hongzhou Lu*

National Clinical Research Center for Infectious Disease, The Second Affiliated Hospital, Southern University of Science and Technology, Shenzhen, Guangdong, China.

SUMMARY The coronavirus disease 2019 (COVID-19) pandemic continues to ravage the world, and the virus' constant evolution has made it increasingly difficult to contain. The combination of the neutralizing antibodies amubarvimab and romlusevimab has recently been introduced as a treatment for COVID-19 in China. Based on its potential to effectively combat severe acute respiratory syndrome coronavirus 2 (SARS-CoV-2) and its Omicron variant at a modest cost and under medical insurance, this controversial biotherapy is anticipated to be widely available in China. Hopefully, whether and how the proposed medication will alter the treatment of COVID-19 in China will be apparent soon, as well as if it will help to reduce hospitalizations, reduce the incidence of severe illness, or even act as pre-exposure prophylaxis.

Keywords COVID-19, SARS-CoV-2, Omicron variant, neutralizing antibody, monoclonal antibody

Coronavirus disease 2019 (COVID-19), a global epidemic caused by the severe acute respiratory syndrome coronavirus 2 (SARS-CoV-2), continues to flare up three years later. As a result of the emergence of Alpha, Beta, Gamma, Delta, and now Omicron variants, COVID-19's level and speed of transmission have substantially increased (*1,2*). Repeated infections and severe, prolonged symptoms pose significant social and economic concerns and cast serious doubts on the efficacy of vaccination. Other than vaccination against COVID-19, systemic treatment options are quite limited in terms of safety and expense. Small molecules and neutralizing antibodies are reliable and effective therapies for COVID-19. Combining neutralizing antibodies in a cocktail therapy decreases the possibility of a resistant virus strain emerging in individuals with COVID-19 and maintains neutralization activity against several emerging mutant strains. Therefore, the successful development of combination therapies with neutralizing antibodies could play a critical role in reshaping the world's ability to combat the epidemic.

The first neutralizing antibody cocktail therapy for COVID-19 to be commercially marketed in China was introduced on July 7, 2022. It consisted of two non-competing, anti-SARS-CoV-2 monoclonal antibodies, amubarvimab (BRII-196) and romlusevimab (BRII-198), obtained from the B cells of eight patients recovering from COVID-19 in the early stages of the 2020 pandemic. In response to promising results of a phase 1 clinical trial conducted in China, BRII-196 and BRII-198 were selected for inclusion in NIH's Accelerating COVID-19 Therapeutic Interventions and Vaccines 2 (ACTIV-2) international multicenter clinical trial. As reported in the ACTIV-2 study, the combination of BRII-196 and BRII-198 reduced hospitalization and the risk of death by 78% compared to a placebo (*3*). After this trial demonstrated the safety and effectiveness of the treatment for COVID-19, the FDA granted it an Emergency Use Authorization (EUA). In December 2021, the State Drug Administration of China approved the combination therapy for the treatment of adult and adolescent patients with mild or general COVID-19 with risk factors for progression, and the National Health Commission included it in the Diagnosis and Treatment Protocol for COVID-19 (Tentative 9th ed.) in March 2022 (*4,5*). These advances have contributed to improved treatment options for COVID-19 and bolstered clinicians' confidence in their ability to combat SARS-CoV-2 in China.

As a thriving avenue of drug discovery, many monoclonal antibodies either singly or in combination have been granted an EUA by authorities in various countries (*6*). Hundreds of monoclonal antibodies are in different stages of clinical studies as COVID-19 therapies. However, the widespread adoption of neutralizing antibodies poses major obstacles. The most

significant problem is loss of neutralizing antibodies' efficacy against emerging SARS-CoV-2 variants, such as Omicron and its sub-variants (BA.1, BA.2, BA.3, and BA.4/5). Among the more than 50 mutations present in Omicron, 32 occurred in the receptor binding domain of the spike protein (*7*). Since the receptor binding domain is the primary target of neutralizing antibodies following infection and immunization, these modifications may result in Omicron's evasion of antibody therapy. Studies have indicated that most of the therapeutic antibodies licensed under an EUA lose their binding and neutralizing properties when combined with Omicron variants. This will provide a serious challenge to the efficacy of neutralizing antibodies. This might be overcome by the newly listed amubarvimab and romlusevimab. A live virus neutralization assay revealed that amubarvimab had reduced neutralizing activity against the Omicron variant while romlusevimab displayed enhanced neutralizing action against the Omicron variant (*8*). The total concentrations of the two drugs in the blood remained 60 times higher than the amount needed to neutralize the live virus isolate BA.2 by 90%.

The normal use of neutralizing antibodies is dependent on availability and affordability, which are ongoing concerns for policymakers and patients. Due to a combination of technical advancements and market demand, the capacity for and price of antibody preparations have changed radically, and once prohibitive prices have become more affordable. As a medication that must be used long-term, the combination therapy will place a significant financial burden on patients. Moreover, injectables pose an obvious challenge for patients at home. Amubarvimab and romlusevimab are covered by medical insurance in China, but if their use is driven by medical necessity, this will put pressure on the Chinese health insurance system.

Overall, the use of neutralizing antibodies to treat COVID-19 presents both opportunities and challenges. Existing policies in China to combat the epidemic have been adjusted in light of the country's economic and social development. A broader selection of therapeutic options will make the strategy more adaptable and flexible, so the healthcare system will not become overburdened or better preventative measures can be taken to reduce the spread of the disease. Amubarvimab and romlusevimab, along with their derivatives, are expected to contribute to achieving these goals.

Acknowledgements

The authors wish to thank all of the participants in this study.

Funding: None.

Conflict of Interest: The authors have no conflicts of interest to disclose.

References

1. Mohapatra RK, Kuppili S, Kumar Suvvari T, Kandi V, Behera A, Verma S, Biswal SK, Al-Noor TH, El-ajaily MM, Sarangi AK. SARS-CoV-2 and its variants of concern including Omicron: A never ending pandemic. Chem Biol Drug Des. 2022; 99:769-788.
2. Zhou P, Yang XL, Wang XG, et al. A pneumonia outbreak associated with a new coronavirus of probable bat origin. Nature. 2020; 579:270-273.
3. Evering TH, Giganti M, Chew KW, Hughes M, Moser C, Wohl DA, Currier J, Eron JJ, Javan A, Margolis DA. LB2. Safety and efficacy of combination SARS-CoV-2 monoclonal neutralizing antibodies (mAb) BRII-196 and BRII-198 in non-hospitalized COVID-19 patients. In: Open Forum Infectious Diseases. Oxford University Press US, 2021; pp. S807-S808.
4. NMPA. The National Medical Products Administration issued emergency approval of an application for registration of injectable ambacizumab (BRII 196) and injectable romisvir (BRII 198) as a combination therapy with neutralizing antibodies for COVID-19 from Tengsheng Huachuang Pharmaceutical Technology (Beijing) Co., Ltd. *https://www.nmpa.gov.cn/yaopin/ypjgdt/20211208212528103.html* (accessed July 15, 2022)
5. NHC. Regimen for the treatment of COVID-19 (Tentative 9th ed.). *http://www.nhc.gov.cn/yzygj/s7653p/202203/b74ade1ba4494583805a3d2e40093d88.shtml* (accessed July 15, 2022)
6. Hurt AC, Wheatley AK. Neutralizing antibody therapeutics for COVID-19. Viruses. 2021; 13:628.
7. Lan J, Ge J, Yu J, Shan S, Zhou H, Fan S, Zhang Q, Shi X, Wang Q, Zhang L. Structure of the SARS-CoV-2 spike receptor-binding domain bound to the ACE2 receptor. Nature. 2020; 581:215-220.
8. Lusvarghi S, Pollett SD, Neerukonda SN, Wang W, Wang R, Vassell R, Epsi NJ, Fries AC, Agan BK, Lindholm DA. SARS-CoV-2 BA. 1 variant is neutralized by vaccine booster–elicited serum but evades most convalescent serum and therapeutic antibodies. Sci Transl Med. 2022; 14:eabn8543.

Received July 20, 2022; Revised July 30, 2022; Accepted August 7, 2022.

**Address correspondence to:*
Hongzhou Lu, National Clinical Research Center for Infectious Disease, The Second Affiliated Hospital, Southern University of Science and Technology, 29 Bulan Road, Long Gang District, Shenzhen 518112, Guangdong, China.
E-mail: luhongzhou@fudan.edu.cn

Released online in J-STAGE as advance publication August 13, 2022.

Letter to the Editor

DOI: 10.5582/ddt.2022.01054

Effects of raltegravir formulation change on medication adherence and medication errors

Sonoe Higashino[1,§], Takeo Yasu[1,2,§,*] , Kenji Momo[1,3], Seiichiro Kuroda[1]

[1] Department of Pharmacy, The Institute of Medical Science Hospital, The University of Tokyo, Tokyo, Japan;
[2] Department of Medicinal Therapy Research, Pharmaceutical Education and Research Center, Meiji Pharmaceutical University, Tokyo, Japan;
[3] Department of Hospital Pharmaceutics, School of Pharmacy, Showa University, Tokyo, Japan.

SUMMARY This study was aimed at assessing the adherence and incorrect drug intake associated with changes in the dosing schedule of raltegravir, the first integrase strand transfer inhibitor, from 400 mg twice a day (BID) to 600 mg × 2 tablets once a day (QD) in human immunodeficiency virus (HIV)-infected patients. Medication adherence over 1 month was evaluated in 25 male patients using the 100-mm visual analog scale (VAS) at the 3-day recall pill count and during pharmacist counseling after the first post-change visit. VAS scores before and after the raltegravir formulation change were compared. Medication adherence increased from 96 ± 4.3 mm (BID) to 100 ± 0.3 mm (QD) ($P < 0.05$). The patients exhibited improved medication adherence; however, three patients incorrectly took the drug when the formulation changed. This discovery can be used to facilitate the treatment of HIV-infected patients to increase treatment suitability and safety.

Keywords Raltegravir, medication adherence, medication error, formulation change

Letter to the Editor,

Raltegravir, the first integrase strand transfer inhibitor, was approved in October 2007. It is a key drug in the treatment of infection with human immunodeficiency virus-1 (HIV-1) (*1*). In 2017, Cahn *et al*. reported that a change in the dosing schedule of raltegravir from 400-mg tablet taken twice a day (BID) to 1,200 mg (2 × 600 mg tablets) once a day (QD) is noninferior in efficacy (*2*). We previously reported a case in which raltegravir underdosing occurred when the formulation changed (*3*). In HIV treatment, a high level of HIV medication adherence increases the likelihood of complete control of the infection. However, the association between formulation changes and medication errors, such as incorrect use of anti-HIV agents, remains unclear. Therefore, we assessed medication adherence and incorrect drug use when the dosing schedule changed from BID to QD in raltegravir-treated patients with HIV infection. We expect that our results can shed light on how formulation changes are associated with errors and could be used by pharmacists to better treat and care for patients with HIV infection in the future.

The medical records of 25 men with HIV infection whose dosing schedules were changed from BID to QD were retrospectively reviewed at the Institute of Medical Science Hospital, the University of Tokyo, from July 2018 to September 2018. A 3-day recall was used to determine the total pill count to discover the patients who incorrectly took anti-HIV drugs. Data on medication adherence was collected from the medical and drug management instruction records. Medication adherence before and after formulation changes was evaluated using a 100-mm visual analog scale (VAS) and 3-day recall pill count. The former was self-assessed by the patients for 1 month according to pharmacist instructions. Comparisons of VAS data between BID and QD were performed using a paired *t*-test. All statistical analyses were performed using EZR (4). All *p*-values were two-sided, and values < 0.05 were considered statistically significant. The study was approved by the Institutional Review Board of our institution.

The dosing schedule for 25 patients who were prescribed raltegravir in our hospital was changed from BID to QD. The mean age of the patients was 51.9 ± 14.4 years. The drugs used by the patients included lamivudine/abacavir ($n = 11$), emtricitabine/tenofovir alafenamide ($n = 11$), and other drugs ($n = 3$), and the number of drugs used per patient was 4.5 ± 2.9. The median duration of HIV treatment was 104 months (range, 50-214 months). Medication adherence as assessed by the VAS score increased from 96 ± 4.3 mm (BID) to 100 ± 0.3 mm (QD) ($p < 0.05$, Figure 1). Three patients were found to have incorrectly taken the anti-HIV agents, including raltegravir. The incorrect drug use

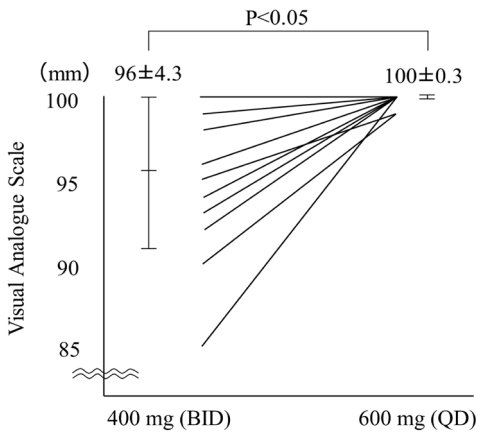

Figure 1. Patient self-assessment data using the 100-mm visual analog scale for medication adherence before and after the raltegravir dosing schedule was changed from BID to QD.

was discovered in the 3-day recall pill count. The three patients who had incorrectly taken drugs after raltegravir formulation change were elderly patients with HIV in their 50s, 60s, and 70s.

In this study, we demonstrated that changing the dosing schedule from BID to QD improved adherence in all patients. This result is similar to previous reports (*2,5-7*). However, the formulation changes caused medication errors in 3 of 25 patients. In HIV-infected patients, medication compliance of less than 95% increases treatment-resistant viral load (*8*). Therefore, our results on medication adherence and medication errors show the need for detailed instructions from pharmacists for each patient when they change dose timings. In addition, aging patients with HIV infection are more prone to medication errors as the number of medications for comorbidities increases and cognitive function declines. In particular, as anti-HIV medications are taken throughout life, the risk of medication errors is expected to increase further as daily treatment regimens, including the timing and frequency of dosing, become habitual. Thus, physicians and pharmacists must also consider polypharmacy and the complex medication treatment strategies used by patients with HIV infection. Based on our results, we can recommend that to discover any errors in dosage and medication adherence in clinical settings, strict monitoring is required using multiple methods, including subjective and objective tools, when a formulation is changed.

This study had a few imitations. First, this was a single-center study with a small number of patients. Second, our patients included many elderly patients. Interestingly, three patients who incorrectly took the anti-HIV agents were elderly. Therefore, their actions may have been influenced by and partially attributable to their age.

Our patients exhibited improved medication adherence after the dosing schedule changed from BID to QD; however, three patients incorrectly took their medications when the raltegravir formulation was changed. Although only a small proportion of patients made an error, this discovery can be used to improve the safety and suitability of HIV treatment. Pharmacists and physicians should closely monitor medication adherence and ensure that each patient takes the correct dose.

Funding: None.

Conflict of Interest: The authors have no conflicts of interest to disclose.

References

1. Steigbigel RT, Cooper DA, Kumar PN, *et al*. Raltegravir with optimized background therapy for resistant HIV-1 infection. N Engl J Med 2008; 359:339-354.
2. Cahn P, Kaplan R, Sax PE, *et al*. Raltegravir 1200 mg once daily versus raltegravir 400 mg twice daily, with tenofovir disoproxil fumarate and emtricitabine, for previously untreated HIV-1 infection: a randomised, double-blind, parallel-group, phase 3, non-inferiority trial. Lancet HIV. 2017; 4:e486-e494.
3. Kobayashi S, Momo K, Yasu T, Higashino S, Kuroda S. A case of under-dosing after raltegravir formulation change in an elderly patient treated for HIV. Pharmazie. 2019; 74:62-63.
4. Kanda Y. Investigation of the freely available easy-to-use software 'EZR' for medical statistics. Bone Marrow Transplant. 2013; 48:452-458.
5. Parienti J-J, Bangsberg DR, Verdon R, Gardner EM. Better adherence with once-daily antiretroviral regimens: A meta-analysis. Clin Infect Dis. 2009; 48:484-488.
6. Cooper V, Horne R, Gellaitry G, Vrijens B, Lange AC, Fisher M, White D. The impact of once-nightly versus twice-daily dosing and baseline beliefs about HAART on adherence to efavirenz-based HAART over 48 weeks: the NOCTE study. J Acquir Immune Defic Syndr. 2010; 53:369-377.
7. Jayaweera D, Dejesus E, Nguyen KL, Grimm K, Butcher D, Seekins DW. Virologic suppression, treatment adherence, and improved quality of life on a once-daily efavirenz-based regimen in treatment-naïve HIV-1-infected patients over 96 weeks. HIV Clin Trials. 2009; 10:375-384.
8. Paterson DL, Swindells S, Mohr J, Brester M, Vergis EN, Squier C, Wagener MM, Singh N. Adherence to protease inhibitor therapy and outcomes in patients with HIV infection. Ann Intern Med. 2000; 133:21-30.

Received July 19, 2022; Revised August 9, 2022; Accepted August 20, 2022.

[§]These authors contributed equally to this work.
**Address correspondence to:*
Takeo Yasu, Department of Medicinal Therapy Research, Pharmaceutical Education and Research Center, Meiji Pharmaceutical University; 2-522-1, Noshio, Kiyose, Tokyo 204-8588, Japan
Email: yasutakeo-tky@umin.ac.jp

Released online in J-STAGE as advance publication August 25, 2022.

Letter to the Editor

DOI: 10.5582/ddt.2022.01033

Portal vein thrombosis as the first presentation of paroxysmal nocturnal hemoglobinuria

Ran Wang[1], Xiaozhong Guo[1], Yufu Tang[2], Xingshun Qi[1,*]

[1] Department of Gastroenterology, General Hospital of Northern Theater Command, Shenyang, China;
[2] Department of Hepatobiliary Surgery, General Hospital of Northern Theater Command, Shenyang, China.

SUMMARY Paroxysmal nocturnal hemoglobinuria (PNH) is a rare, acquired clonal hematopoietic stem cell disorder, characterized by hemolytic anemia, bone marrow failure and thrombosis. Portal vein thrombosis (PVT) is relatively rare in patients with PNH. In this paper, we reported PVT as the first clinical presentation of PNH in a female patient. PVT related symptoms resolved after anticoagulation therapy.

Keywords paroxysmal nocturnal hemoglobinuria, portal vein thrombosis, anticoagulation therapy

Letter to the Editor:

Paroxysmal nocturnal hemoglobinuria (PNH) is a rare, life-threatening, clonal hematopoietic stem cell disorder (*1*). PNH arises from a somatic mutation in the phosphatidylinositol N-acetylglucosaminyltransferase subunit A (*PIG-A*) gene located on chromosome X (*1*). It is characterized by a deficiency of glycosylphosphatidylinositol (GPI) anchored proteins, including CD55 and CD59, leading to complement-mediated hemolysis (*2*). The incidence of PNH is approximately 1-1.5 per 1,000,000 individuals worldwide with a 5- and 10-year mortality of 35% and 50%, respectively (*3-5*). Thrombosis, is a common complication of PNH, however, the most commonly involved site of thrombosis is hepatic vein, portal vein thrombosis (PVT) is rarely reported (*6*). Herein, we describe the disease course of and anticoagulation treatment for PVT in a PNH patient. Notably, no obvious clinical symptom was observed during a 15-year history of PNH. Abdominal pain secondary to PVT should be considered as the first presentation of PNH in this patient and was soon resolved after anticoagulation therapy.

A 55-year-old woman presented with fever and right upper abdominal pain for 30 days. She was accidentally diagnosed with PNH 15 years ago. Because she had not suffered any significant clinical symptoms potentially related to PNH, no specific medical treatment had been given for PNH. Neither regular medications nor family history of thrombosis was reported. On August 5, 2021, the patient was admitted to our hospital. On laboratory tests, hemoglobin was 84 g/L (reference range: 115-150 g/L), mean corpuscular volume was 107.6 fL (reference range: 82.0-100.0 fL), and platelets count was 38 × 10^9 cells/L (reference range: 125-350 × 10^9 cells/L), white blood cell was 3.3 × 10^9 cells/L (reference range: 3.5-9.5 × 10^9 cells/L) with 68.4% granulocytes, 8.7% monocytes, and 21.8% lymphocytes, lactate dehydrogenase (LDH) was elevated at 642 U/L (reference range: 109-245 U/L), total bilirubin level was 24.1 μmol/L (reference range: 5.1-22.2 μmol/L), alkaline phosphatase level was 269.28 U/L (reference range: 35-135 U/L), and γ-glutamyl transferase level was 245.3 U/L (reference range: 7-45 U/L). The Coombs test was negative, and the D-dimer was 3.71 mg/L (reference range: 0.00-0.55 mg/L). On August 6, contrast-enhanced abdominal computed tomography (CT) revealed portal vein, superior mesenteric vein, and splenic vein thrombosis with portal cavernoma (Figure 1). Endoscopy demonstrated mild varices on gastric fundus. On August 6, she received anticoagulation therapy of PVT at our department. Low molecular weight heparin (LMWH) was given at a dosage of 5,000 IU subcutaneously twice a day. Three days later, abdominal pain and fever completely disappeared. Fourteen days later, a repeat CT was performed, and showed that portal vein, superior mesenteric vein, and splenic vein thrombosis remained, but inflammatory exudate around the superior mesenteric vein was resolved (Figure 2). On November 20, follow-up CT still showed portal vein thrombosis, and superior mesenteric vein thrombosis with portal cavernoma. LMWH was converted to rivaroxaban (Figure 3). At the last follow-up on April 15, 2022, her general condition was stable without any complaints.

PNH can be characterized as hemolytic anemia, bone marrow failure, renal dysfunction, erectile dysfunction, pulmonary hypertension, infection, and unexplained

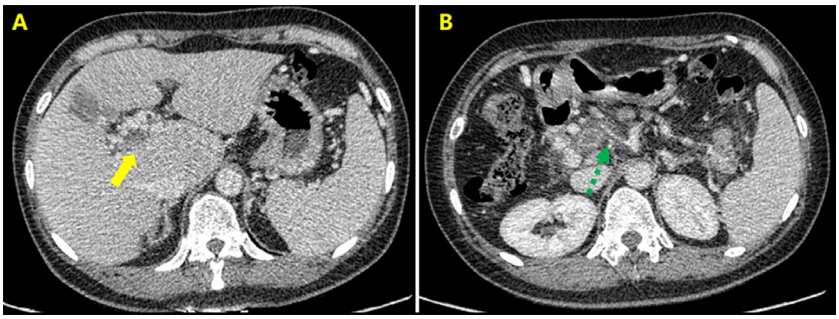

Figure 1. Computed tomography scans performed on August 6, 2021, at admission. Computed tomography showed portal vein thrombosis (solid arrow) **(A)** and superior mesenteric vein thrombosis (dotted arrow) **(B)**.

Figure 2 Computed tomography scans performed on August 20, 2021, after anticoagulation. Axial computed tomography scans showed portal vein thrombosis (solid arrow) **(A)** and superior mesenteric vein thrombosis (dotted arrow) **(B)**. Coronal computed tomography scans showed portal vein thrombosis (solid arrow) **(C)**.

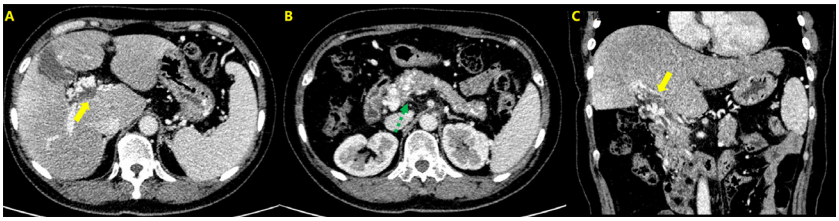

Figure 3. Computed tomography scans performed on November 20, 2021, during follow-up. Axial computed tomography scans showed portal vein thrombosis (solid arrow) **(A)** and superior mesenteric vein thrombosis (dotted arrow) **(B)**. Coronal computed tomography scans showed portal vein thrombosis (solid arrow) **(C)**.

thrombosis (*7*). However, some PNH cases do not have any clinical presentations (*8*). Similarly, despite PNH was diagnosed 15 years ago, our case did not have any classical manifestations until abdominal pain secondary to PVT developed as the first clinical presentation.

There are some possible mechanisms of thrombosis in patients with PNH. 1) PNH clone. The risk of thrombotic events appears to be directly associated with the size of PNH clone, especially the percentage of GPI protein-free granulocytes (PNH granulocytes > 50%). The 10-year cumulative thrombosis rate was 34.5% for PNH granulocytes > 50%, but only 5.3% for PNH granulocytes < 50% ($p < 0.01$) (*9*). The International PNH Registry analysis, the largest PNH study to date, also found that the incidence of thrombotic events was significantly higher in patients with PNH granulocytes > 50% than those with PNH granulocytes < 10% and PNH granulocytes within 10-50% (*10*). 2) Endothelial cell (EC) damage. EC damage can occur during any thrombotic event. In PNH patients, the free hemoglobin released from lysed PNH erythrocytes and its breakdown oxidative product heme can directly activate EC, increase the production of tissue factors, and further promote inflammation and coagulation (*11,12*). 3) Platelets activations. The absence of CD59 in PNH patients makes platelets vulnerable to complement attack, resulting in complement-mediated activation and disruption (*13*). Activated platelets also interact with neutrophils to promote thrombosis through the release of serine proteases and nucleosomes from neutrophils, which synergistically activate factor X to initiate coagulation primarily through the extrinsic pathway (*14*). 4) Intravascular hemolysis. Elevated hemoglobin from intravascular hemolysis may lead to nitric oxide depletion, which has also been reported to contribute to thrombosis (*11*).

Thrombosis is the leading cause of death in PNH patients. A thrombotic event increases the relative risk of death in PNH patients by 5- to 10- fold (*15,16*). There are some risk factors that help identify thrombosis in PNH patients, including LDH level ≥ 1.5 times the upper limit of normal (ULN), high PNH symptom burden,

ethnicity, and infection. In a Korean registry study of patients with PNH, LDH ≥ 1.5 times ULN at diagnosis was independently associated with increased odds of thrombotic events after adjusting for age, gender, and bone marrow failure (odds ratio 7.0; 95% confidence interval 1.5-32; $p = 0.013$) (17). In our case, the LDH level was 642 U/L, which is 2.6 times of the ULN. PNH symptom burdens include abdominal pain, fatigue, dyspnea, hemoglobinuria, and dysphagia. Higher PNH symptom burdens had a positive correlation with the GPI-deficient granulocyte clone size, and was also recognized as a risk factor for thrombosis (*10,17*). Ethnicity may be another risk factor for the development of thrombosis in PNH patients, because the incidence of thrombotic events was 13-17% in Asian PNH patients (*17,18*) and 29-44% in Western PNH patients (*5,8*). Taken together, venous thrombosis should be regularly observed in PNH patients, especially those with above-mentioned risk factors. On the other hand, Western studies have also suggested that routine screening for PNH should be considered in PVT patients (*19*). However, there was a very low prevalence of PNH in Chinese patients with PVT (*19,20*), which did not support the necessity of routine screening for PNH in such patients.

In PNH patients with acute thrombosis, eculizumab and anticoagulation should be given immediately with a duration of 3-6 months, and anticoagulation can be discontinued if thrombotic symptoms are resolved (*1*). Eculizumab is recommended as the first-line therapy for PNH, can improve long-term survival and quality of life, and reduce hemolysis and thrombotic events (*21-24*). However, high costs and difficulty to access limit the use of eculizumab in China (*25*). Additionally, anticoagulation can reach an overall response rate of more than 70% in patients with acute non-cirrhotic, non-malignant PVT (*26*). In a systematic review, complete or partial portal vein recanalization was observed in 38.3% and 14% of cases after initiation of anticoagulation therapy, respectively, but in 16.7% of cases without anticoagulation (*27*). Direct oral anticoagulants, such as rivaroxaban, are likely equivalent, but have not been well studied in PNH (*28*). Notably, anticoagulation also potentially increases the morbidity of variceal bleeding. A risk-benefit ratio of anticoagulants in non-cirrhotic PVT may be evaluated based on grade of gastroesophageal varices, recent bleeding events, prothrombotic disorders, and thrombocytopenia (*29*). Our case had PNH as a permanent thrombotic risk factor with low-risk varices without any previous bleeding events, so anticoagulation might be less risky. Alternative treatments would be considered if anticoagulation failed or was not feasible. Transjugular intrahepatic portosystemic shunt can be considered for the treatment of portal hypertension in patients with non-malignant and non-cirrhotic portal vein thrombosis (*30*), even those with portal cavernoma (*31*).

In conclusion, thrombosis should be routinely screened in patients with PNH, especially in high-risk patients. It is probable that PVT should be the first clinical presentation of PNH. Early anticoagulation therapy may be preferred in PNH patients with PVT.

Funding: None.

Conflict of Interest: The authors have no conflicts of interest to disclose.

References

1. Hill A, DeZern AE, Kinoshita T, Brodsky RA. Paroxysmal nocturnal haemoglobinuria. Nat Rev Dis Primers. 2017; 3:17028.
2. Parker CJ. The pathophysiology of paroxysmal nocturnal hemoglobinuria. Exp Hematol. 2007; 35:523-533.
3. Socie G, Schrezenmeier H, Muus P, *et al*. Changing prognosis in paroxysmal nocturnal haemoglobinuria disease subcategories: an analysis of the International PNH Registry. Intern Med J. 2016; 46:1044-1053.
4. Brodsky RA. Paroxysmal nocturnal hemoglobinuria. Blood. 2014; 124:2804-2811.
5. Hillmen P, Lewis SM, Bessler M, Luzzatto L, Dacie JV. Natural history of paroxysmal nocturnal hemoglobinuria. N Engl J Med. 1995; 333:1253-1258.
6. Parvataneni S, Sunkara T, Gaduputi V. Rare hematological disease of paroxysmal nocturnal hemoglobinuria with profound implications for a gastroenterologist: A case report and literature review. Cureus. 2020; 12:e8941.
7. Devos T, Meers S, Boeckx N, Gothot A, Deeren D, Chatelain B, Chatelain C, Devalet B. Diagnosis and management of PNH: Review and recommendations from a Belgian expert panel. Eur J Haematol. 2018; 101:737-749.
8. Parker C, Omine M, Richards S, Nishimura J, Bessler M, Ware R, Hillmen P, Luzzatto L, Young N, Kinoshita T, Rosse W, Socie G, International PNHIG. Diagnosis and management of paroxysmal nocturnal hemoglobinuria. Blood. 2005; 106:3699-3709.
9. Hall C, Richards S, Hillmen P. Primary prophylaxis with warfarin prevents thrombosis in paroxysmal nocturnal hemoglobinuria (PNH). Blood. 2003; 102:3587-3591.
10. Schrezenmeier H, Roth A, Araten DJ, Kanakura Y, Larratt L, Shammo JM, Wilson A, Shayan G, Maciejewski JP. Baseline clinical characteristics and disease burden in patients with paroxysmal nocturnal hemoglobinuria (PNH): updated analysis from the International PNH Registry. Ann Hematol. 2020; 99:1505-1514.
11. Van Bijnen ST, Van Heerde WL, Muus P. Mechanisms and clinical implications of thrombosis in paroxysmal nocturnal hemoglobinuria. J Thromb Haemost. 2012; 10:1-10.
12. Rother RP, Bell L, Hillmen P, Gladwin MT. The clinical sequelae of intravascular hemolysis and extracellular plasma hemoglobin: a novel mechanism of human disease. JAMA. 2005; 293:1653-1662.
13. Wiedmer T, Hall SE, Ortel TL, Kane WH, Rosse WF, Sims PJ. Complement-induced vesiculation and exposure of membrane prothrombinase sites in platelets of paroxysmal nocturnal hemoglobinuria. Blood. 1993; 82:1192-1196.
14. Massberg S, Grahl L, von Bruehl ML, *et al*. Reciprocal coupling of coagulation and innate immunity via

neutrophil serine proteases. Nat Med. 2010; 16:887-896.
15. Socie G, Mary JY, de Gramont A, Rio B, Leporrier M, Rose C, Heudier P, Rochant H, Cahn JY, Gluckman E. Paroxysmal nocturnal haemoglobinuria: long-term follow-up and prognostic factors. French Society of Haematology. Lancet. 1996; 348:573-577.
16. Hill A, Kelly RJ, Hillmen P. Thrombosis in paroxysmal nocturnal hemoglobinuria. Blood. 2013; 121:4985-4996; quiz 5105.
17. Lee JW, Jang JH, Kim JS, Yoon SS, Lee JH, Kim YK, Jo DY, Chung J, Sohn SK. Clinical signs and symptoms associated with increased risk for thrombosis in patients with paroxysmal nocturnal hemoglobinuria from a Korean Registry. Int J Hematol. 2013; 97:749-757.
18. Nishimura JI, Kanakura Y, Ware RE, Shichishima T, Nakakuma H, Ninomiya H, Decastro CM, Hall S, Kanamaru A, Sullivan KM, Mizoguchi H, Omine M, Kinoshita T, Rosse WF. Clinical course and flow cytometric analysis of paroxysmal nocturnal hemoglobinuria in the United States and Japan. Medicine (Baltimore). 2004; 83:193-207.
19. Qi X, He C, Han G, Yin Z, Wu F, Zhang Q, Niu J, Wu K, Fan D. Prevalence of paroxysmal nocturnal hemoglobinuria in Chinese patients with Budd-Chiari syndrome or portal vein thrombosis. J Gastroenterol Hepatol. 2013; 28:148-152.
20. Qi X, Wu F, He C, Fan D, Han G. Thrombotic risk factors in Chinese nonmalignant and noncirrhotic patients with portal vein thrombosis: an observational study with a systematic review of the literature. Eur J Gastroenterol Hepatol. 2015; 27:77-83.
21. Cancado RD, Araujo ADS, Sandes AF, Arrais C, Lobo CLC, Figueiredo MS, Gualandro SFM, Saad STO, Costa FF. Consensus statement for diagnosis and treatment of paroxysmal nocturnal haemoglobinuria. Hematol Transfus Cell Ther. 2021; 43:341-348.
22. Hillmen P, Muus P, Roth A, Elebute MO, Risitano AM, Schrezenmeier H, Szer J, Browne P, Maciejewski JP, Schubert J, Urbano-Ispizua A, de Castro C, Socie G, Brodsky RA. Long-term safety and efficacy of sustained eculizumab treatment in patients with paroxysmal nocturnal haemoglobinuria. Br J Haematol. 2013; 162:62-73.
23. Ikezoe T, Noji H, Ueda Y, *et al*. Long-term follow-up of patients with paroxysmal nocturnal hemoglobinuria treated with eculizumab: post-marketing surveillance in Japan. Int J Hematol. 2022; 115:470-480.
24. Zhou S, Dong X, Chen C, Ma L, Wu Y, Zhou Y, Cui Y. Efficacy and safety of eculizumab for paroxysmal nocturnal hemoglobinuria: A systematic review and meta-analysis. J Pediatr Hematol Oncol. 2021; 43:203-210.
25. Liang HY, Xie XD, Jing GX, Wang M, Yu Y, Cui JF. Posthepatectomy jaundice induced by paroxysmal nocturnal hemoglobinuria: A case report. World J Clin Cases. 2021; 9:10046-10051.
26. Rossle M, Bettinger D, Trebicka J, *et al*. A prospective, multicentre study in acute non-cirrhotic, non-malignant portal vein thrombosis: comparison of medical and interventional treatment. Aliment Pharmacol Ther. 2020; 52:329-339.
27. Hall TC, Garcea G, Metcalfe M, Bilku D, Dennison AR. Management of acute non-cirrhotic and non-malignant portal vein thrombosis: a systematic review. World J Surg. 2011; 35:2510-2520.
28. Brodsky RA. How I treat paroxysmal nocturnal hemoglobinuria. Blood. 2021; 137:1304-1309.
29. Qi X, Han G, Bai M, Yuan S, Fan D. Anticoagulation and variceal bleeding in non-cirrhotic patients with portal vein thrombosis. Intern Emerg Med. 2011; 6:93-94; author reply 95-96.
30. Qi X, Guo X. An early decision of transjugular intrahepatic portosystemic shunt may be considered for non-malignant and non-cirrhotic portal vein thrombosis with ascites: a concise review of the theoretical possibility and practical difficulty. Arch Med Sci. 2016; 12:1381-1383.
31. Qi X, Han G, Yin Z, He C, Wang J, Guo W, Niu J, Zhang W, Bai M, Fan D. Transjugular intrahepatic portosystemic shunt for portal cavernoma with symptomatic portal hypertension in non-cirrhotic patients. Dig Dis Sci. 2012; 57:1072-1082.

Received April 17, 2022; Revised June 27, 2022; Accepted August 13, 2022.

**Address correspondence to:*
Xingshun Qi, Department of Gastroenterology, General Hospital of Northern Theater Command (formerly General Hospital of Shenyang Military Area), No. 83 Wenhua Road, Shenyang, 110840 Liaoning Province, China.
E-mail: xingshunqi@126.com

Released online in J-STAGE as advance publication August 21, 2022.

DD&T
Drug Discoveries & Therapeutics

Guide for Authors

1. Scope of Articles

Drug Discoveries & Therapeutics (Print ISSN 1881-7831, Online ISSN 1881-784X) welcomes contributions in all fields of pharmaceutical and therapeutic research such as medicinal chemistry, pharmacology, pharmaceutical analysis, pharmaceutics, pharmaceutical administration, and experimental and clinical studies of effects, mechanisms, or uses of various treatments. Studies in drug-related fields such as biology, biochemistry, physiology, microbiology, and immunology are also within the scope of this journal.

2. Submission Types

Original Articles should be well-documented, novel, and significant to the field as a whole. An Original Article should be arranged into the following sections: Title page, Abstract, Introduction, Materials and Methods, Results, Discussion, Acknowledgments, and References. Original articles should not exceed 5,000 words in length (excluding references) and should be limited to a maximum of 50 references. Articles may contain a maximum of 10 figures and/or tables. Supplementary Data are permitted but should be limited to information that is not essential to the general understanding of the research presented in the main text, such as unaltered blots and source data as well as other file types.

Brief Reports definitively documenting either experimental results or informative clinical observations will be considered for publication in this category. Brief Reports are not intended for publication of incomplete or preliminary findings. Brief Reports should not exceed 3,000 words in length (excluding references) and should be limited to a maximum of 4 figures and/or tables and 30 references. A Brief Report contains the same sections as an Original Article, but the Results and Discussion sections should be combined.

Reviews should present a full and up-to-date account of recent developments within an area of research. Normally, reviews should not exceed 8,000 words in length (excluding references) and should be limited to a maximum of 10 figures and/or tables and 100 references. Mini reviews are also accepted, which should not exceed 4,000 words in length (excluding references) and should be limited to a maximum of 5 figures and/or tables and 50 references.

Policy Forum articles discuss research and policy issues in areas related to life science such as public health, the medical care system, and social science and may address governmental issues at district, national, and international levels of discourse. Policy Forum articles should not exceed 3,000 words in length (excluding references) and should be limited to a maximum of 5 figures and/or tables and 30 references.

Case Reports should be detailed reports of the symptoms, signs, diagnosis, treatment, and follow-up of an individual patient. Case reports may contain a demographic profile of the patient but usually describe an unusual or novel occurrence. Unreported or unusual side effects or adverse interactions involving medications will also be considered. Case Reports should not exceed 3,000 words in length (excluding references).

Communications are short, timely pieces that spotlight new research findings or policy issues of interest to the field of global health and medical practice that are of immediate importance. Depending on their content, Communications will be published as "Comments" or "Correspondence". Communications should not exceed 1,500 words in length (excluding references) and should be limited to a maximum of 2 figures and/or tables and 20 references.

Editorials are short, invited opinion pieces that discuss an issue of immediate importance to the fields of global health, medical practice, and basic science oriented for clinical application. Editorials should not exceed 1,000 words in length (excluding references) and should be limited to a maximum of 10 references. Editorials may contain one figure or table.

News articles should report the latest events in health sciences and medical research from around the world. News should not exceed 500 words in length.

Letters should present considered opinions in response to articles published in *Drug Discoveries & Therapeutics* in the last 6 months or issues of general interest. Letters should not exceed 800 words in length and may contain a maximum of 10 references. Letters may contain one figure or table.

3. Editorial Policies

For publishing and ethical standards, *Drug Discoveries & Therapeutics* follows the Recommendations for the Conduct, Reporting, Editing, and Publication of Scholarly Work in Medical Journals (*http://www.icmje.org/recommendations*) issued by the International Committee of Medical Journal Editors (ICMJE), and the Principles of Transparency and Best Practice in Scholarly Publishing (*https://doaj.org/bestpractice*) jointly issued by the Committee on Publication Ethics (COPE), the Directory of Open Access Journals (DOAJ), the Open Access Scholarly Publishers Association (OASPA), and the World Association of Medical Editors (WAME).

Drug Discoveries & Therapeutics will perform an especially prompt review to encourage innovative work. All original research will be subjected to a rigorous standard of peer review and will be edited by experienced copy editors to the highest standards.

Ethics: *Drug Discoveries & Therapeutics* requires that authors of reports of investigations in humans or animals indicate that those studies were formally approved by a relevant ethics committee or review board. For research involving human experiments, a statement that the participants gave informed consent before taking part (or a statement that it was not required and why) should be indicated. Authors should also state that the study conformed to the provisions of the Declaration of Helsinki (as revised in 2013). When reporting experiments on animals, authors should indicate whether the institutional and national guide for the care and use of laboratory animals was followed.

Conflict of Interest: All authors are required to disclose any actual or potential conflict of interest including financial

interests or relationships with other people or organizations that might raise questions of bias in the work reported. If no conflict of interest exists for each author, please state "There is no conflict of interest to disclose".

Submission Declaration: When a manuscript is considered for submission to *Drug Discoveries & Therapeutics*, the authors should confirm that 1) no part of this manuscript is currently under consideration for publication elsewhere; 2) this manuscript does not contain the same information in whole or in part as manuscripts that have been published, accepted, or are under review elsewhere, except in the form of an abstract, a letter to the editor, or part of a published lecture or academic thesis; 3) authorization for publication has been obtained from the authors' employer or institution; and 4) all contributing authors have agreed to submit this manuscript.

Cover Letter: The manuscript must be accompanied by a cover letter prepared by the corresponding author on behalf of all authors. The letter should indicate the basic findings of the work and their significance. The letter should also include a statement affirming that all authors concur with the submission and that the material submitted for publication has not been published previously or is not under consideration for publication elsewhere. The cover letter should be submitted in PDF format. For example of Cover Letter, please visit: Download Centre (*https://www.ddtjournal.com/downcentre)*.

Copyright: When a manuscript is accepted for publication in *Drug Discoveries & Therapeutics*, the transfer of copyright is necessary. A JOURNAL PUBLISHING AGREEMENT (JPA) form will be e-mailed to the authors by the Editorial Office and must be returned by the authors as a scan. Only forms with a hand-written signature are accepted. This copyright will ensure the widest possible dissemination of information. Please note that your manuscript will not proceed to the next step in publication until the JPA form is received. In addition, if excerpts from other copyrighted works are included, the author(s) must obtain written permission from the copyright owners and credit the source(s) in the article.

Peer Review: *Drug Discoveries & Therapeutics* uses single-blind peer review, which means that reviewers know the names of the authors, but the authors do not know who reviewed their manuscript. The external peer review is performed for research articles by at least two reviewers, and sometimes the opinions of more reviewers are sought. Manuscripts sent out for peer review are evaluated by independent reviewers. Peer reviewers are selected based on their expertise and ability to provide high quality, constructive, and fair reviews. For research manuscripts, the editors may, in addition, seek the opinion of a statistical reviewer. Consideration for publication is based on the article's originality, novelty, and scientific soundness, and the appropriateness of its analysis.

Suggested Reviewers: A list of up to 3 reviewers who are qualified to assess the scientific merit of the study is welcomed. Reviewer information including names, affiliations, addresses, and e-mail should be provided at the same time the manuscript is submitted online. Please do not suggest reviewers with known conflicts of interest, including participants or anyone with a stake in the proposed research; anyone from the same institution; former students, advisors, or research collaborators (within the last three years); or close personal contacts. Please note that the Editor-in-Chief may accept one or more of the proposed reviewers or may request a review by other qualified persons.

Language Editing: Manuscripts prepared by authors whose native language is not English should have their work proofread by a native English speaker before submission. If not, this might delay the publication of your manuscript in *Drug Discoveries & Therapeutics*.

The Editing Support Organization can provide English proofreading, Japanese-English translation, and Chinese-English translation services to authors who want to publish in *Drug Discoveries & Therapeutics* and need assistance before submitting a manuscript. Authors can visit this organization directly at *http://www.iacmhr.com/iac-eso/support.php?lang=en.* IAC-ESO was established to facilitate manuscript preparation by researchers whose native language is not English and to help edit works intended for international academic journals.

4. Manuscript Preparation

Manuscripts are suggested to be prepared in accordance with the "Recommendations for the Conduct, Reporting, Editing, and Publication of Scholarly Work in Medical Journals", as presented at *http://www.ICMJE.org*.

Manuscripts should be written in clear, grammatically correct English and submitted as a Microsoft Word file in a single-column format. Manuscripts must be paginated and typed in 12-point Times New Roman font with 24-point line spacing. Please do not embed figures in the text. Abbreviations should be used as little as possible and should be explained at first mention unless the term is a well-known abbreviation (*e.g.* DNA). Single words should not be abbreviated.

Title page: The title page must include 1) the title of the paper (Please note the title should be short, informative, and contain the major key words); 2) full name(s) and affiliation(s) of the author(s), 3) abbreviated names of the author(s), 4) full name, mailing address, telephone/fax numbers, and e-mail address of the corresponding author; and 5) conflicts of interest (if you have an actual or potential conflict of interest to disclose, it must be included as a footnote on the title page of the manuscript; if no conflict of interest exists for each author, please state "There is no conflict of interest to disclose"). Please visit Download Centre and refer to the title page of the manuscript sample.

Abstract: The abstract should briefly state the purpose of the study, methods, main findings, and conclusions. For article types including Original Article, Brief Report, Review, Policy Forum, and Case Report, a one-paragraph abstract consisting of no more than 250 words must be included in the manuscript. For Communications, Editorials, News, or Letters, a brief summary of main content in 150 words or fewer should be included in the manuscript. Abbreviations must be kept to a minimum and non-standard abbreviations explained in brackets at first mention. References should be avoided in the abstract. Three to six key words or phrases that do not occur in the title should be included in the Abstract page.

Introduction: The introduction should be a concise statement of the basis for the study and its scientific context.

Materials and Methods: The description should be brief but with sufficient detail to enable others to reproduce the experiments. Procedures that have been published previously should not be described in detail but appropriate references should simply be cited. Only new and significant modifications of previously published procedures require complete description. Names of products and manufacturers with their locations (city and state/country) should be given and sources of animals and cell lines should always be indicated. All clinical investigations must have been conducted in accordance with Declaration of Helsinki principles. All human and animal studies must have been approved by the appropriate institutional review board(s) and a specific declaration of approval must be made within this section.

Results: The description of the experimental results should be succinct but in sufficient detail to allow the experiments to be analyzed and interpreted by an independent reader. If necessary, subheadings may be used for an orderly presentation. All figures and tables must be referred to in the text.

Discussion: The data should be interpreted concisely without repeating material already presented in the Results section. Speculation is permissible, but it must be well-founded, and discussion of the wider implications of the findings is encouraged. Conclusions derived from the study should be included in this section.

Acknowledgments: All funding sources should be credited in the Acknowledgments section. In addition, people who contributed to the work but who do not meet the criteria for authors should be listed along with their contributions.

References: References should be numbered in the order in which they appear in the text. Citing of unpublished results, personal communications, conference abstracts, and theses in the reference list is not recommended but these sources may be mentioned in the text. In the reference list, cite the names of all authors when there are fifteen or fewer authors; if there are sixteen or more authors, list the first three followed by *et al*. Names of journals should be abbreviated in the style used in PubMed. Authors are responsible for the accuracy of the references. The EndNote Style of *Drug Discoveries & Therapeutics* could be downloaded at **EndNote** (*https://www.ddtjournal.com/examples/Drug_Discoveries_Therapeutics.ens*).

Examples are given below:

Example 1 (Sample journal reference):

Nakata M, Tang W. Japan-China Joint Medical Workshop on Drug Discoveries and Therapeutics 2008: The need of Asian pharmaceutical researchers' cooperation. Drug Discov Ther. 2008; 2:262-263.

Example 2 (Sample journal reference with more than 15 authors):

Darby S, Hill D, Auvinen A, *et al*. Radon in homes and risk of lung cancer: Collaborative analysis of individual data from 13 European case-control studies. BMJ. 2005; 330:223.

Example 3 (Sample book reference):

Shalev AY. Post-traumatic stress disorder: Diagnosis, history and life course. In: Post-traumatic Stress Disorder, Diagnosis, Management and Treatment (Nutt DJ, Davidson JR, Zohar J, eds.). Martin Dunitz, London, UK, 2000; pp. 1-15.

Example 4 (Sample web page reference):

World Health Organization. The World Health Report 2008 – primary health care: Now more than ever. *http://www.who.int/whr/2008/whr08_en.pdf* (accessed September 23, 2010).

Tables: All tables should be prepared in Microsoft Word or Excel and should be arranged at the end of the manuscript after the References section. Please note that tables should not in image format. All tables should have a concise title and should be numbered consecutively with Arabic numerals. If necessary, additional information should be given below the table.

Figure Legend: The figure legend should be typed on a separate page of the main manuscript and should include a short title and explanation. The legend should be concise but comprehensive and should be understood without referring to the text. Symbols used in figures must be explained. Any individually labeled figure parts or panels (A, B, *etc*.) should be specifically described by part name within the legend.

Figure Preparation: All figures should be clear and cited in numerical order in the text. Figures must fit a one- or two-column format on the journal page: 8.3 cm (3.3 in.) wide for a single column, 17.3 cm (6.8 in.) wide for a double column; maximum height: 24.0 cm (9.5 in.). Please make sure that artwork files are in an acceptable format (TIFF or JPEG) at minimum resolution (600 dpi for illustrations, graphs, and annotated artwork, and 300 dpi for micrographs and photographs). Please provide all figures as separate files. Please note that low-resolution images are one of the leading causes of article resubmission and schedule delays.

Units and Symbols: Units and symbols conforming to the International System of Units (SI) should be used for physicochemical quantities. Solidus notation (*e.g*. mg/kg, mg/mL, mol/mm^2/min) should be used. Please refer to the SI Guide *www.bipm.org/en/si/* for standard units.

Supplemental data: Supplemental data might be useful for supporting and enhancing your scientific research and *Drug Discoveries & Therapeutics* accepts the submission of these materials which will be only published online alongside the electronic version of your article. Supplemental files (figures, tables, and other text materials) should be prepared according to the above guidelines, numbered in Arabic numerals (*e.g*., Figure S1, Figure S2, and Table S1, Table S2) and referred to in the text. All figures and tables should have titles and legends. All figure legends, tables and supplemental text materials should be placed at the end of the paper. Please note all of these supplemental data should be provided at the time of initial submission and note that the editors reserve the right to limit the size and length of Supplemental Data.

5. Submission Checklist

The Submission Checklist will be useful during the final checking of a manuscript prior to sending it to *Drug Discoveries & Therapeutics* for review. Please visit Download Centre and download the Submission Checklist file.

6. Online Submission

Manuscripts should be submitted to *Drug Discoveries & Therapeutics* online at *https://www.ddtjournal.com*. The manuscript file should be smaller than 5 MB in size. If for any reason you are unable to submit a file online, please contact the Editorial Office by e-mail at *office@ddtjournal.com*.

7. Accepted Manuscripts

Proofs: Galley proofs in PDF format will be sent to the corresponding author *via* e-mail. Corrections must be returned to the editor (*proof-editing@ddtjournal.com*) within 3 working days.

Offprints: Authors will be provided with electronic offprints of their article. Paper offprints can be ordered at prices quoted on the order form that accompanies the proofs.

Page Charge: Page charges will be levied on all manuscripts accepted for publication in *Drug Discoveries & Therapeutics* (Original Articles / Brief Reports / Reviews / Policy Forum / Communications: $140 per page for black white pages, $340 per page for color pages; News / Letters: a total cost of $600). Under exceptional circumstances, the author(s) may apply to the editorial office for a waiver of the publication charges at the time of submission.

Misconduct: *Drug Discoveries & Therapeutics* takes seriously all allegations of potential misconduct and adhere to the ICMJE Guideline (*http://www.icmje.org/recommendations*) and COPE Guideline (*http://publicationethics.org/files/Code_of_conduct_for_journal_editors.pdf*). In cases of suspected research or publication misconduct, it may be necessary for the Editor or Publisher to contact and share submission details with third parties including authors' institutions and ethics committees. The corrections, retractions, or editorial expressions of concern will be performed in line with above guidelines.

(As of February 2022)

Drug Discoveries & Therapeutics
Editorial and Head Office
Pearl City Koishikawa 603,
2-4-5 Kasuga, Bunkyo-ku,
Tokyo 112-0003, Japan.
E-mail: office@ddtjournal.com